STRUCTURAL ABNORMALITIES WITHIN THE EPISODIC PROSPECTION AND DECISION MAKING CIRCUITRY IN CIGARETTE SMOKERS: A DTI AND SMRI ANALYSIS

Audrey Rose Verde

A dissertation submitted to the faculty of the University of North Carolina at Chapel Hill in partial fulfillment of the requirements for the degree of Doctor of Philosophy in the Neurobiology Curriculum.

Chapel Hill
2014

Approved by:

Charlotte Boettiger

Martin Styner

Kelly Giovanello

J.C. Garbutt

Hongtu Zhu

Donita Robinson

ABSTRACT

AUDREY ROSE VERDE: STRUCTURAL ABNORMALITIES WITHIN THE EPISODIC PROSPECTION AND DECISION MAKING CIRCUITRY IN CIGARETTE SMOKERS: A DTI AND SMRI ANALYSIS.
(Under the direction of Charlotte Boettiger and Martin Styner)

Smokers characteristically show a heightened tendency to select smaller, sooner over larger, delayed rewards, and the neurobiology of such decision−making is beginning to come to light. For instance, recent studies in healthy people show that engaging episodic prospection during such decision−making can reduce impulsive choices, and that this effect is mediated by enhanced functional connectivity between medial temporal lobe regions implicated in episodic prospection and frontal areas. Through this study we sought to determine if there are any structural differences between cigarette smokers and non−smokers in the episodic prospection and decision making circuitry through the use of diffusion tensor imaging (DTI) and structural MRI (sMRI) analysis. Further, we investigated whether there were any structural changes in this circuitry within smokers that correlated with measurements of cigarette consumption (cigarettes per day, breath carbon monoxide), and addiction severity (cigarette dependence scale). Specifically we studied the white matter (WM) tracts the cingulum, fornix, and uncinate, and the grey matter (GM) regions that these tracts connect, namely regions of the medial temporal lobe and the prefrontal cortex. Our hypotheses were that smokers would have decreased WM structural integrity in the tracts bilaterally compared to nonsmokers, and that the brain regions served by these tracts would have decreased volume and thickness in smokers compared to non−smokers. Within smokers, we hypothesized that with increasing cigarette consumption and addiction severity there would be decreased

WM integrity, and decreased regional GM volume and thickness. We acquired diffusion weighted and anatomical MR images from nonsmokers (n=15) and smokers (n=10 (11 for sMRI)), aged 19−40 years old. We developed and utilized a novel framework for DTI analysis, the UNC−Utah NA−MIC Framework for DTI Fiber Tract Analysis. We found smokers to have decreased WM integrity in the fornix crus, and decreased hippocampal volume compared to nonsmokers. Looking just within smokers, we found positive correlations between WM integrity and measurements of cigarette consumption and addiction severity for the fornix and cingulum. GM analysis though showed negative correlations between these same smoking indices and measurements of cortical thickness and volume in the inferior frontal gyrus, lateral orbitofrontal cortex, cingulate, and amygdala. Together these results demonstrate that the circuitry for episodic prospection, decision making, and cognitive control are altered in cigarette smokers and that the structural aberration correlates with measures of cigarette consumption and dependence.

This dissertation is dedicated to my husband, Barrett Green. I could not have done this without your love and support.

ACKNOWLEDGMENTS

I would first like to thank my advisors, Martin Styner and Charlotte Boettiger, who challenged, encouraged, and supported me for the past 2.75 years of my PhD. I was in a tough position switching labs and research fields a year into my PhD studies, but joining their labs was the best decision I made in graduate school. Through their mentoring I have developed into the scientist and critical thinker I am today. I am incredibly grateful for their guidance and support.

I would also like to thank my thesis committee, Drs. Kelly Giovanello, J.C. Garbutt, Hongtu Zhu, and Donita Robinson, for their advice, guidance, and honest feedback during the course of my project. I am particularly thankful for my committee chair, Dr. Kelly Giovanello, whose positivity, advice, and belief in my abilities kept me going when times were tough.

In addition to my research committee I would also like to thank my clinical advisors, Drs. Ana Felix, J.C. Garbutt, and Mauricio Castillo, who provided me with the opportunity to see how my research on addiction and memory neuroimaging can translate to the clinic. Every day I spent in Neurology, Psychiatry, or Neuroradiology, the experiences I had and the lessons I learned rejuvenated my excitement about science and research, and the career of a physician scientist. Additionally, I would like to thank Dr. Richard Murrow for his support, mentorship, and intellectually stimulating conversations.

There are so many people that made this project possible. I would not have succeeded in this endeavor without all of you. I would like to thank all of my lab mates in Martin's and Charlotte's labs. Particularly, Aditya Gupta and Francois Budin, my success in the lab is largely due to the time you spent with me over the years teaching me the ways of scripting, how our tools work, and how to fix them when they break. Thank you Amanda Lyall for always keeping me in check anytime I was too stressed out, and for teaching me how to relax. A provider of unwavering support, a big thank you to Ipek Oguz for your friendship, guidance, and words of encouragement. Chris Smith, you are a beam of positivity and I am so grateful to have been in Charlotte's lab with you. Your upbeat attitude always centered me and reminded me that there are big deals and there are little deals; most things are little deals. Thank you to Mihye Ahn for your help and support with FADTTS and statistics on this project. And a HUGE thank you to my two undergraduate students, Nicole Seider and Kirsten Consing, without whom I would have been far less productive. Thank you both for your hard work and partnership.

I came to UNC for the incredibly supportive environment of the UNC MD−PhD program. The program developed and led by Dr. Orringer, Dr. Rathmell, Dr. Deshmuhk, Alison Regan, and Carol Herion, is truly one where all of our students are encouraged to reach their full potential as a scientist, as a doctor, and as an individual. Their support, and the amazing students in our program have made the past 6 years an incredibly fun journey. A special place in my heart is held for my MD−PhD classmates; going through this experience with you all is an honor. You all have taught me how to enjoy life and knowing you all has made me a better person.

I also would like to thank the Neurobiology Curriculum, and in particular Drs. Ann Stuart and Richard Weinberg for your support, critical feedback, insightful conversations, and for always challenging me to better myself.

My friends have kept me going over the years, and they always make sure I remember to laugh and enjoy life. I would particularly like to thank Kate Hacker, Chris O'Conor, Melody Chou, Nick Taylor, Rachel Blasiak, Ryan Gessner, Kari Hacker, Justin Brown, Melissa Gough, Sal Gough, my friends from undergrad, and everyone else who I don't have enough space to list. Also, a special thanks to one of my undergraduate research mentors and close friend, Dr. Darnell Graham. Thank you for always challenging me and supporting me in my goals.

I would not be who I am today without the support of my parents, Rose-Marie and Jeffrey Nelson, and my family. While we had meager means, my parents instilled in me that I could achieve anything I put my mind to with hard work and determination. I am infinitely grateful to them for the support they have given me throughout life, for all of my different goals and passions.

Lastly I would like to thank my wonderful husband, Barrett Green. It has been so hard living apart during my PhD and I so look forward to when you can come home from the Navy. I truly could not have done this without your incredible love, support, and belief in me. Thank you, and I love you very much.

And while they can't read this, I am super thankful for my awesome cats, Karmen and Bollox, who keep me company and make me laugh with their ridiculous personalities and antics.

TABLE OF CONTENTS

LIST OF FIGURES

LIST OF TABLES

LIST OF ABBREVIATIONS

ACC	Anterior cingulate cortex
AD	Axial diffusivity
ANTS	Advanced normalization tools
AUDIT	Alcohol use disorders identification test
BMI	Body mass index
CC	Corpus callosum
CDS	Cigarette dependence scale
CO	Carbon monoxide
COMT	Catechol-O-methyl transferase
CSF	Cerebrospinal fluid

CSV Comma separated values

DA Dopamine

dACC Dorsal anterior cingulate cortex

DAT Dopamine transporter

dlPFC Dorsolateral prefrontal cortex

DSM Diagnostic and statistical manual

DTI Diffusion tensor imaging

DWI Diffusion weighted imaging

EM Episodic memory

FA Fractional anisotropy

FADTTS Functional analysis of diffusion tensor tract statistics

fMRI Functional magnetic resonance imaging

FTND Fagerstrom test for nicotine dependence

GABA	Gamma-aminobutyric acid
GM	Gray matter
GUI	Graphical user interface
IBIS	Infant brain imaging study
IDWI	Isotropic diffusion weighted image
IFG	Inferior frontal gyrus
LDTn	Laterodorsal tegmental nucleus
MD	Mean diffusivity
ml	Milliliters
mm	Millimeters
MNI	Montreal neurological institute
mPFC	Medial prefrontal cortex
MPRAGE	Magnetization prepared rapid acquisition with gradient echo

MRI Magnetic resonance imaging

NA-MIC National alliance for medical image computing

NAc Nucleus accumbens

nAChR Nicotinic acetylcholine receptor

nBM Nucleus basalis of meynert

NITRC The neuroimaging informatics tools and resources clearinghouse

NRT Nicotine replacement therapy

PCC Posterior cingulate cortex

PFC Prefrontal cortex

PHC Parahippocampal cortex

PPn Pedunculopontine nucleus

QC Quality control

RD Radial diffusivity

ROI	Region of interest
sMRI	Structural magnetic resonance imaging
SNP	Single nucleotide polymorphism
SNR	Signal to noise ratio
TBSS	Tract based spatial statistics
UNC	University of North Carolina at Chapel Hill
VBA	Voxel based analysis
VBM	Voxel based morphometry
vlPFC	Ventrolateral prefrontal cortex
VTA	Ventral tegmental area
WM	White matter

CHAPTER 1

INTRODUCTION

1.1 Cigarettes – a global epidemic

This year marks the 50−year anniversary of the first US public health warning from the Surgeon General stating that cigarettes play a causative role in cancer and disease. Since then research has continued to uncover the role cigarettes play in causing disease and death. However, even after half a century of research and public health warnings, one billion people continue to smoke cigarettes worldwide [1]. Cigarettes are the number one preventable cause of death and disease, killing more than five million people worldwide each year [2]. One person dies from a tobacco related disease every six seconds, accounting for one in ten deaths worldwide [1] and one in five deaths in the US [3]. More deaths are caused by cigarettes than alcohol use, illegal drug use, HIV, motor vehicle accidents, murders, and suicides combined [4; 3; 5]. Ultimately, half of smokers will die due to a tobacco related illness [6].

While cigarette smoking has dropped in the US from 42% of adults in 1964 to 18% in 2012, the consumption of tobacco products is increasing worldwide [7; 1]. Tobacco is the only legal drug that the act of consumption affects not only the smoker, but everyone around them. Six hundred thousand deaths each year worldwide are due to second hand smoke exposure alone. At the current increase in use, it is anticipated that tobacco will kill more than a billion people in just the 21st century [1]. It is imperative that we as a global community do something to prevent further people from starting

to smoke cigarettes, and to help those who are currently addicted to quit.

Of those that try cigarettes once, 32% will progress to dependence. This experiment to addiction ratio for cigarettes is higher than that of heroin (23%), cocaine (17%), or alcohol (15%), indicating the habit−forming power of cigarettes [8]. Of current smokers, approximately 70% report wishing to quit and 50% report a past year quit attempt, but only 5% successfully abstain at one year out from their quit date [9; 10]. With the use of available therapies quit success can be raised to 30% [11], however, 95% of smokers will not seek help in their quit attempt. While new, more effective therapies are needed, we also need to begin to understand why currently available therapies are underused. Further understanding the neurobiology of cigarette addiction may help to shed light on both of these pressing issues.

DSM-V
Tobacco Use Disorder
maladaptive pattern of substance use leading to clinically significant impairment or distress, as manifested by 2 (or more) of the following, occurring within a 12-month period: 1. Recurrent substance use resulting in a failure to fulfill major role obligations at work, school, or home 2. Recurrent substance use in situations in which it is physically hazardous 3. Continued substance use despite having persistent or recurrent social or interpersonal problems caused or exacerbated by the effects of the substance 4. Tolerance, as defined by either of the following: a) need for markedly increased amounts of the substance to achieve intoxication or desired effect b) markedly diminished effect with continued use of the same amount of the substance 5. Withdrawal, as manifested by either of the following: a) the characteristic withdrawal syndrome for the substance; b) the same (or a closely related) substance is taken to relieve or avoid withdrawal symptoms 6. The substance is often taken in larger amounts or over a longer period than was intended 7. There is a persistent desire or unsuccessful efforts to cut down or control substance use 8. A great deal of time is spent in activities necessary to obtain the substance, use the substance, or recover from its effects 9. Important social, occupational, or recreational activities are given up or reduced because of substance use 10. The substance use is continued despite knowledge of having a persistent or recurrent physical or psychological problem that is likely to have been caused or exacerbated by the substance 11. Craving or a strong desire or urge to use a specific substance

Table 1.1: Tobacco use disorder diagnosis criteria from the DSM−V. *Adapted from [12]*

1.2 Diagnosis and treatment of cigarette dependence

The extremely low success rate of smoking cessation attempts may in part be due to the fact that cigarettes are both physiologically and psychologically addictive. Physiologic or somatic addiction refers to the development of tolerance and withdrawal symptoms. Psychological addiction refers to changes in behavior characterized by compulsive use of the substance, craving, addiction memory, loss of control, and continuing to use the substance despite negative consequences and the desire to quit [12]. While the physical symptoms of withdrawal will cease after a few weeks, the psychological symptoms of addiction such as craving and addiction memory can last a lifetime. It is this mental aspect of addiction that leads many to relapse.

The diagnosis of cigarette dependence is made using clinical criteria from the newest version of the Diagnosis and Statistical Manual of Mental Disorders (DSM). In the DSM−V, the diagnosis terminology was changed from a two stepped Nicotine Abuse and Nicotine Dependence, to just Tobacco Use Disorder. Further, the criteria for diagnosis were changed to now only require two or more symptoms within the past twelve months from a list of 11 criteria as seen in Table 1.1. Notably, the new criteria list includes craving, as much research has centered on this aspect of cigarette addiction and how it relates to relapse.

Cigarette dependence is a chronic relapsing disorder that often requires multiple quit attempts to succeed [12]. As most cigarette smokers start as teenagers, the majority of successful quit attempts do not occur until age 40 [13]. However, quit rates can improve through the implementation of several available tools for cessation. First, physicians of all specialties can make a significant difference in quit rates by just screening for tobacco use, assessing willingness to quit, and providing information about available resources and therapies that can aid in quitting smoking [14]. Identifying smokers that are considering quitting and providing information on cessation is important, because

the younger a smoker quits the better their health outcomes [15].

However, most smokers who try to quit prefer to attempt cessation cold turkey and do not seek out professional help [10; 9]. Unfortunately, this technique results in a one−year cessation success rate of 5%. Long−term cessation success rates can be improved through physician assistance and the use of available over the counter and prescription therapies [9]. Treatments available consist of informational counseling, cognitive behavioral therapy, nicotine replacement therapy (NRT), and pharmacological agents.

Today there is broad array of ways to start a quit attempt. Resources are available online such as smokefree.gov, and by telephone via quit lines like 1−800−Quit Now that allow patients a way to seek counseling from the safety of their own home [16]. Also, physicians can provide individual or group cognitive behavioral therapy sessions meant to create a community of support, construct a quit plan, and to outline strategies for how to deal with cravings and relapse. While both providing information and formal therapy improve the chance of successfully quitting, the most benefit comes from combining these efforts with one or more pharmacological agents for smoking cessation.

The goal of nicotine replacement therapy is to provide nicotine throughout the day without the use of cigarettes. Through using NRT options, smokers can wean down of their number of cigarettes each day without experiencing the main deterrent of quitting, withdrawal symptoms. NRT comes now in many forms and doses for nicotine: gum, lozenge, patch, nasal spray, and inhaler. The gum, lozenge, and patch provide slow release of nicotine meant to help keep the blood concentration of nicotine at the smokers normal level, while the nasal spray and inhaler are meant to mimic the sharp bolus of nicotine provided by smoking a cigarette. Quit success rates while using one form of NRT doubles the quit success rate to 10%, and the success of cessation rises further

when combining multiple forms of NRT [17; 18]. Effectiveness of NRT options varies though by BMI, number of cigarettes consumed daily, nicotine metabolism, and sex [19; 20; 21; 22; 23].

After NRT, other first line pharmacological agents used for the treatment of cigarette dependence are bupropion and varenicline. Bupropion was first approved for use as an antidepressant and is thought to be a weak inhibitor of dopamine and norepinephrine reuptake, although the true therapeutic mechanism is unknown [24]. It has been shown to be as effective as NRT in aiding smoking cessation [25]. Varenicline is another first line pharmacological agents for the treatment of nicotine dependence that works as a partial agonist for the $\alpha 4\beta 2$ nicotinic acetylcholine receptor [26]. As varenicline binds to the same receptor as does nicotine, varenicline is thought to reduce withdrawal symptoms, and to also reduce the euphoric effect of nicotine by blocking the receptors, preventing nicotine from binding [26]. Of the pharmacological agents available, Varenicline has been found to have the best cessation success rates, and treatment outcome further improves by combining it with NRT [27].

Second line pharmacological agents for smoking cessation are the $\alpha 2$ adrenoreceptor agonist clonidine, and the tricyclic antidepressant nortriptyline. While both medications yielded cessation rates similar to NRT and bupropion respectively, the side effect profile for these two medications makes them rarely prescribed [28; 29]. Other medications investigated for use in treating cigarette dependence but that have had mixed results are naltrexone, fluoxetine, mecamylamine, and monoamine oxidase inhibitors [29; 30; 31].

New efforts have been placed in designing a nicotine vaccine to aid in smoking cessation. The concept behind the vaccine is to create an immune response to nicotine so when vaccinated individuals smoke a cigarette, the nicotine would be bound in the bloodstream, keeping it from reaching the brain, and ultimately preventing the

rewarding effects of smoking. While the vaccine has shown promising results in small trials, stage III clinical trials failed to show efficacy [32]. Further work to improve immune response to the vaccine is ongoing.

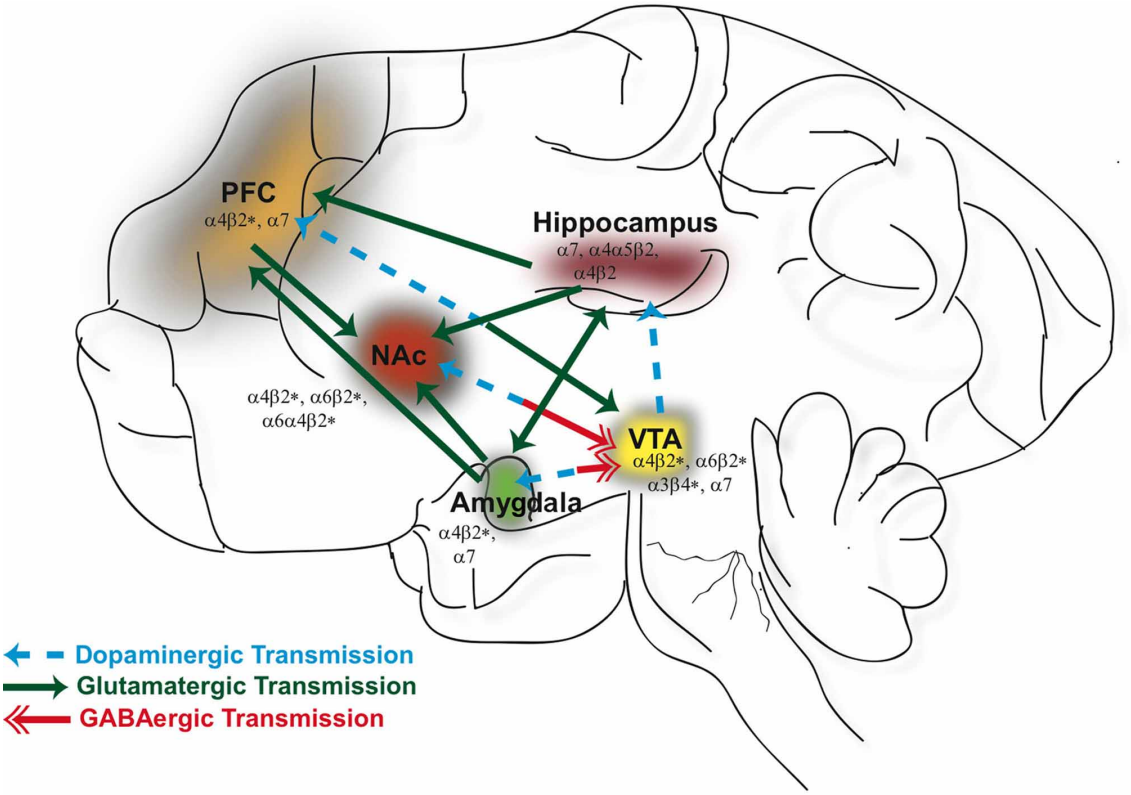

Figure 1.1: Neuronal nicotinic acetylcholine receptors (nAChRs) are widely distributed in different brain regions that include the ventral tegmental area (VTA), nucleus accumbens (NAc), hippocampus, prefrontalcortex (PFC), and amygdala. Activation of nAChRs in these brain areas significantly contribute to the rewarding effects of nicotine and play a role in modulating synaptic plasticity. GABAergic (red), glutamatergic (green), and dopaminergic (blue) connections between these structures constitute a major neural circuitry underlying addictive disorders. *Printed with permission from* © *[33]*

1.3 Neurobiology of cigarette dependence

While cigarette smoke is composed of over 7000 chemicals, the ingredient identified to play the main role in the addictive properties of cigarettes is nicotine. Nicotine

is a volatile alkaloid naturally occurring in the tobacco leaf and other plants of the nightshade family. When the end of a cigarette is lit, the air within the cigarette heats up volatilizing the nicotine from the dried tobacco leaf. As the air is pulled through the cigarette towards the smokers mouth the air cools and condenses the nicotine on to particles of smoke for efficient travel to the lungs. Here nicotines small size and lipophilic nature allows the alkaloid to pass across the alveolar space to enter the blood stream and reach the brain in 15−20 seconds after being inhaled [16].

Once in the brain, the partial agonist nicotine binds acetylcholine receptor subtypes distributed throughout the brain termed nicotinic acetylcholine receptors (nAChRs) [34; 35]. nAChR are ligand gated ion channels composed of hetero or homo pentameric combinations of alpha (α 2−10) and beta (β 2−4) subunits [36; 37]. The most common nAChR in the brain is the high affinity $\alpha 4(3)\beta$ 2(2) heteromeric pentamer, with the next most prevalent being the low affinity $\alpha 7(5)$ homomeric receptor. Receptor subtypes and functions vary by brain region, cell type, location on the cell, type of stimulus, and time course of synaptic events (Figure 1.1). Most nAChRs are located on the soma, perisynaptically, or presynaptically and play a modulatory role in synaptic transmission [38]. When nicotine binds the nAChR alpha subunits there is a conformational change in the receptor subunits that allows for the influx of cations (Na^{2+} and Ca^{2+}) into the cell. This influx of cations causes the cell to depolarize and to fire an action potential, causing the release of neurotransmitter [39].

Important for the rewarding aspects of cigarette smoking, nicotine binds the $\alpha 4\beta 2$ and $\alpha 6$ containing nAChRs on the soma of the dopamine (DA) neurons in the posterior ventral tegmental area (VTA). This causes the VTA DA neurons to release DA in the nucleus accumbens (NAc), prefrontal cortex (PFC), and hippocampus [33]. Further, the pattern of DA release changes from tonic to phasic burst firing, rapidly increasing the concentration of DA in the ventral striatum, PFC, and hippocampus, resulting in

the euphoric and reinforcing aspect of cigarettes, as well as the formation of addiction memory [40; 41; 42; 43].

Regulating this release of DA from the VTA DA neurons are inputs from glutamatergic, gabaergic, and cholingeric cells from other regions of the brain, and within the VTA (Figure 1.2). Within the VTA, nicotine binds the presynaptic $\alpha 4\beta 2$ nAChRs on VTA GABA interneurons and $\alpha 7$ nAChRs on VTA glutamatergic neurons, both of which take part in regulating dopamine release. The VTA DA neurons receive further excitatory glutamatergic inputs from the PFC, NAc, amygdala, bed nucleus of stria terminalis, and pontomesencephalic tegmental area [33]. While the $\alpha 4\beta 2$ receptors quickly desensitize within seconds, the $\alpha 6$ and $\alpha 7$ receptors continue to exert their effect on the VTA DA neurons for minutes, leading to long$-$term plasticity of behavior and reinforcement of the addiction [44; 45; 46].

After a brief activation by nicotine the $\alpha 4\beta 2$ receptors enter a state of desensitization. By continuing to smoke, the continued presence of nicotine keeps these receptors in a desensitized state. This desensitization causes a scenario where the same drag from a cigarette does not cause the expected release of dopamine, and is the physical definition of tolerance. Neurons throughout the brain also respond to this increased desensitization in the presence of nicotine by creating more nAChRs and by modifying their subunit composition [47]. The $\alpha 4(3)\beta 2(2)$ receptors are replaced by $\alpha 4(2)\beta 2(3)$, that have increased sensitivity to nicotine, therefore causing the release of DA at lower concentrations of nicotine, but continuing to increase the desensitization period and thus creating the constant loop of increased tolerance, and physical addiction [48]. At the same time this upregulation of receptors leads to a larger release in DA, the absence of which causes craving during nicotine withdrawal.

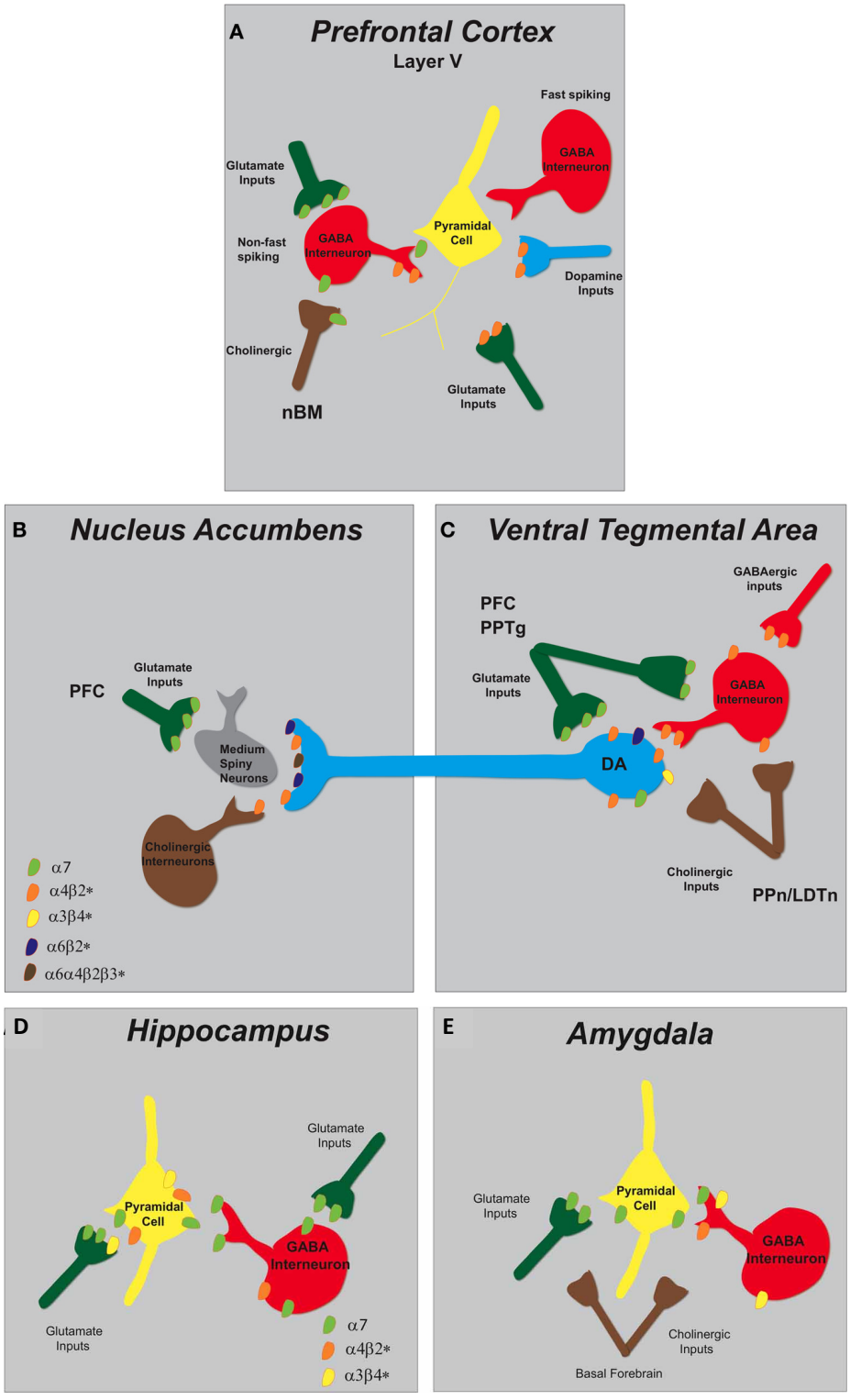

Figure 1.2: Schematic representation of nAChR subtypes for areas important for cigarette dependence. Caption on following page.

1.4 Nicotine's effect − greater than just dopamine release

The presence of nicotine in the brain and body does more than just release DA. The influx of nicotine with each cigarette causes an increase in signaling for multiple other neurotransmitter systems including acetylcholine, glutamate, $\gamma-$aminobutyric acid (GABA), serotonin, norepinephrine, and beta−endorphin (Figure 1.3) [49; 50]. The upregulation of all of these other neurotransmitter systems, along with that of DA combine to make the rewarding and reinforcing properties of cigarette addiction. Further, it is this upregulation and alteration in receptor expression across neurotransmitter systems that creates the physiological and psychological symptoms of withdrawal. These symptoms include agitation, irritability, anxiety, depression, decreased cognition, headaches, hunger, and cigarette craving.

Figure 1.2. Schematic representation of nAChR subtypes for areas important for cigarette dependence A. Pyramidal cell activity in layer V of the PFC is modulated by excitatory and inhibitory neurons expressing nAChRs. Non−fast spiking GABAergic interneurons bear nAChRs ($\alpha7$ and $\alpha4\beta2$). Distinct populations of glutamatergic inputs express either $\alpha7$ or $\alpha4\beta2$ nAChRs while DA terminals projecting from the VTA contain $\alpha4\beta2$ nAChRs. Cholinergic inputs into the PFC arise from the nucleus basalis of Meynert (nBM). B. In the NAc, nAChRs ($\alpha4\beta2$, $\alpha6\beta2$, and $\alpha6\alpha4\beta2$) expressed on DAergic terminals from the VTA mediate DA release based on the neuronal activity firing rate. A small population of tonically active cholinergic interneurons (2%) is synchronized with DA cell firing. Glutamatergic inputs from the PFC endow $\alpha7$ nAChRs. C. The VTA receives cholinergic innervation from the pedunculopontine (PPn) and laterodorsal tegmental nuclei (LDTn). In addition to the nAChRs localized on DA cell bodies, DAergic cell firing is modulated by $\alpha4\beta2$ (and possibly $\alpha7$) nAChRs expressed on GABAergic interneurons and excitatory glutamatergic afferents from the PFC and the PPn. D. In the hippocampus, $\alpha7$ and $\alpha4\beta2$ nAChRs are abundantly expressed on pyramidal cells and inhibitory interneurons. GABAergic interneurons have pre−synaptic $\alpha7$ nAChRs and somato−dendritic expression of $\alpha7$ and $\alpha4\beta2$ nAChRs. Glutamatergic afferents have predominately pre−synaptic $\alpha7$ nAChRs and only low levels of $\alpha3\beta4$. E. In the amygdala, cholinergic inputs from the basal forebrain synapse in proximity to pre−synaptic nAChRs that modulate both excitatory and inhibitory synaptic transmission. Glutamatergic afferents and pyramidal neurons endow $\alpha7$ nAChRs and GABAergic interneurons express multiple nAChRs ($\alpha7$, $\alpha4\beta2$, and $\alpha3\beta4$). *Adapted and printed with permission from [33].*

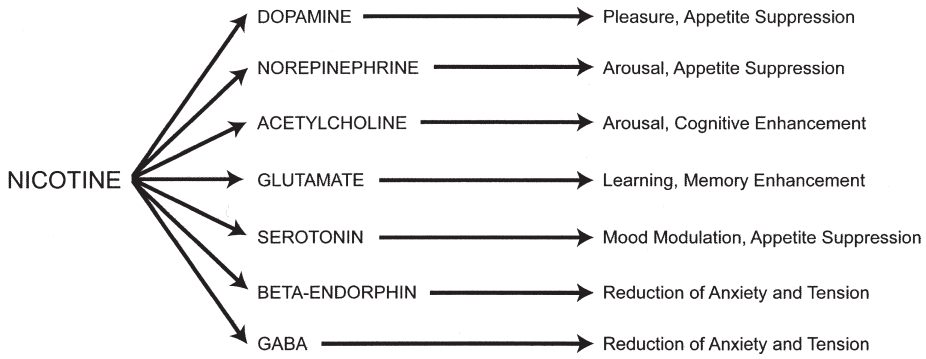

Figure 1.3: Nicotine receptor activation promotes the release of neurotransmitters, which then mediate various effects of nicotine use. GABA = $\gamma-$aminobutyric acid. *Printed with permission from © [49]*

1.5 There is more to cigarettes than nicotine

Most of what we know about the neurobiology of cigarette addiction has come from work in animal models of nicotine addiction, as nicotine is identified as the primary addictive ingredient in cigarettes [49]. However, recently the cigarette dependence research community has stepped back to acknowledge the existence of the 7000 other chemicals in cigarette smoke and that studying just the effect of nicotine on the brain and behavior is not the same as studying the effects of cigarettes on the brain and behavior. To study the effect cigarette smoke has on neurobiology, investigators are turning to the use of actual cigarette smoke in experiments or by creating cigarette smoke extract via the condensation of cigarette smoke into a liquid. This new direction of study is promising, and will help to paint a more realistic and complete understanding of cigarette dependence, and how cigarettes affect brain biology, structure, and function.

1.6 Smoking and Neuroimaging

The study of cigarette dependence using human neuroimaging, however, affords us with the ability to study cigarette addiction in its natural state, examining the addiction to nicotine as well as all other components of cigarette smoke. However, due

to the large comorbidity of cigarette smoking with other human disorders (alcohol use disorders, schizophrenia, depression, etc), imaging literature looking singularly at the effects of cigarette dependence in otherwise healthy individuals is scarce. Of the existing literature in just cigarette smokers, most investigations utilize functional imaging to understand the anatomical underpinnings of craving, attention to smoking cues, memory, cognition, and impulsivity. Studies looking at structural abnormalities in the brains of cigarette smokers using anatomical magnetic resonance imaging (sMRI) or diffusion tensor imaging (DTI) are few, and have been largely limited by the analytical methods employed. Thankfully, due to advancements in image acquisition and analysis techniques, the field is at an exciting time to study the structural abnormalities in the brains of cigarette smokers.

1.7 Measurements of smoking consumption and addiction severity

While most studies are cross sectional, investigators are interested to know if structural or functional differences in the brains of cigarette smokers correlate with total cigarette exposure. There are two main self−report measures used to capture the amount of cigarette exposure consisting of: a reported average number of cigarettes/day and pack years, with pack years generally computed from cigarettes/day and years smoking. In addition to self−report, there are biological measures that can be used to quantify the level of cigarette consumption, including exhaled carbon monoxide (CO) concentration, and urine or saliva levels of cotinine, a metabolite of nicotine. Continine measurements are the most sensitive way to determine the level of recent smoking, however, no truly quantitative rapid measures of continine are currently available, making it difficult to assess smoking status in real time. Exhaled CO provides an easy alternative for measuring smoking within the past 24 hours, with CO having a half life of 3−6 hours [51].

While clinical diagnosis of nicotine dependence is made using a structured interview and DSM criteria, in the lab it is useful to have shorter questionnaires with continuous scales in order to capture a range of addiction severity. In almost all cigarette dependence studies investigators use the Fagerstrom Test for Nicotine Dependence (FTND) [52]. While several other similar measures exist, even some that have been shown to perform superiorly to the FTND, the field continues to use the FTND. This may be in part due to tradition, and in part due to the fact that at this point some 30 years of research has been performed using this test where it has been found to correlate with many important aspects of cigarette addiction. One of the available tests that has been shown to perform better than the FTND on measures of construct and predictive validity is the Cigarette Dependence Scale (CDS) [53; 54]. With the exception of tolerance, the CDS covers the main criteria for ICD−10 and DSM−IV definitions of dependence: withdrawal symptoms, compulsion, loss of control, time allocation, neglect of other activities, and persistence despite harm [55]. We believe the CDS provides a more accurate measurement of cigarette addiction severity and thus it is the measure that we use in this study.

1.8 Measuring behavioral impulsivity – the delay discounting task

One feature of addiction that may play into the cycle of quit attempt and relapse, is that people with addictive disorders, including cigarette dependence, characteristically display impulsive choice behavior [56; 57; 58]. In the lab, one way to measure this impulsive choice behavior is through the use of a delay discounting task. Generically this task is composed of multiple trials where the participant is presented with a choice between two options, a choice of a small reward available immediately or a larger reward available at various delays. Across multiple forms of addiction, those with addiction disorders are far more likely to choose the smaller sooner reward than normal controls.

This impulsive choice behavior holds true for those dependent on cigarettes as well [56; 57; 58]. While this task originated on paper, it has since been modified to work on a computer, as well as for use in a MRI scanner to allow for functional imaging during the task [59].

1.9 The circuitry of episodic memory

Episodic Memory (EM) is the ability to retrieve event−specific information from your life, which is accompanied by a feeling of re−experiencing the event at retrieval [60; 61]. In the lab, EM has been subdivided into distinct event−specific information (e.g. what words were on a list you memorized, what was their location, and did you see a certain word before this other word?) and personally significant (i.e. autobiographical) EM (e.g. what did you wear to your senior prom?) [62]. Outside of the lab, however, recalling episodes from ones past involves specifically autobiographical memory with the associated details, emotions, and rich context [63; 64; 65; 66; 67]. This capacity to re−experience memories from our own past relies upon a rich network of brain regions known as the episodic memory network. The episodic memory circuit includes nodes in the temporal lobe (the hippocampus, parahippocampal cortex (PHC), amygdala, rhinal cortex, temporopolar cortex, lateral temporal cortex), the frontal lobe (medial prefrontal cortex (mPFC), ventrolateral prefrontal cortex (vlPFC), dorsolateral PFC (dlPFC), frontopolar cortex, orbitofrontal cortex (OFC), anterior cingulate cortex (ACC)), the parietal lobe (retrosplenial/posterior cingulate cortex (PCC), inferior parietal lobe, temporoparietal junction), the insula, the occipital cortex, and several subcortical structures (caudate, anterior thalamus, mammillary bodies, cerebellum) [68; 67; 63; 66; 61; 69; 70; 65; 71; 72; 73; 66; 64; 74; 75]. White matter tracts implicated in episodic memory connect these nodes, including the uncinate fasciculus, cingulum bundle, and fornix [73; 76; 77]. Critically, this circuitry is the same as that

needed for episodic prospection [78; 68; 75; 71; 79; 78].

1.10 Imagining future events reduces delay discounting – Implications for cigarette dependence

Two recent studies have shown that episodic prospection (imagining future events) reduces discounting of delayed rewards in healthy control participants via enhanced connectivity between the frontal lobe and mediotemporal regions mediating episodic prospection [80; 81]. As noted above, cigarette smokers have a heightened tendency to discount delayed rewards; however the neural bases of this tendency are not fully understood. Thus, a possible neural mechanism underlying enhanced delay discounting in cigarette smokers is impaired connectivity between frontal regions and the circuitry engaged during episodic prospection. Moreover, behavioral studies have demonstrated that those with cigarette dependence commonly exhibit impaired episodic memory, suggesting possible specific structural deficits in the episodic circuitry [82; 83]. Together, these observations have led us to the following hypothesis:

Hypothesis: Individuals with cigarette dependence show variations in the structural properties of the episodic memory circuitry that correlate with cigarette addiction severity, particularly its connections to frontal elements of decision−making circuits.

We investigated this hypothesis using a novel framework for diffusion tensor imaging (DTI) tractography analysis (Chapter 3), and an established framework for the analysis of cortical and subcortical volumes, and cortical thickness, FreeSurfer (Chapter 4) [84; 85; 86; 87; 88; 89; 90; 91; 92; 93; 94; 95; 96; 97].

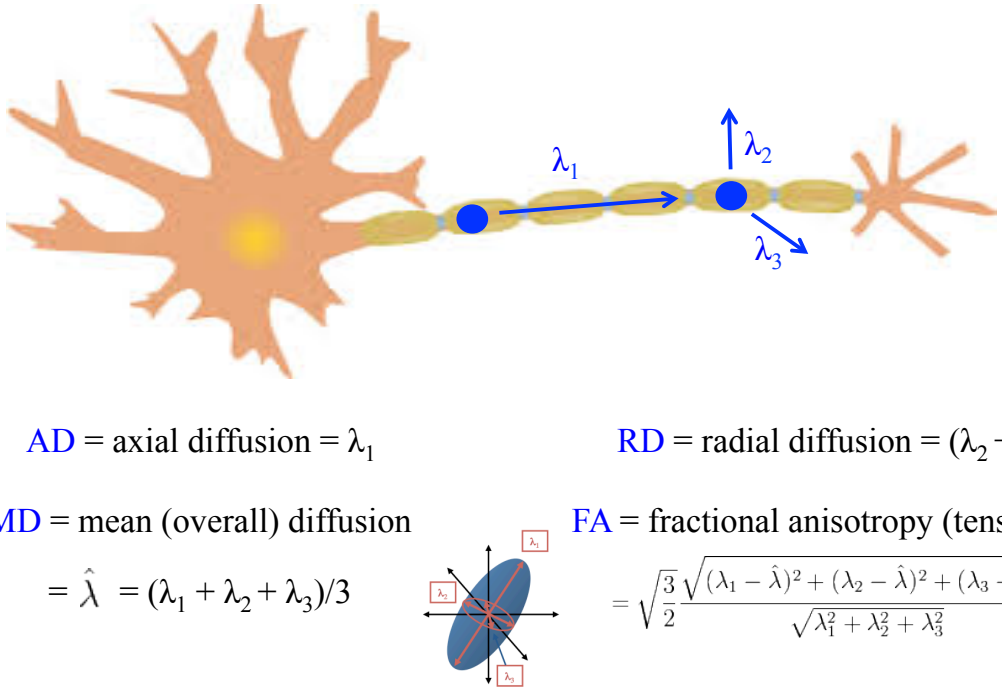

Figure 1.4: Measurements of diffusion used in DTI analysis. Diffusion parameters for DTI analysis are calculated from the first three primary eigenvalues ($\lambda 1$, $\lambda 2$, $\lambda 3$). The top image shows how the three primary eigenvalues would describe diffusion for a single water molecule moving down a neuronal axon. The primary direction of diffusion is defined as the first eigenvalue ($\lambda 1$). A combination of the second and third eigenvalues describe water diffusion orthogonal to the axon ($\lambda 2$, $\lambda 3$). Together, the first three eigenvalues of diffusion are used to compute the fractional anisotropy (FA), which describes the shape of the diffusion tensor (bottom center image). *Adapted and printed with permission from:* `http://www.clker.com/clipart-9828.html`

1.11 Prior neuroimaging findings in smokers within the circuitry implicated in episodic prospection and decision−making

1.11.1 Diffusion Tensor Imaging (DTI)

Diffusion tensor imaging (DTI) is the study of the movement of water molecules, with the assumption that the diffusion of water is restricted by the macro and microstructure of its environment. Thus water molecules located in the lateral ventricle with a large space for diffusion, will likely diffuse by Brownian motion in an isotropic (spherical) manner. However, water molecules located within a fiber bundle or neuronal

axon will have their diffusion limited by the dense macrostructure of many surrounding axons in a white matter tract, as well as the microstructure of myelin surrounding axons, and organelles and microtubules within individual axons making their diffusion described as more anisotropic (linear) in nature. Under these assumptions we can then measure to what degree water diffusion is linear, or the fractional anisotropy (FA), in regions of interest in the brain. Composing the measurement of FA are the measurements of axial, radial, and mean diffusivity. Axial diffusivity (AD) is the primary direction of water diffusion, or the first eigenvalue, and is also described as the diffusion of water that is parallel to the fiber bundle or axon. Radial diffusivity (RD) is the average of the second and third eigenvalues, which describe the magnitude of diffusion orthogonal to the axon or fiber bundle. Mean diffusivity (MD), is then an average of the first three eigenvalues, and describes the overall amount of diffusion. FA combines all three of these other measurements to describe the overall shape of the diffusion tensor (Figure 1.4).

As FA and MD combine multiple measurements into one reading, they are generally considered to be more stable measurements of diffusion and often are the only two reported diffusion parameters in manuscripts. Traditionally FA is taken to represent a measurement of microstructural integrity and/or fiber bundle organization, and is the diffusion parameter of primary interest. However, interpretation of FA is only possible by referring to the diffusion parameters of axial, radial, and mean diffusivity. Changes in radial diffusivity are often seen as alterations in myelin integrity, but can also represent changes in fiber bundle organization. Decreases in axial diffusivity are often interpreted as cell death that has lead to axon degeneration, but again can suggest alterations in fiber bundle organization [98].

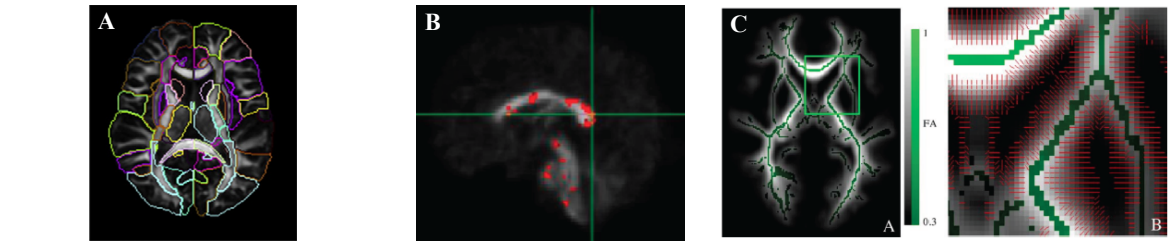

Figure 1.5: Prior methods used for DTI analysis. A. Region of interest (ROI) analysis displayed here with ROIs from the Susumu Mori atlas. DTI analysis performed with large ROIs as displayed here often average the diffusion within the entire ROI for a single measurement, combining readings from multiple white matter tracts into one region, as well as combining together diffusion in white matter and grey matter. This leads to results that are not localizable to a specific tract or a specific region on a tract. *Adapted and printed with permission from [99].* B. Whole brain voxel based analysis used to find single voxels of significance. This method assumes perfect registration on the voxel level between participants, which is often not possible. This method is a great way to generate hypotheses for future studies using a more specific method of analysis. *unpublished figure from our lab.* C. Tract based spatial statistics (TBSS) is a form of voxel based analysis. For this method a white matter skeleton is constructed and the max FA located perpendicularly to the skeleton is assigned to that location on the skeleton. Like ROI analysis, this method also often combines information of multiple white matter tracts into a single measurement. Thus findings are not truly localizable to a single tract. Further, the use of max FA is not a very reliable measurement of diffusion. A weighted average of diffusion in the environment is a better measure of diffusion that protects against outliers and takes into account the neighborhood of diffusion. TBSS does work better than whole brain voxel based analysis, as it does not require absolutely perfect registration. *Adapted and printed with permission from [100].*

Prior investigations of DTI in smoking

To date, little work has investigated the relationship between cigarette smoking and white matter (WM) integrity of the brain using DTI. Of the studies that exist, most utilize voxel wise analysis, TBSS (a form of voxel wise analysis), or large nonspecific regions of interest (ROIs), and do not perform specific along the tract tractography analysis (Figure 1.5) [101; 99; 100; 102]. Thus previously reported DTI findings in smokers are not truly localizable to specific tracts or to exact locations along tracts (Figure 1.5). When comparing smokers to nonsmokers using these DTI analysis techniques, findings have been mixed. While most studies report smokers to have increased FA in regions of the brain compared to nonsmokers [103; 104; 105; 106; 107], others find smokers to have decreased FA [108; 109], or no difference in FA [110; 111]. Likewise there are varying conclusions as to how cigarette consumption and addiction severity relate to WM integrity in smokers. Studies have found a negative correlations [104; 110; 106; 107], positive correlations [103], or no correlation [105; 109] between measures of addiction severity and FA.

There may be several reasons for these discrepancies in findings, one of which is the use of nonspecific voxel wise or ROI−based analyses. With these analytical techniques, single average measurements of diffusion parameters (FA, MD, RD, AD) are used to represent entire fiber bundles, when the regions analyzed may consist of multiple WM tracts, or may contain both white and grey matter. In order to better understand how cigarette smoking addiction affects WM integrity, a more specific and localizable technique needs to be applied.

To address this gap in the literature, we developed a DTI analysis framework (Chapter 2) for along the tract investigation of diffusion in cigarette smokers and non−smokers (Chapter 3).

1.11.2 Structural MRI (sMRI)

Study of structural (anatomical) MRI images aids in determining differences in brain region volumes between smokers and non−smokers. Two forms of methods available for this form of analysis are voxel based morphometry (VBM) and surface based morphometry (FreeSurfer). VBM uses a previously segmented atlas to compute tissue probability maps for each subject in order to segment the brain into white matter, grey matter, and cerebrospinal fluid (CSF). VBM does this segmentation and the following statistical tests on a voxel by voxel basis [112]. Results from VBM are typically reported as either measurements of volume or density.

In addition to segmenting cortical and subcortical brain volumes like VBM, FreeSurfer is also capable of computing cortical thickness and white matter surface area measurements. The publicly available FreeSurfer[1] software assesses bilateral regional cortical and subcortical volumes, and regional cortical thickness [85; 86; 87; 88; 89; 90; 91; 92; 93; 94; 95; 96; 97]. Briefly, this processing includes T1 motion correction [93], removal of non−brain tissue using a hybrid watershed/surface deformation procedure [86], automated Talairach transformation, segmentation of the subcortical white matter and deep gray matter volumetric structures [87; 94], intensity normalization Sled1998, tessellation of the gray matter white matter boundary, automated topology correction [89; 90], and surface deformation following intensity gradients to optimally place the gray/white and gray/cerebrospinal fluid borders at the location where the greatest shift in intensity defines the transition to the other tissue class [85; 91; 92]. Once the cortical models are complete, a number of deformable procedures can be performed for in further data processing and analysis including surface inflation [95], registration to a

[1] `http://surfer.nmr.mgh.harvard.edu/`

spherical atlas which utilized individual cortical folding patterns to match cortical geometry across subjects [96], parcellation of the cerebral cortex into units based on gyral and sulcal structure [97], and creation of a variety of surface based data including maps of curvature and sulcal depth. This method uses both intensity and continuity information from the entire three dimensional MR volume in segmentation and deformation procedures to produce representations of cortical thickness, calculated as the closest distance from the gray/white boundary to the gray/CSF boundary at each vertex on the tessellated surface [92]. The maps are created using spatial intensity gradients across tissue classes and are therefore not simply reliant on absolute signal intensity. The maps produced are not restricted to the voxel resolution of the original data thus are capable of detecting submillimeter differences between groups.

Prior investigations of sMRI in smoking

When compared to nonsmokers, previous studies using these VBM or FreeSurfer found smokers to have decreased grey matter volume and density in the anterior cingulate, prefrontal cortex (PFC), orbital frontal cortex (OFC), frontal cortex, parahippocampal gyrus, temporal lobe, hippocampus, hippocampus subfields, thalamus, substantia nigra, insula, and total brain [113; 114; 110; 115; 116]. These decreases in volume/density in smokers negatively correlated with pack years for the frontal lobe, temporal lobe, left PFC, hippocampus, subiculum, and presubiculum [113; 110; 115]. Decreased cortical thickness was also found in the anterior cingulate cortex, insula, total brain reward system, total frontal cortex, and medial OFC, with the decrease in the OFC cortical thickness correlating with cigarettes per day and pack years [117; 118]. While several studies have investigated cortical and subcortical volumes, cortical thickness evaluation is new to the field and it is of great interest to specifically investigate cortical thickness and volume for the brain regions implicated in episodic prospection

and decision−making. Thus to add to existing literature, we utilized FreeSurfer to investigate the cortical and subcortical volumes, and cortical thickness of brain regions implicated in episodic memory and decision−making (Chapter 4).

Benefits of multi−modal analysis

Using both DTI and sMRI to analyze the same dataset of cigarette smokers and non-smokers allows us to acquire information about the same story from different angles. DTI affords us the knowledge of what is happening to water diffusion in the brain and how these changes may be related to structural alterations in white matter tracts. How diffusion parameters change provides clues as the biology occurring and what may be causing the structural alterations in the WM. sMRI analysis provides information on the brain grey matter. Again, whether it is cortical volume or thickness changing provides information as to the biological process occurring in the tissues. If we had fMRI data, this could further help to complete the picture of what biologically is going on in cigarette smokers. It could help answer whether the structural alterations we see in the WM and GM are correlated with functional changes or behavioral alterations. Each imaging modality provides a different piece of the puzzle with information on the potential biological process that compliments findings from other modalities. The challenge is then taking all of the puzzle pieces and trying to figure out how they all fit together to make the full picture of disease.

CHAPTER 2

UNC–UTAH NA–MIC FRAMEWORK FOR DTI FIBER TRACT ANALYSIS

[1]

2.1 Foreword

Dr. Styner's lab is specialized in creating cutting edge, open source processing and analysis tools for use in the investigation of diffusion tensor images (DTI), anatomical magnetic resonance images (MRI), and MRI shape analysis. When I joined the lab in the summer of 2011 many tools for the processing and analysis of DTI were available in command line format, but were not accessible to investigators without a computer science background. In order to make these tools usable by any researcher that collects DTI data, graphical user interfaces (GUIs) and advanced visualization options had to be created for the existing tools, and new programs were required to make the analysis pipeline seamless. Computer science students and research staff in Dr. Styner's lab set to work coding these new tool interfaces and as they finished testing the tools from a development standpoint, I then assisted in testing them from the viewpoint of a nave user providing design feedback, option ideas to improve usability, and help in

[1]This chapter is modified from Audrey R Verde, Francois Budin, Jean−Baptiste Berger, Aditya Gupta, Mahshid Farzinfar, Adrien Kaiser, Mihye Ahn, Hans J Johnson, Joy Matsui, Heather C Hazlett, Anouja Sharma A, Casey Goodlett, Yundi Shi, Sylvian Gouttard, Clement Vachet, Joseph Piven, Hongtu Zhu, Guido Gerig, Martin A. Styner, *UNC− Utah NA−MIC Framework for DTI Fiber Tract Analysis.*, Frontiers in Neuroinformatics, 2014 Jan 9; 7(51). All previously published material was reprinted with permission from the publishers.

troubleshooting bugs that became apparent in processing.

I helped with the development, testing, and debugging of our DTI analysis framework tools for the first two years of my thesis work. While the Styner lab focuses mostly on neonatal and infant neurodevelopment analysis, my project is the only one to study a disease of adulthood. Thus, since our goal was to create a DTI analysis framework that any investigator could use, regardless of participant group age range, it was to our advantage for me to test our proven infant DTI analysis framework with an adult dataset. Assuring the ability of our tools to be broadly applied in the field of DTI analysis.

However, when it came time to share our framework with the DTI field it was important for us to include a companion dataset as a reference. This would allow new investigators to use our freely available tools to process their data, and to check each of the intermediate steps of analysis to the images provided in the example dataset. In order to provide such a dataset, it required me to process images from a study where the data could be made freely accessible. Unfortunately, my smoking dataset could not fill this role. Thus, we turned to a different study that the Styner lab is involved in, the Infant Brain Imaging Study (IBIS). This is a large, multisite, longitudinal, clinical study of infants and their sibling at high and low risk for autism. Since much of this dataset has already been published on, the images could be uploaded for public access. Thus, we went forward to use this infant dataset to illustrate the power and outputs of our DTI analysis tools. The manuscript describing our framework through the use of this data can be found in Chapter 2, and contains a set of links where all of our tools are accessible for download free of charge. While we are motivated and committed to keeping these tool websites updated with the most current version of programs and to address bugs and/or feature requests, we are not obligated nor supported by the NIH for tool maintenance.

While Chapter 2 illustrates our DTI analysis framework through the use of a neonatal dataset, the programs in our framework were first developed with and tested on my smoking dataset, proving these tools to be powerful analysis techniques for both infant and adult DTI. The resulting analysis of the smoking dataset with our DTI analysis framework is showcased in Chapter 3. Thus with this framework freely accessible at `http://www.nitrc.org/projects/namicdtifiber`, researchers in any field, cigarette smoking or otherwise, have the tools and an example dataset available to them to help in the successful processing and analysis of their own DTI data.

2.2 Introduction

Since its invention in the 1980s diffusion weighted imaging has become increasingly popular for the analysis of brain pathologies and development. It is now standard practice for investigators to collect diffusion weighted images (DWI) concurrently with other modalities of interest without any expertise on how to preprocess or analyze DWI. To address this growing wealth of DWI data, we have created a coherent framework of tools for the pre−processing and analysis of DWI and diffusion tensor images (DTI) that is accessible for the non−technical user. It is the aim of this paper to describe our DTI processing workflow and to provide example data processed with this framework for increased workflow clarity.

Diffusion weighted images (DWI) capture the movement of water molecules. When locally unconstrained, such water molecules move by Brownian motion in an isotropic spherical fashion, for example as is the case within the brain lateral ventricles. However when locally confined, the diffusion of water molecules is constrained by local boundaries, such as cell membranes. Within the human brain white matter, largely composed of neuronal axons, the diffusion of water is more ellipsoid or anisotropic in shape due to the confines of the internal microstructure and the myelin surrounding neuron axons.

Characterizing the properties of diffusion can inform us about the integrity of white matter micro−structure and provides insight on the mechanisms and progression of disease. To date DTI has been used in research to further the understanding of pathology in many neurologic diseases including multiple sclerosis [119], Alzheimer's [120], and Parkinson's [121], as well as normal neurodevelopment [122] and aging [123]. The most common properties measured in DWI/DTI are axial (AD, $\lambda \parallel$), radial (RD, $\lambda \perp$), and mean diffusivity (MD), as well as fractional anisotropy (FA). Axial diffusivity has been shown to decrease in the case of cell death, while radial diffusivity will increase in the case of myelin damage [98]. Alterations in fractional anisotropy reflect changes of AD, RD, and MD and describe the overall pattern of diffusion.

Several analysis frameworks exist for the study of DWI/DTI data, typically falling into one of 3 categories: region of interest (ROI) based analysis, voxel based analysis, and quantitative tractography. ROI driven analysis can be performed by registering individual subject DWI images either to their corresponding anatomical images or by registering the DWI of all individuals to a prior existing atlas. In the first type of ROI analysis, regional segmentations from structural (T1w, T2w) MRIs of the same subject are propagated via linear or deformable co−registration of the structural images to the diffusion image data and mean statistics are collected [101]. However, the structural white matter parcellations are commonly lobar based and thus cannot separate the measurements from different fiber tracts located in the same cortical lobe/region. In the second type of region of interest analysis co−registration with a prior white matter fiber atlas is performed [99]. This type of analysis again requires deformable registration and results in a single measure per fiber region, potentially combining regions that show significantly different fiber situations. The positive aspects of both of these types of region based analysis is that processing is relatively simple and it is robust against imperfect registration. On the other hand, the analysis of large ROIs means

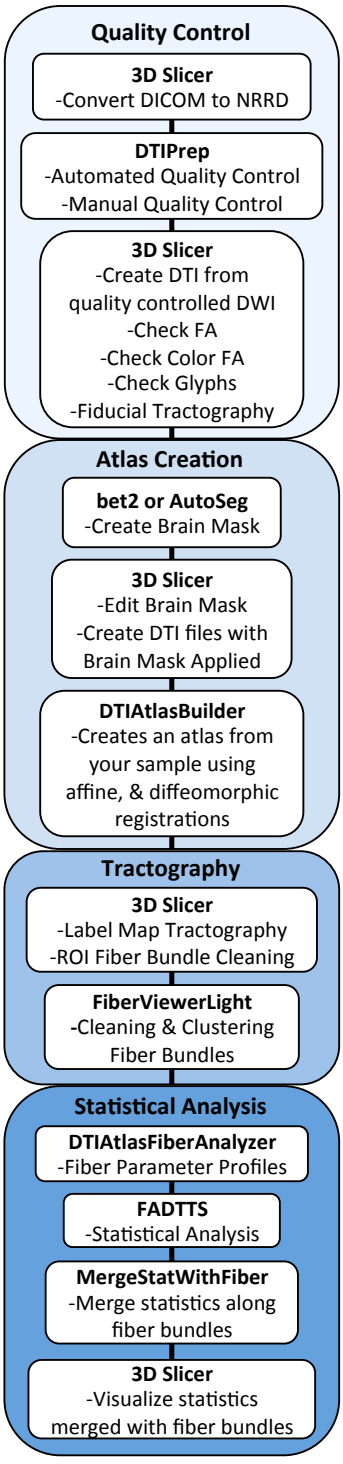

Figure 2.1: UNC−Utah NA−MIC DTI Framework. Step 1 is Quality Control. Step 2 is Atlas Creation. Step 3 is Interactive Tractography. Step 4 is Parameter Profile Creation and Statistical Analysis.

non−specific findings as ROIs can contain multiple fiber tracts and multiple fiber situations (single, fanning, crossing fiber situations). This form of analysis thus leads to limited localization of findings.

Another DTI processing framework is voxel based analysis (VBA). This style of analysis requires registration of each subject into a study specific reference space and then all voxels are tested individually for significance [124]. While this technique allows for whole brain analysis and is suitable for hypothesis generation, this analysis assumes absolutely perfect registration on a voxel by voxel basis and is thus highly sensitive to the deformable co−registration. Another form of voxel based analysis is FSL's Tract Based Spatial Statistics (TBSS). Here a white matter (WM) skeleton is created for the brain, maximal FA values are projected to the WM skeleton, and voxel wise analysis of the skeleton is performed [100]. Due to the projection to the WM skeleton, TBSS is less sensitive to registration accuracy compared to standard VBA. While FSL's TBSS tool provides a coherent framework that works well with imperfect registration, it does not have an explicit tract representation and instead provides a skeletal voxel representation that cannot be uniquely linked to individual fibers throughout the brain. Further, the use of maximal FA values renders TBSS sensitive to DWI artifacts.

Our framework falls into the category of quantitative tractography, where anatomically informed curvilinear regions are used to analyze diffusion at specific locations all along fiber tracts. Diffusion property profiles are computed as weighted averages taking into account the neighborhood at each step along the fiber bundles [125]. This form of analysis results in highly localized statistics that can be visualized back on the individual fiber bundles.

In this paper, we propose the use of our 3D Slicer based UNC−Utah NA−MIC DTI framework for a coherent atlas fiber tract based DTI analysis. Most steps of the framework utilize graphical user interfaces (GUI) to simplify interaction and provide

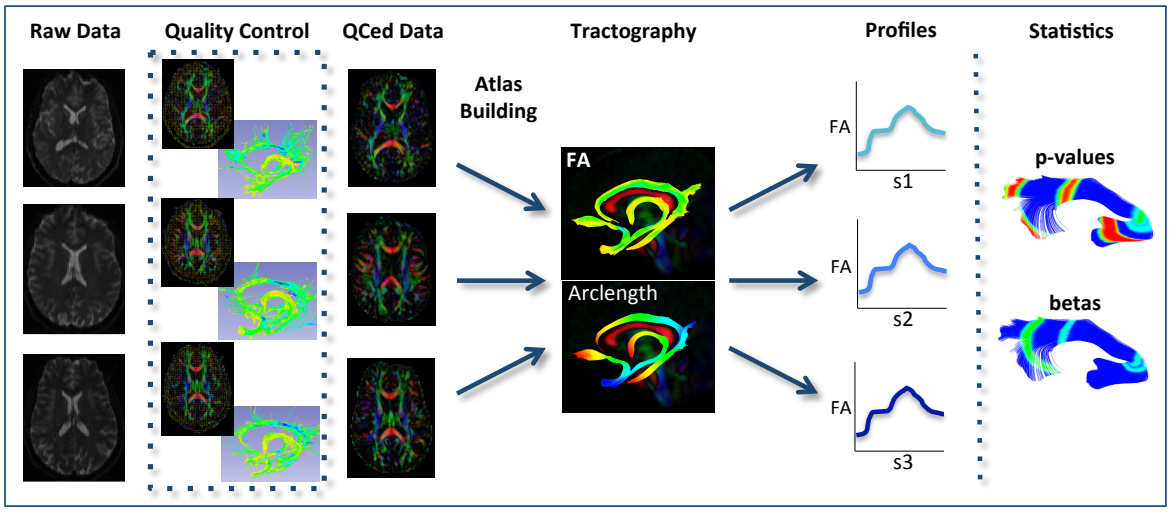

Figure 2.2: Schematic of DTI processing workflow. The input raw DWI data first undergoes vigorous quality control before the final conversion to DTI for Atlas Building. Interactive tractography is performed on the Atlas. From these fiber bundles, diffusion parameter profiles are extracted and analyzed along with other study variables to determine significant correlations.

accessibility for non−technical researchers. At the heart of the framework is a set of tools anchored around the multi−purpose image analysis platform 3D−Slicer. Several workflow steps are handled via external modules called from Slicer in order to provide an integrated approach. Our workflow starts with data conversion from DICOM format, followed by an automatic as well as interactive DWI and DTI quality control (QC) steps. Though under appreciated in the field, appropriate and thorough QC is a must for every DTI study. Our framework then centers around a DTI atlas that is either provided as a prior template or computed directly as an unbiased average atlas from the study data via deformable atlas building [125]. Fiber tracts are defined via interactive label map tractography on that atlas followed by consecutive interactive fiber cleaning steps. Individual subject DTI fiber tract profiles of FA, MD, RD, and AD are extracted automatically using the atlas mapping information. These fiber tract profiles are then analyzed using our statistics toolbox (FADTTS) [126]. The local statistical results are then mapped back on to the fiber bundles for visualization within 3D Slicer [127].

This framework has been developed over several years and we continuously improve the current toolset. Within the past year we have added entropy−based detection of vibration artifacts as part of the automatic QC and an interactive atlas building tool called DTIAtlasBuilder. All tools that are part of the UNC−Utah NA−MIC DTI framework are open source and available on NITRC, providing the neuroimaging field with a transparent and coherent toolset for DTI fiber tract based analysis.

We illustrate the use of our framework on a small sample, cross sectional neuroimaging study of 8 healthy 1 year old children from the Infant Brain Imaging Study (IBIS) Network (`http://www.ibisnetwork.org/UNC`). In this paper, we demonstrate our method by quantifying the diffusion properties within the genu and splenium fiber tracts. The corresponding raw data, intermediate files, and final results for data presented in this manuscript have been made freely available on NITRC.

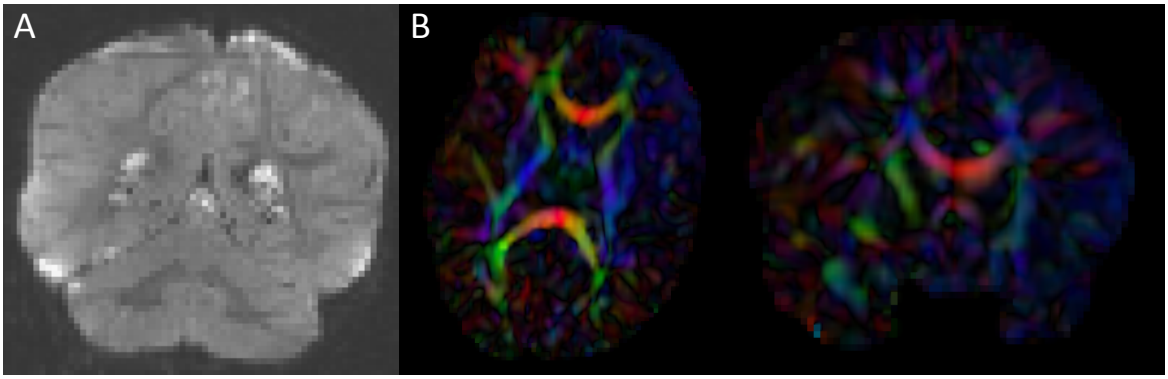

Figure 2.3: Artifacts encountered during quality control. A.) DWI artifact missed by automatic quality control run of DTIPrep, but caught in the visual quality control. You can see the horizontal lines running through this coronal view of the brain. Towards the top, almost an entire slice is missing. In cases like this, the gradient containing this artifact would be excluded from the saved DWI volume. B.) Axial and coronal view of DTI color FA volume. The large area of blue in the left frontal and temporal lobes indicates that a dominant direction artifact remains after DTIPrep quality control. Thus this artifact was too large to correct and this participant was excluded from analysis.

2.3 Material and Methods

Our framework for the fiber tract based analysis of DTI images is composed of four essential segments: 1. Quality Control, 2. Atlas Creation, 3. Interactive Tractography, and 4. Statistical Analysis. The tool workflow can be seen in Figure 2.1 and an overall conceptual schematic of the process is displayed in Figure 2.2. All of the tools referenced in the description of our workflow can be utilized as stand−alone command line applications to facilitate scripting and grid computing, or interactively as part of 3D Slicer as external modules. While the first segment of our framework is termed Quality Control (QC), it is critical to perform quality assessment of the processing at every step in the framework to ensure the data that is analyzed is correct.

2.3.1 DWI and DTI Quality Control

DWI Quality Control – DTIPrep

Analysis starts by converting the raw diffusion weighted images (DWI) from DICOM to NRRD format using a tool called DicomToNrrdConverter in 3D Slicer. This tool is capable of computing diffusion weighted images via the b−matrix information stored in Siemens DICOM headers, as well as recognizing many other manufacturer specific tags. A tool called DTIPrep [102] is then used to check for and correct several common artifacts found in DWI. In summary, DTIPrep performs image information checking, slice−wise artifact detection, creates a baseline average, corrects for subject motion and eddy current induced deformations, and finally detects dominant direction artifacts [128]. To carry out the automatic QC a protocol must be created that contains all parameters of the DTIPrep QC. Protocols are fully modifiable for individual studies and include a significant number of parameters for every step. DTIPrep gives the option of creating a default protocol from a given scan. On completion of the automatic QC it is further advised to perform additional visual quality control. Here artifacts that

may be missed by the automatic QC step can be detected and gradients still containing artifacts or motion can be excluded from the final DWI (Fig 3A). After visual quality control, the DTI tensor and property images are then automatically estimated from the DWI data via the dtiestim and dtiprocess modules.

DTI Quality Control – 3D Slicer

In addition to checking the DWIs for artifacts, the resulting DTI must also undergo visual quality control using 3D Slicer. This QC step is to ensure the correct directional encoding, sufficient signal−to−noise (SNR) in the FA data, and to test the overall quality of the data by performing landmark−based/fiducial tractography.

Visual DTI QC begins by loading the FA image and scrolling through the slices for each plane (axial, sagittal, coronal) to assess the apparent level of SNR for the volume. Next, the DTI volume is analyzed to determine if the header information encoding directionality for the volume is correct. The DTI image is colored by tract direction with tracts moving right to left colored red, tracts moving anterior to posterior colored green, and tracts moving inferior to superior colored blue. The corpus callosum should appear red, the cingulum green and the corticospinal tract should be blue. Also special attention is directed to detect dominant directional artifacts if low FA regions (such as the gray matter) display a single color throughout most of the DTI image, as seen in Figure 2.3B. Visualization of the primary direction via line glyphs is the next step to ensure the correctness of the diffusion measurement frame. Glyphs should follow the direction of the main fiber tracts. If the glyphs are incorrect (due to incorrect DICOM information or scanner software malfunction), then the corrected measurement frame must be determined and edited in the volume header.

Once the header information is confirmed to be correct for the volume, fiducial based

tractography will provide information whether tractography is feasible, and anatomically accurate. Fiducial tractography is commonly performed for the major fiber tracts (corpus callosum (CC) genu and splenium, cingulum, and corticospinal tract) as well as any tracts of particular interest for the neuroimaging study at hand. In the resulting fiber tracts, it is important to observe a) sufficient quantity of fibers delineating a fiber tract, b) whether fibers completely track between the expected terminal regions, and whether the fiber location is anatomically accurate throughout the length of the fiber tract. If artifacts remain in the volume, then fibers may break prematurely, appear warped or incorrectly localized, or if the data has a very low SNR the fiber bundles of interest may be impossible to track. If tracking is not feasible or anatomically incorrect, then exclusion of this dataset is suggested.

2.3.2 Atlas Building

Brain Mask Creation, Editing and Application – bet2/AutoSeg

The first step in atlas building is to extract out the brain regions for each DTI image. To do this, a brain mask must be computed, edited, and applied to the DWIs in order to create a skull−stripped DTI. Many tools are available for brain mask creation, such as the Brain Mask from DWI module in 3D Slicer, bet2 within DTIPrep, or a tissue segmentation based approach in AutoSeg [129]. Brain mask creation by bet2 can be computed using the baseline image or the IDWI (isotropic DWI), while both are used jointly to compute the brain mask with AutoSeg. Mask editing is performed also within 3D Slicer, but any editing tools with Slicer compatible format (NRRD, Nifti, GIPL, Analyze) can be employed such as itk−SNAP [130]. The edited brain mask can then be applied to the DWIs, creating a skull stripped DTI (referred to as Original DTI in this paper) ready for atlas building.

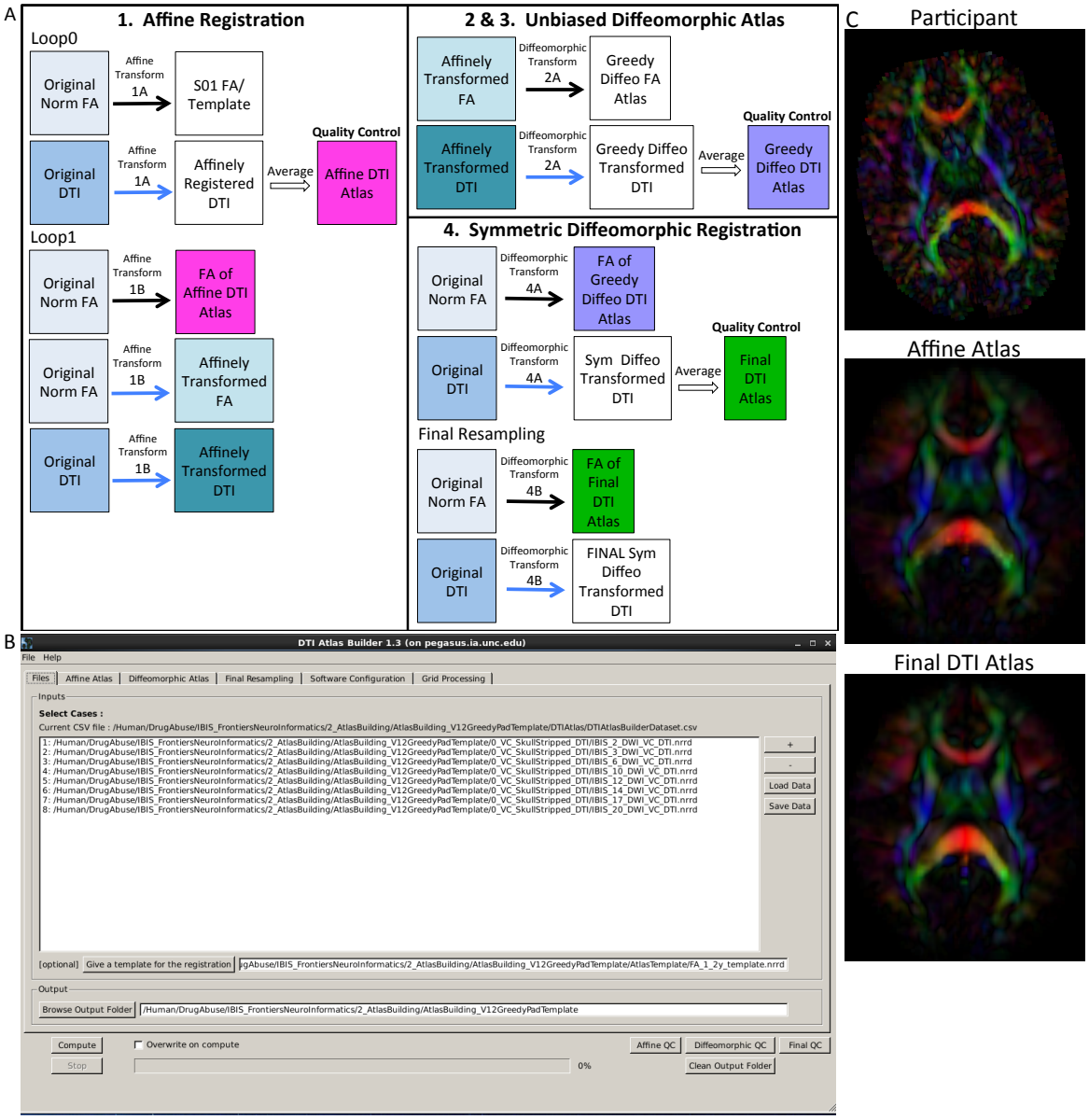

Figure 2.4: DTIAtlasBuilder steps, GUI, and registration progression. Caption on following page.

Atlas Creation – DTIAtlasBuilder

The main atlas building step is performed with a tool called DTIAtlasBuilder, detailed in Figure 2.4. This program allows the user to create an atlas image as an unbiased average of all co−registered DTI images in the study. Atlases are created iteratively starting from affine atlases (step 1) and moving to deformable diffeomorphic atlases (step 2, 3, and 4). The registration is done in three steps: 1) affine registration with the Slicer General Registration module (called BRAINSFit) [131], 2) unbiased diffeomorphic atlas computation [132] with the GreedyAtlas module within AtlasWerks [132], and 3) a refinement step via symmetric diffeomorphic registration with the Slicer DTI registration module DTI−Reg using the Advanced Normalization Tools (ANTS) [133; 134]. The final, refinement step significantly improves registration accuracy in our experience, most likely attributable to the use of local normalized cross−correlation as the image similarity metric. A final step will combine multiple transforms to compute the overall transformation (GlobalDisplacementFields) from the original DTI images to the Final DTI Atlas. This final transform is required for the analysis of fiber tract properties in the individual subject space.

Figure 2.4. DTIAtlasBuilder steps, GUI, and registration progression. A.) DTIAtlasBuilder steps. Black solid arrows indicate transform computation. Blue solid arrows indicate transform application. Hollow black arrows indicate an averaging of transformed images. Before the Affine registration in step 1, FA is normalized so that FA intensity difference between subject images does not bias the atlas creation. The FA is also filtered to remove negative eigenvalues, which will adjust the resulting FA values to scale between zero and one. The transform computed in step 4 Final Resampling, Diffeomorphic Transform 4B, is termed the Final (or Global) Displacement Field. It is this transform that is required to extract fiber tract profiles from each individual subject DTI when using DTIAtlasFiberAnalyzer later in the workflow. B.) DTIAtlasBuilder GUI. Here one can see the first tab with the input list of quality controlled and skull−stripped DTI volumes. Along the top of the GUI, the tabs for adjusting parameters and tool paths are visible. C.) Progression of the atlas building from a single participant volume to the affine atlas, and the final unbiased diffeomorphically registered DTI Atlas in the presented experimental pediatric population.

In the first step, DTIAtlasBuilder will generate scalar FA images from the skull stripped DTIs. The affine atlas building starts by registering subject images to a pre−exiting FA template in MNI−normative space or to the first subject in case no prior template is specified. In order to avoid biasing the subsequent analysis, the image intensities are calibrated with the templates intensities using standard histogram quantile normalization available in ITK. The affine transforms are applied to the original DTIs and the transformed images are averaged to create the Affine DTI Atlas (see Figure 2.4A,B). Each images affine transform is then updated by recomputing the affine registration in a second loop to the Affine DTI Atlas (rather than to the initial template as in the first loop). This transform, Affine Transform 1B, is then applied to the original DTI to create affinely co−registered DTIs for each subject.

In the second step of atlas building, the unbiased diffeomorphic atlas is computed from the affinely registered FAs via diffeomorphic, fluid flow based atlas building. This results in deformation fields from the affine space to the unbiased atlas space. These deformation fields are then applied to the affinely registered DTIs and the transformed images are averaged to create a Greedy Diffeomorphic DTI Atlas (Figure 2.4A).

The last stage of atlas building utilizes DTI−Reg to refine the diffeomorphic registration computed in the previous step. To start, FA images from the original subject DTIs are histogram normalized to the Greedy Diffeomorphic FA Atlas, and then diffeomorphically registered to it. The resulting deformation fields are then applied to the original subject DTI and the resulting diffeomorphically registered DTIs are averaged to create the Final DTI Atlas. The deformation fields are then updated with another loop of registrations with DTI−Reg in order to co−register the images with the Final DTI Atlas (rather than with the Greedy Diffeomorphic FA Atlas as in the first loop). The overall Global Displacement Fields are finally computed by composing the affine transform from step 1, as well as the affine and deformation transform from this last

step. These displacement fields will be used to map the fiber tracts created in atlas space to the individual subject spaces for analysis. The final atlas co−registered DTI images are computed by applying these final deformations fields. It is noteworthy that this deformation of the DTI images is unlike the processing in TBSS/FSL, where FA images are deformed. Furthermore, all DTI image interpolations are performed using standard Log Euclidean based resampling [135].

With the atlas building complete, it is important to perform quality control on the Affine, Greedy Diffeomorphic, and Final DTI Atlases, simply accessible with a single button within DTIAtlasBuilder. In this quality control step we can visually determine the point to point correspondence between the subject images and the atlas to determine if computed registration transforms are appropriate. The progression of atlas sharpness can be seen in Figure 2.4C.

Software path configuration for the tool can be performed automatically or manually, and the settings can be saved for future use. This tool also has a no GUI/command line option, given that the data file, parameter file, and software configuration file are available (all can be determined and saved via the GUI). There is also direct support for the GRID software LSF (Load Sharing Facility, Platform Computing, Inc).

2.3.3 Tractography

Label Map Single Tensor Tractography − 3D Slicer

While atlas building is fully automatic, the definition of fiber tracts of interest needs to be performed interactively. Fiber tractography only needs to be performed once on the Final DTI Atlas built in the prior step. In our framework, fiber tractography is performed via the label map tractography module or the full brain tractography module within 3D Slicer. If using label map tractography, each fiber tract has a separate anatomically informed label created in the editor module and is tracked individually

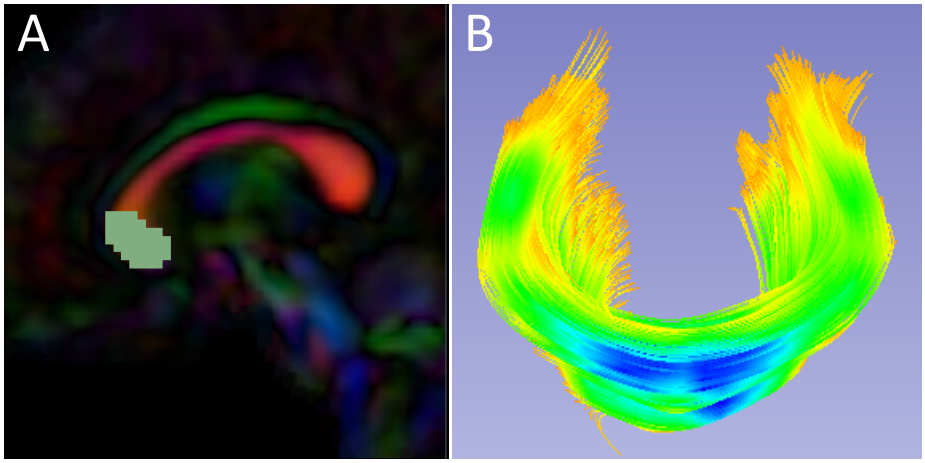

Figure 2.5: Slicer label map tractography. A.) Sagittal view of the corpus callosum genu label map in the Final DTI Atlas. B.) Resulting genu bundle fibers from label map tractography within 3D Slicer. The bundle is colored by FA values along the fibers with cooler colors indicating higher FA.

(Figure 2.5). Alternative fiber tracking tools can be employed as long as the resulting fibers are stored in standardized vtk−based file format. Resulting DTI fiber bundles require post−processing via ROIs to remove unwanted, erroneous fibers.

Coarse fiber bundle editing with ROIs – 3D Slicer

The results of label map tractography may contain fibers in addition to the fiber bundle of interest. Coarse cleaning is performed with interactive 3D regions of interest (ROIs) in 3D Slicers tractography display module. Here fibers to be kept or removed are selected using ROIs iteratively. ROIs should also be utilized for separating tracts that run within the left and right hemispheres in order to allow separate analysis of the right and left portions (for example the left and right hemispheric portions of the fornix).

Fine fiber bundle editing – FiberViewerLight

Fiber tracts often need additional, finer editing via clustering and cleaning within FiberViewerLight. Fiber length based cleaning and several fiber clustering algorithms

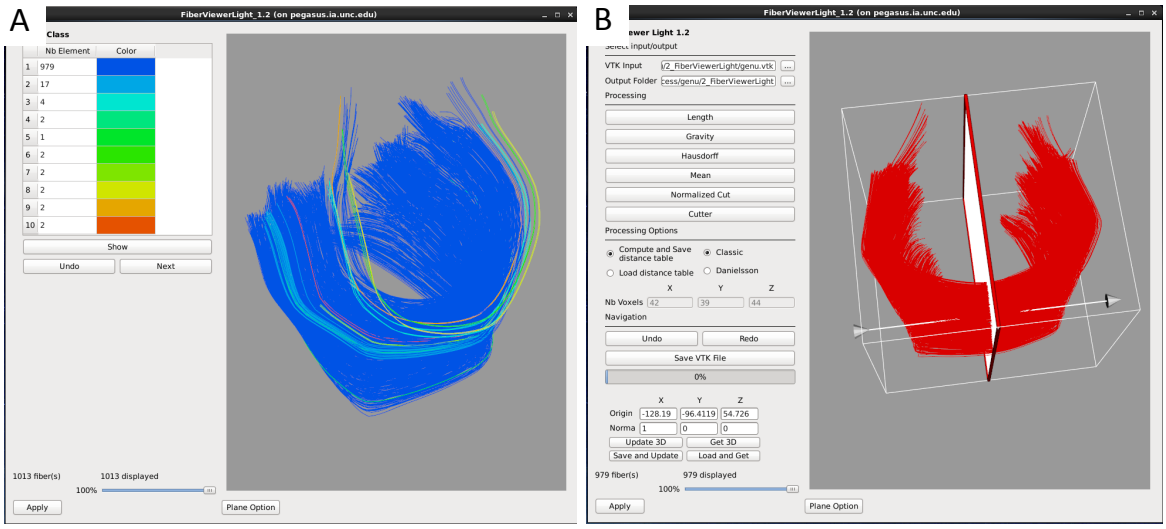

Figure 2.6: FiberViewerLight clustering, cleaning, and plane creation. A.) Example of genu fiber clustering based on the center of gravity. B.) In the left panel all of the fiber clustering algorithms are visible, as well as the different styles of computation (Classic vs Danielsson). In the right panel the plane function is visualized for the genu. This tool is used to set a plane of origin from which the fiber bundle will be parameterized for further analysis.

(center of gravity, Hausdorff distance, mean distance, normalized cut) to further delineate which fibers belong in the bundle of interest and which ones do not (Figure 2.6). The decision for inclusion or exclusion is based on expected fiber tract anatomy. Once fiber bundles are deemed appropriate, diffusion property profiles for each fiber tract and subject image are extracted as described in the next section.

2.3.4 Property profiles and statistical analysis

Diffusion Property Profiles – DTIAtlasFiberAnalyzer

As a final step prior to statistical analysis, diffusion properties along the fiber tracts, called fiber property profiles, are extracted. For that purpose, a fiber tract parameterization needs to be established, which is achieved via arclength parameterization [136] starting from each fibers intersection with an origin plane. While DTIAtlasFiberAnalyzer automatically determines an appropriate origin plane, investigators can choose

to interactively determine that plane in order to associate a specific anatomical fiber location to this origin within FiberViewerLight (see Figure 2.6B).

The parameter profile generation and processing is performed with a tool called DTIAtlasFiberAnalyzer, shown in Figure 2.7. The profile extraction operates on the original DTI data in order to avoid the need for tensor deformation by deforming the parameterized fibers into original space via the previously computed Global Deformation Field. At the deformed fiber locations the tool can then calculate the different fiber property profiles along each fiber in the bundle (FA, RD, AD, MD, GA, Fro, $\lambda 2$, and $\lambda 3$) in subject space. Figure 2.7B shows example FA profiles of the genu calculated and visualized with DTIAtlasFiberAnalyzer for this study. Visualization of these fiber property profiles for each subject versus the fiber bundle in atlas space allows an alternative assessment of the registration quality to atlas space (Figure 2.7B). Inspecting the atlas fiber bundle parameterization is an additional quality control step to confirm correct parameterization (Figure 2.7C). An error in parameterization usually requires a change in origin plane to correct the problem.

The fiber property profiles are the input for the analysis tool called Functional Analysis of Diffusion Tensor Tract Statistics (FADTTS) [126] that performs statistical analysis on the fiber bundle profiles. This tool has the ability to compute group difference and correlational analyses (Figure 2.8). Currently the FADTTS tool is Matlab (MathWorks Inc, MA) based, and requires a user familiar to Matlab to operate. The Matlab scripts used to analyze the data for this paper are available with the sample data at www.nitrc.org.

Statistical Analysis of Diffusion Properties Along the Fiber Tract – FADTTS

Using the diffusion profiles obtained from DTIAtlasFiberAnalyzer, it is possible to test how these diffusion properties relate to other variables of interest within the sample

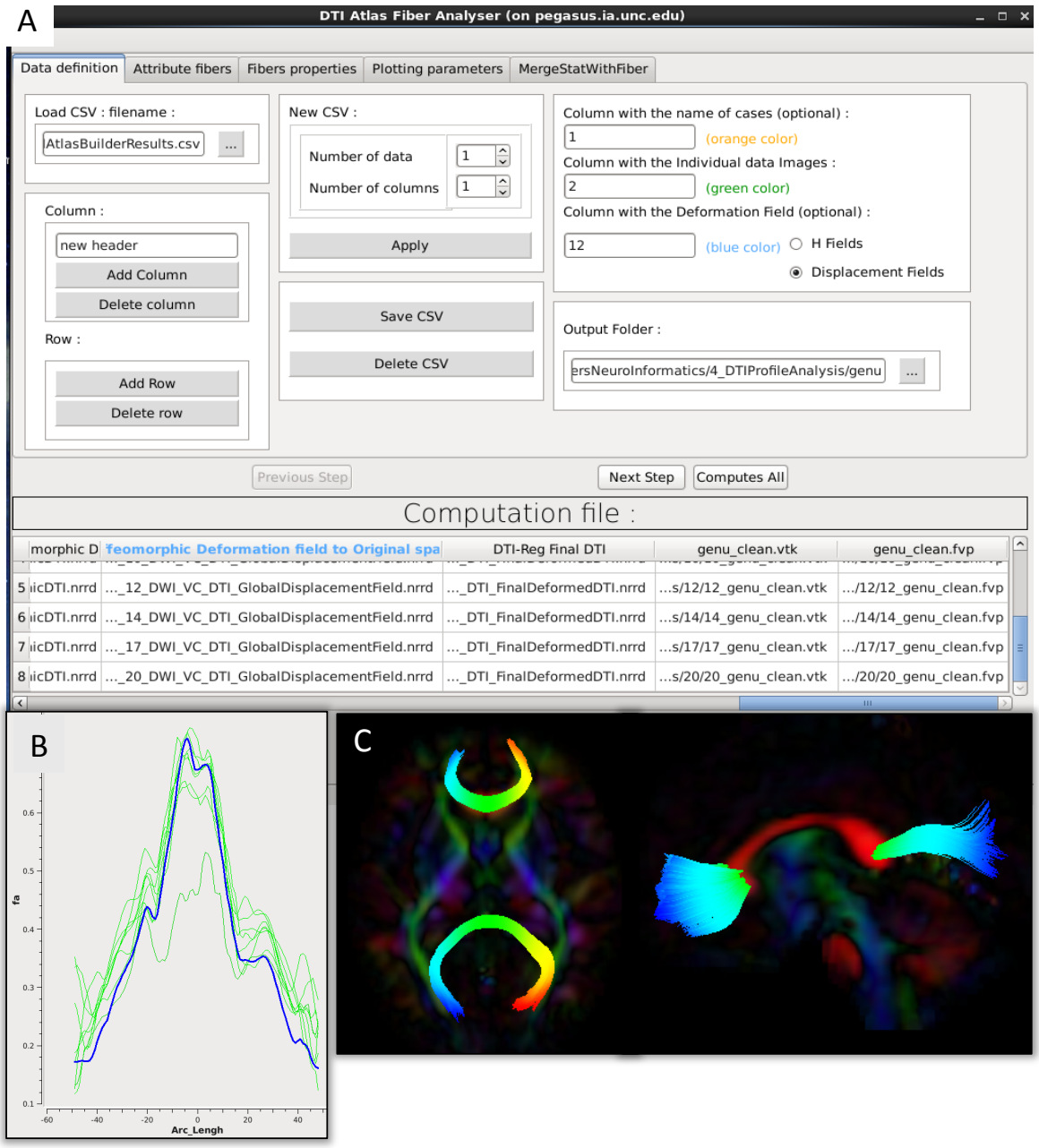

Figure 2.7: DTIAtlasFiberAnalyzer GUI. Caption on following page.

data. FADTTS performs several statistics tests including a multi−variate coefficient model, weighted least squares estimation, and functional principal component analysis. These tests produce both global and local test statistics with confidence bands and the local values are corrected for multiple comparisons with false discovery rate (FDR). Several statistical plots are commonly created, a sample of which can be seen in Figure 2.8. From the beta plots, the direction, magnitude, and significance of the relationship of interest can be assessed by the beta sign, distance from zero, and the significance marker (a filled circle) on the curve respectively (Figure 2.8C,D).

Mapping covariate p−values on fiber bundles for visualization – MergeStatWithFiber

Upon computation of test statistics with FADTTS, the statistics can be mapped to their corresponding location on the fiber bundle using a tool called MergeStatWithFiber. The input for MergeStatWithFiber is the comma−separate−value (csv) file resulting from FADTTS with the addition of arclength as the first column, and a header row containing column labels. The result of this merge is then visualized in 3D Slicer (Figure 2.8E). The color map shown is determined by the significance threshold set in MergeStatWithFiber, as such that all points on the fiber that have a p−value above

Figure 2.7. DTIAtlasFiberAnalyzer GUI. A.) In the first tab of this tool the input data is defined: the label for each participant, the original quality controlled skull−stripped DTI, and the GlobalDeformationField computed in Atlas Building. B.) After DTIAtlasFiberAnalyzer has sampled the intended diffusion parameters, DTI property profiles for individual images (green) and the DTI atlas (blue) can be visualized in the Plot Parameters tab. Inspecting these profiles allows for a different type of quality control of the atlas registrations. The FA profiles of the subjects (pictured here) should be similarly shaped to the atlas. C.) Visualization of the parameterized genu and splenium fibers in the axial and sagittal views. Fibers that have been correctly parameterized with DTIAtlasFIberAnalyzer via the origin plane will be colored by FiberLocationIndex (arclength) from red to blue. Red indicates low arclength and blue high arclengths. The corresponding profile plots of these genu and splenium fibers would run from the right to the left hemisphere.

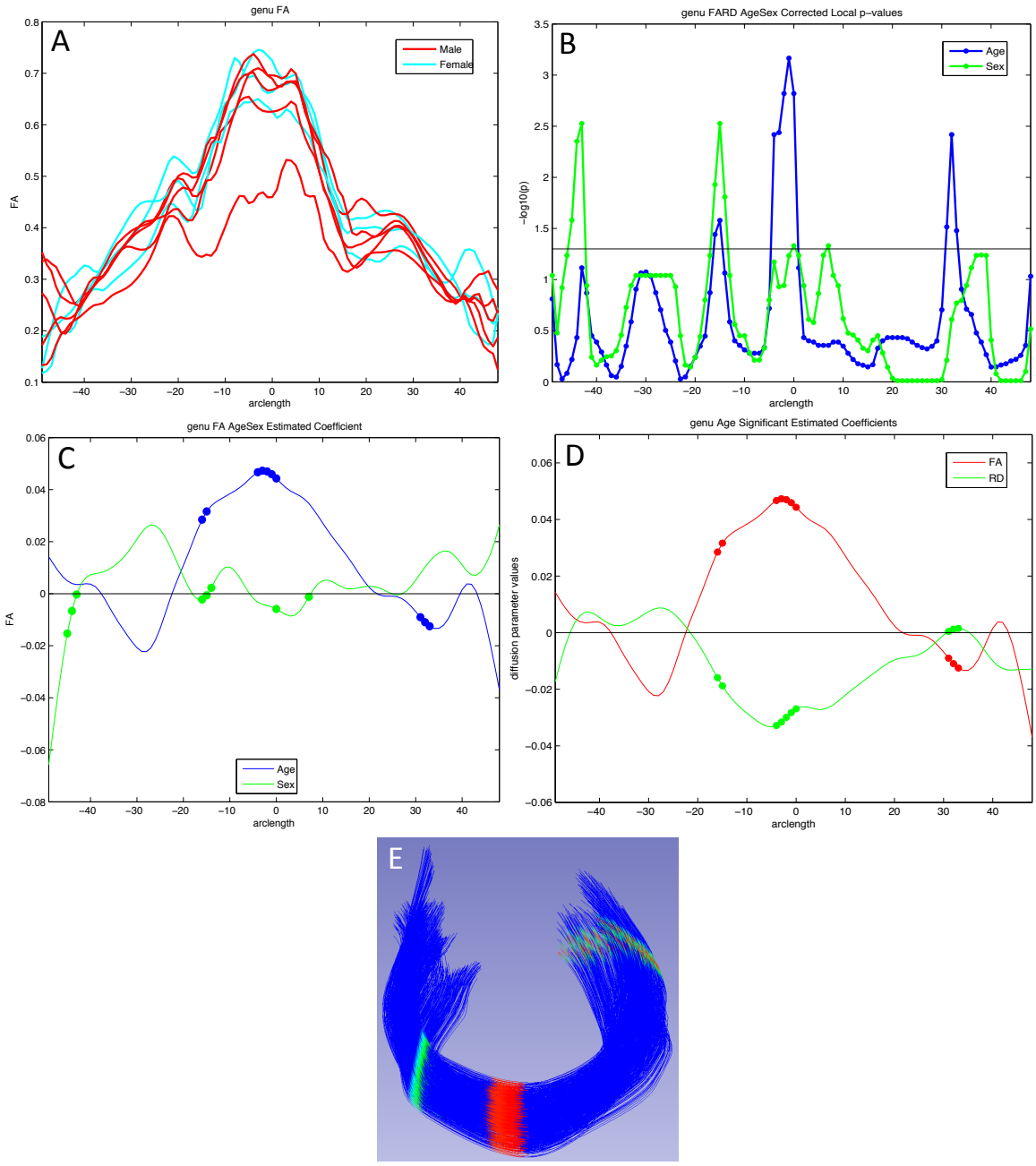

Figure 2.8: Examples of possible plots from Functional Analysis of Diffusion Tensor Tract Statistics (FADTTS) and MergeStatWithFiber. Caption on following page.

the significance threshold are colored blue, and all points with values below the significance threshold are colored from cyan to red, with points indicated in red signifying the areas of greatest significance. If desired, this color map can be altered within Slicer to another color table. MergeStatWithFiber can be used as a command line tool or through the final tab in the DTIAtalsFiberAnalyzer GUI (Figure 2.7).

2.4 Results

For our example data we created an unbiased diffeomorphic atlas with eight 12 month old IBIS participant scans, and performed interactive tractography of the genu and splenium on this atlas. Diffusion parameter profiles were created for these two fiber bundles and these profiles were further analyzed with FADTTS. While each of the participants were categorized as 12 month olds for the IBIS study, the correlation between a subjects actual age in months (ranging from 11.8 to 14.5 months) and the DTI properties was analyzed to illustrate the use of our tools. On the genu, 3 areas showed significant correlation between Age and FA, but no areas of significant correlation were found on the splenium (data not shown). Figure 2.8C shows the graphical output of this result from FADTTS in the blue line for Age with the filled in circles indicating

---

Figure 2.8. Examples of possible plots from Functional Analysis of Diffusion Tensor Tract Statistics (FADTTS) and MergeStatWithFiber. A.) Plot the raw data. B.) Output of FDR corrected local log p−values along the length of the fiber tract. C.) Separate beta plots for all of the covariates entered into the model and how they correlate with each diffusion parameter. D.) Separate beta plots for how all the investigated diffusion parameters correlate with each covariate in the model. For both beta plots, the filled in circles along the curves indicate areas of significance post FDR correction. E.) Visualization of local statistics along the tract with 3D Slicer. Specifically this image reflects the corrected local p−values for the correlation between Age and FA for the genu (C. blue line, D. red line). All non−significant points are assigned a single value and color (dark blue here). Points that are significant then proceed from the next value on the color bar until the furthest end of the color bar. In the color bar shown, areas of significance are colored from cyan to red, with red areas indicating most significance. Any color bar available can be used.

significance. Figure 2.8E portrays the same information of significance mapped back on to the original genu fiber bundle.

2.5 Discussion and Conclusion

With the use of diffusion tensor imaging on the rise, the field of neuroimaging is in need of a coherent paradigm for localized fiber tract based diffusion tensor imaging (DTI) analysis. Here, we illustrate the UNC−Utah NA−MIC framework for DTI fiber tract analysis assessing the genu and splenium in one year olds from the UNC arm of the IBIS study. To demonstrate the use of our framework we analyzed the relationship of subject age in months with diffusion tensor properties. For the genu there were three locations of significant correlation as visible in Figure 2.8. The splenium demonstrated no areas of significant correlation. To facilitate utilization of our workflow, all of the data, intermediate files, scripts, and tools are freely available on NITRC.

Over the past few years we have created and tested our tools to provide maximum usability and a detailed analysis of diffusion at each point along fiber bundles. As these are tools for research, the tools in our framework are constantly evolving as we improve their function and incorporate new options. For example, we are currently enhancing DTIPrep to allow for simulation based error estimation, enhancing DTIAtlasBuilder to improve its unbiased atlas building step, as well as providing a GUI (non−Matlab) based interface to FADTTS directly within DTIAtlasFiberAnalyzer.

While all tools employed here are individually available online (see appendix below), all needed modules of this framework are directly available for download via the 3D Slicer extension manager (version 4.3 and above) (Figure 2.9). We hope our workflow will fill the void in the field for the many neuroimaging investigators that need to analyze their DTI data with a localized fiber based approach.

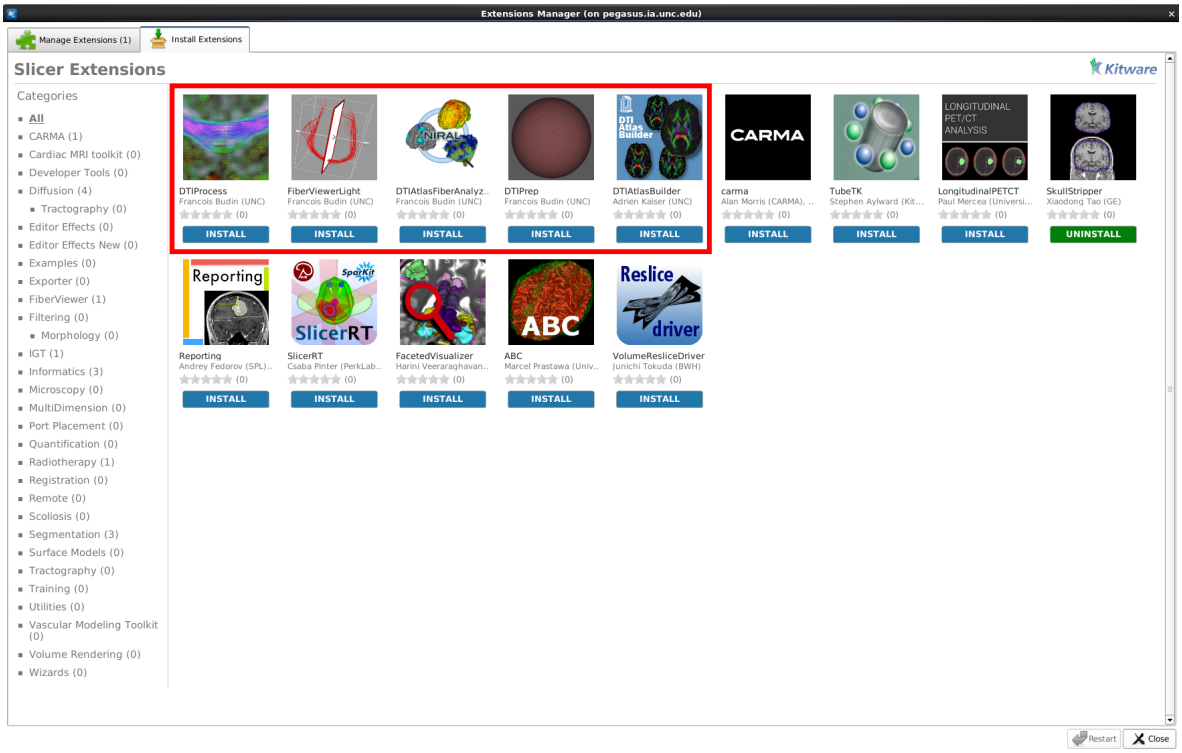

Figure 2.9: A screenshot displaying our tools as available extensions in 3D Slicer (box highlighted to indicate our Slicer modules).

2.6 Software and Example Dataset

3D Slicer: `http://www.slicer.org`

DTIPrep: `http://www.nitrc.org/projects/dtiprep/`

AutoSeg: `http://www.nitrc.org/projects/autoseg/`

itk−SNAP: `http://www.itksnap.org/pmwiki/pmwiki.php`

DTIAtlasBuilder: `http://www.nitrc.org/projects/dtiatlasbuilder/`

MriWatcher: `http://www.nitrc.org/projects/mriwatcher/`

AtlasWerks: `http://www.sci.utah.edu/software/13/370$-$atlaswerks.html`

DTI−Reg: `http://www.nitrc.org/projects/dtireg/`

BRAINS: `http://www.nitrc.org/projects/brains/`

ANTS: `http://www.picsl.upenn.edu/ANTS/`

FIberViewerLight: http://www.nitrc.org/projects/fvlight/

DTIAtlasFiberAnalyzer: http://www.nitrc.org/projects/dti_tract_stat

FADTTS: http://www.nitrc.org/projects/fadtts/

Matlab: http://www.mathworks.com/products/matlab/

Dataset: http://www.nitrc.org/projects/namicdtifiber/

CHAPTER 3

WHITE MATTER MICROSTRUCTURE ABNORMALITIES IN THE FORNIX AND CINGULUM OF CIGARETTE SMOKERS: A TRACTOGRAPHY BASED ANALYSIS

[1]

3.1 Introduction

Fifty years after the 1964 surgeons generals report on *Smoking and Health*, cigarette smoking is still the single most preventable cause of death worldwide, killing almost 6 million people each year [1]. In the US alone cigarette smoking is responsible for 1 in every 5 deaths; more than all other drug deaths combined [3; 5; 4]. Despite approximately 70% of cigarette smokers wanting to quit and 50% trying to quit each year, only 5% are successful in their cessation 1 year from their quit date [9]. To improve the success rate of cessation attempt, more effective therapies are needed. A better understanding of the neurobiology of cigarette addiction may help in creating more effective therapies.

A promising approach to this issue is to investigate the neural bases of intermediate phenotypes for smoking addiction. For instance, a growing focus in this intermediate phenotype approach to addictive disorders is the tendency to more often select smaller, sooner over larger, delayed rewards [137], a characteristic of cigarette among smokers

[1]This chapter is in preparation for submission to NeuroImage Clinical

[56; 57; 58]. Such delayed reward discounting is a feature of addiction that may critically play into the cycle of quit attempt and relapse. Excessive discounting of delayed rewards can be reduced by engaging in episodic prospection during decision−making in healthy people, an effect mediated by enhanced synchrony between medial temporal lobe regions implicated in episodic prospection and medial prefrontal areas implicated in decision−making [80; 81]. As such, we hypothesized that smokers would show structural abnormalities in the white−matter tracts through which these brain areas communicate: the cingulum, fornix, and uncinate. We investigated this hypothesis using a novel framework for diffusion tensor imaging (DTI) tractography based analysis [84].

DTI captures the diffusion of water molecules within brain tissue via several diffusion parameters: fractional anisotropy (FA), axial diffusivity (AD), radial diffusivity (RD), and mean diffusivity (MD). FA is used as a measure of overall white matter microstructure integrity, describing the extent to which diffusion of water is linear along a fiber bundle as compared across the fiber. The primary eigenvalue, AD, is the component of FA that describes diffusion along the length of the fiber bundle, whereas an average of the second and third eigenvalues, RD, describes diffusion orthogonal to the length of the fiber bundle. MD is an average of the first three eigenvalues and characterizes the overall magnitude of diffusion. Axial diffusivity is known to decrease in the case of neuron death, while RD increases in settings of myelin damage [98]. An alteration in FA can be caused by changes in fiber bundle organization, myelination, cell death, or inflammation.

To date, few studies have investigated how cigarette smoking independently affects white matter (WM) integrity in the brain using DTI. Studies to date have primarily utilized voxelwise analysis, including Tract−based Spatial Statistics (TBSS) [100], or relatively large, nonspecific regions of interest (ROI) analyses. To date, none have performed analyses along WM fiber tracts. Thus, previously reported DTI findings

in smokers are not truly localizable to specific tracts or exact locations along a tract. Moreover, when comparing smokers to nonsmokers using the above mentioned DTI analysis techniques, findings have been mixed. While most studies have reported increased FA in the brains of smokers compared to nonsmokers [103; 104; 105; 106; 107], others have found decreased FA among smokers [108; 109], or no difference in FA between smokers and nonsmokers [110; 111]. Likewise a variety of conclusions have been drawn as to how cigarette consumption and addiction severity relate to WM integrity in smokers. Some studies have found a negative correlation between measures of addiction severity and FA [104; 110; 106; 107], while others have observed a positive [103] or no [105; 109] correlation.

Several factors may contribute to these discordant findings, one of which is the use of nonspecific voxelwise or ROI−based analyses. With these analysis techniques, single average measurements of diffusion parameters (FA, MD, RD, AD) are used to represent regions that may encompass multiple WM tracts, or even contain both WM and grey matter. In order to better understand how cigarette smoking addiction affects WM integrity, here we applied a more specific and localizable WM fiber based technique.

Using DTI data collected from current cigarette smokers and non−smoking controls, we investigated the WM microstructural integrity of tracts implicated in the processes of episodic prospection and decision making: the cingulum, fornix, and uncinate. The goal of this investigation is to answer two questions: Does WM microstructural integrity differ between smokers and non−smokers along these tracts? Within smokers, does WM microstructural integrity differ as a function of measures of smoking dependence (cigarettes/day, CO, Cigarette Dependence Scale)? To address these questions, we performed DTI tractography, creating anatomically specific curvilinear ROI, analyzing the diffusion properties at each millimeter along the fiber bundle, a novel method of analysis for the cigarette addiction field.

Table 1 Participant demographics and smoking measures

Participants	Smokers (n=10)			Nonsmokers (n=15)			
	Mean / %	SD	(Range)	Mean / %	SD	(Range)	p-value
Age (years)	25.4	7.4	(19-40)	23.4	3.6	(19-29)	0.376
Sex (% Female)	50%			40%			0.697
Ethnicity (% Caucasian)	70%			47%			0.414
Education (years)	14.8	2	(12-18)	16.6	2.5	(12-21)	0.055
Smoking Measures:							
Average Cigarettes/Day	13.9	6.5	(5-25)				
CO concentration (parts/million)	13.3	11.6	(0-34)				
Cigarette Dependence Scale	42.2	11.1	(27-59)				
Age of Onset	17.5	2.5	(13-22)				
Years Smoking	7.9	7.5	(1-25)				

Table 3.1: Participant demographics and smoking measures. CO = carbon monoxide, SD = standard deviation.

3.2 Methods

3.2.1 Participant sample and demographics

Participants were recruited from the University of North Carolina at Chapel Hill (UNC) and surrounding areas by advertisement. Participants were all healthy, right−handed, native English speakers, 18−40 years old, without a known history of disorders of the nervous system, psychoactive medications, or contraindications to magnetic resonance imaging (MRI). Non−smokers reported no past or current regular smoking, and smokers were defined by self−reported smoking of ≥ 5 cigarettes per day. Participants provided written informed consent as approved by the UNC Office of Human Research Ethics, and received monetary compensation for participating. We acquired diffusion weighted images (DWI) from 29 participants, 15 non−smokers and 14 smokers. Data from n=4 smokers were excluded due to artifacts and low signal to noise ratio in the DWI data. Thus all analyses reported here derive from 25 participants (15 non−smokers, 10 smokers). The groups did not differ significantly by age, sex, or ethnicity, but the non−smokers did have an average of almost two additional years of education (p = 0.05; Table 4.1).

3.2.2 Measurements

Smokers were instructed to smoke as usual on the day of the scan. Prior to scan acquisition participants completed questionnaires and provided a breath carbon monoxide (CO) measurement. The questionnaires included a lab developed questionnaire about smoking habits [138] and the Cigarette Dependence Scale (CDS; [55]). We chose the CDS over the more frequently employed Fagerstrom Test for Nicotine Dependence (FTND), as evidence demonstrates that the CDS performs better than the FTND on measures of construct and predictive validity [53; 54].

3.2.3 Magnetic resonance imaging

All MRI scans were acquired on a head−only 3T Siemens Allegra scanner (Siemens Medical System, Erlangen, Germany). A single−shot echo−planar DTI sequence was used to acquire diffusion weighted images (DWI) using the following parameters: TR = 1000 ms, TE = 88 ms, slice thickness = 2 mm, in−plane resolution = 2 x 2 mm^2, and 66 slices; total duration = 10.67 min). 63 separate images were acquired for each DTI scan: 9 images without diffusion sensitization (b = 0 images) and 54 diffusion weighted images along unique gradient directions (b = 1000 s/mm^2).

3.2.4 Image analysis framework

Raw DWI images were processed and DTI tractography analysis was performed using the UNC−Utah NA−MIC Framework for DTI Fiber Tract Analysis Verde2014, which is schematized in Figure 3.1. In brief, DWI images first underwent rigorous quality control, eddy current, and motion correction with DTIPrep[2] [102; 128]. We next evaluated DTI signal to noise and tractography feasibility using 3D Slicer [127]. Here it was discovered that the right−left glyph direction was flipped, and image measurement

[2] `http://www.nitrc.org/projects/dtiprep`

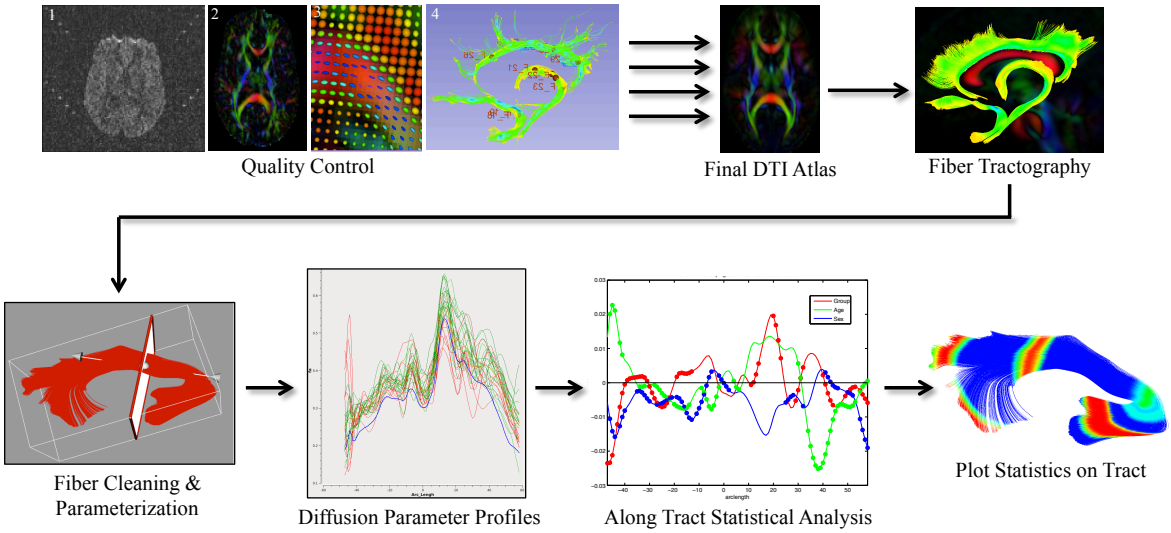

Figure 3.1: UNC−Utah NA−MIC framework for DTI fiber tract analysis. The framework begins with rigorous quality control of individual participant data inspecting for DWI artifacts (1), DTI direction encoding (2), glyph orientation (3), and landmark (fiducial) tractography. Together these steps correct common DWI artifacts, assess data quality, and tractography feasibility. Quality controlled DTI from each participant is then used to create a study specific DTI atlas via linear and nonlinear registration. On this atlas, fiber bundle tractography is performed. Fiber tracts are then cleaned and parameterized so each location along the tract has a relative address. Then diffusion parameters at each address along the tract are extracted from native space for individual participants, creating diffusion parameter profiles for each tract. These profiles are then entered into statistical analysis. Resulting p−values and/or betas can then be visualized on the fiber bundle.

frames were edited in the original DWI header file to correct this directionality for all participants. Then DWI and DTI quality control was repeated with the correct measurement frame. Brain masks were created from the b=0 (b_0) images and the isotropic diffusion weighted (IDWI) images with AutoSeg[3] [129], and edited in ITK−SNAP[4] [130]. A study specific atlas was then built using linear, unbiased diffeomorphic, and symmetric diffeomorphic registrations of skull−stripped DTIs as detailed in [84]. We next performed interactive fiber tractography for the bilateral cingulum, fornix, and

[3] `http://www.nitrc.org/projects/autoseg/`

[4] `www.itksnap.org`

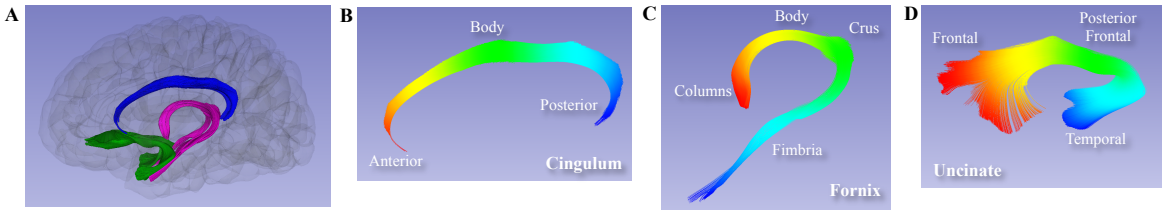

Figure 3.2: Fiber tracts analyzed and anatomical definitions. A. Fiber bundles of interest are represented in their anatomical location in a glass brain, with the cingulum in blue, the fornix in pink, and the uncinate in green. B−D display the individual fiber bundles with locations along the tract labeled to clarify findings. These fibers are colored by the parameterized addresses along each tract (arclength). B. Cingulum, C. Fornix, and D. Uncinate.

uncinate on the Final DTI Atlas in 3D Slicer. See Figure 3.2 for anatomical orientation of each tract investigated. We executed gross fiber bundle cleaning in 3D Slicer utilizing ROIs, followed by fine scale clustering based processing in FiberViewerLight[5] . In order to analyze only the properties of the main fiber bundle, cortical projections were removed from the cingulum bundle using the cutter option in FiberViewerLight. A fiber origin plane was then manually placed for each fiber bundle for tract spatial parameterization, i.e. defining the corresponding arclengths per fiber [139]. Diffusion properties along each tract were extracted for each individual participant employing the final transform computed during atlas building using DTIAtlasFiberAnalyzer[6]. Within DTIAtlasFiberAnalyzer, these diffusion parameters are then plotted as diffusion profiles along the length of each tract, and FA profiles were visually quality controlled for participant profiles with poor correlation to the atlas FA profile. An example of FA profile plots for all participants is displayed in Figure 3.3, which depicts the left and right fornices. Diffusion parameter measurements were then statistically analyzed via Functional Analysis of Diffusion Tensor Tract Statistics (FADTTS)[7] [126]. Local

[5] `http://www.nitrc.org/projects/fvlight`

[6] `http://www.nitrc.org/projects/dti_tract_stat/`

[7] `https://www.nitrc.org/projects/fadtts/`

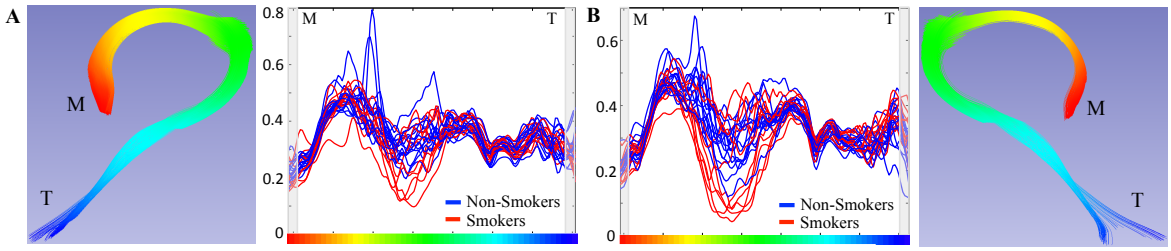

Figure 3.3: Participant fornix fractional anisotropy (FA) profiles. Measurements of FA along the tract for all participants in the left (A) and right (B) fornices. FA profiles are plotted in the middle panels, with nonsmokers indicated in blue, and smokers indicated in red. The color bar on the x axis of the FA profile plots corresponds to the location along the left or right fornix, as depicted in the outer panels. M− medial, T− temporal.

p−values and betas computed with FADTTS were plotted onto the fiber bundle and visualized in 3D Slicer or ShapePopulationViewer[8].

Tractography ROIs

Region of interest label maps for use in the tractography of each tract were based on tract anatomy. Label maps for each tract were manually constructed to be inclusive, but specific for individual tracts. Left and right tract label maps were created at the same time in Slicer, using unique label identifiers. Simultaneous label creation aids in assuring the bilateral consistency of the label map extent for each tract.

Tractography algorithm

Tracts were seeded in 3D Slicer using label maps as described above. Tracks between 10mm and 800mm were computed with a seed spacing of 0.5mm, stopping FA value of 0.18, stopping curvature of 0.7mm, and step length of 0.5mm. Tracts were then cleaned utilizing negative and positive ROIs until only the fibers of the desired tract remained.

[8] `http://www.nitrc.org/projects/shapepopviewer/`

3.2.5 Statistical analysis

For between group comparisons, we used Students t−tests for continuous measures, and χ^2 tests for dichotomous variables. We used FADTTS to analyze the relationship between diffusion parameters and variables of interest at each millimeter along the fiber bundles [126]. FADTTS is composed of several steps: multivariate varying coefficient model, weighted least squares estimation, functional principal component analysis, hypothesis testing (with wild bootstrapping) for global and local test statistics, confidence band computation, false discovery rate (FDR) correction of omnibus local test statistics, and posthoc analysis for individual diffusion parameter significance assessment with false discovery rate correction of local test statistics. For each model, a single variable of interest was investigated while controlling for effects of age and sex.

3.2.6 Result visualizations

The FADTTS plots included in this manuscript depict beta magnitudes for each diffusion parameter (FA− green, RD− red, AD− blue, MD− magenta) along the length of the fiber tract for each variable of interest. Although included in our correction for multiple comparisons, diffusion correlations for the terminal 6mm of all fiber bundles were disregarded (denoted by grey rectangles at plot edges), as diffusion parameters extracted at fiber ends are considered less reliable. The fiber bundle figures map the significant FA beta locations on the left and right tracts. Coloration for the fiber tract figures is by significant FA effect magnitude and direction for each tract, where non−significant areas along the tract are shown in grey.

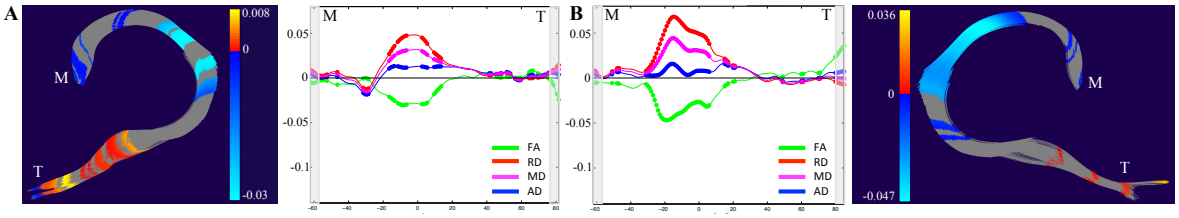

Figure 3.4: Smokers have decreased microstructural integrity in bilateral fornix crus and body. Effect of Group on white matter integrity in the left fornix (A) and right fornix (B). Medial plots depict diffusion parameter beta values for the effect of Group. Positive betas indicate higher diffusion parameter values among smokers. Filled circles indicate significant correlations after FDR correction. Lateral panels localize the significant findings for FA. Cool colors indicate decreased FA among smokers compared to nonsmokers. FA− fractional anisotropy, RD− radial diffusivity, AD− axial diffusivity, MD− mean diffusivity, M− medial, T− temporal.

3.3 Results

3.3.1 Group differences in white matter microstructure

White matter microstructure integrity is decreased in the body and crus of the left and right fornix of cigarette smokers when compared to non−smokers (Figure 3.4). While there is a significant difference between groups when considering all diffusion parameters together, *posthoc* tests of individual diffusion parameters did not find any significant group effects. In addition to these findings in the fornix, we also observed sporadic areas of significant group difference in the bilateral cingulum and uncinate. However, the effect sizes for these findings were minimal, with abundant sign reversals, precluding robust interpretation (data not shown). As detailed in the following sections, we next analyzed the relationship between WM integrity in the same tracts of interest and measures of cigarette consumption and addiction severity within the smokers.

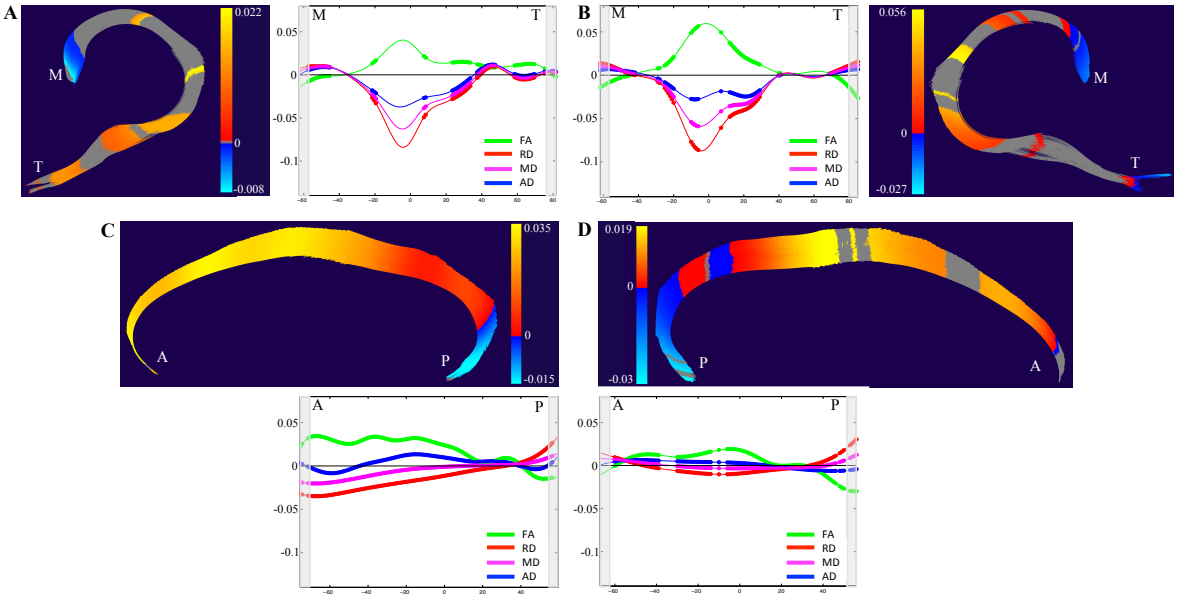

Figure 3.5: White matter integrity in smokers positively correlates with cigarettes per day. Relationship between cigarettes per day and WM in the left fornix (A), right fornix (B), left superior cingulum (C), and right superior cingulum (D). Plots depict beta values for the correlation between cigarettes per day and WM diffusion parameters. Positive beta values indicate a positive correlation with cigarettes per day and the indicated diffusion parameter. Filled circles indicate significant correlations after FDR correction. The tract panels render FA beta values spatially localized to sites along the tract where WM diffusion significantly correlated with cigarettes per day. Coloration conventions as for Figure 4. FA− fractional anisotropy, RD− radial diffusivity, AD− axial diffusivity, MD− mean diffusivity, M− medial, T− temporal, A− anterior, P− posterior.

3.3.2 WM and measures of cigarette consumption

WM and self reported cigarette consumption

Given the findings reported above, to our surprise, WM microstructure integrity in the bilateral fornices positively correlated with self−reported number of cigarettes smoked per day (Figure 3.5A, B). In other words, WM integrity increased with increasing intensity of cigarette smoking. This result was most evident in the left and right fornix body, crus and fimbria. Moreover, we observed the same relationship between self−reported cigarettes per day and WM integrity in the left and right cingulum body, and left anterior cingulum (Figure 3.5 C, D).

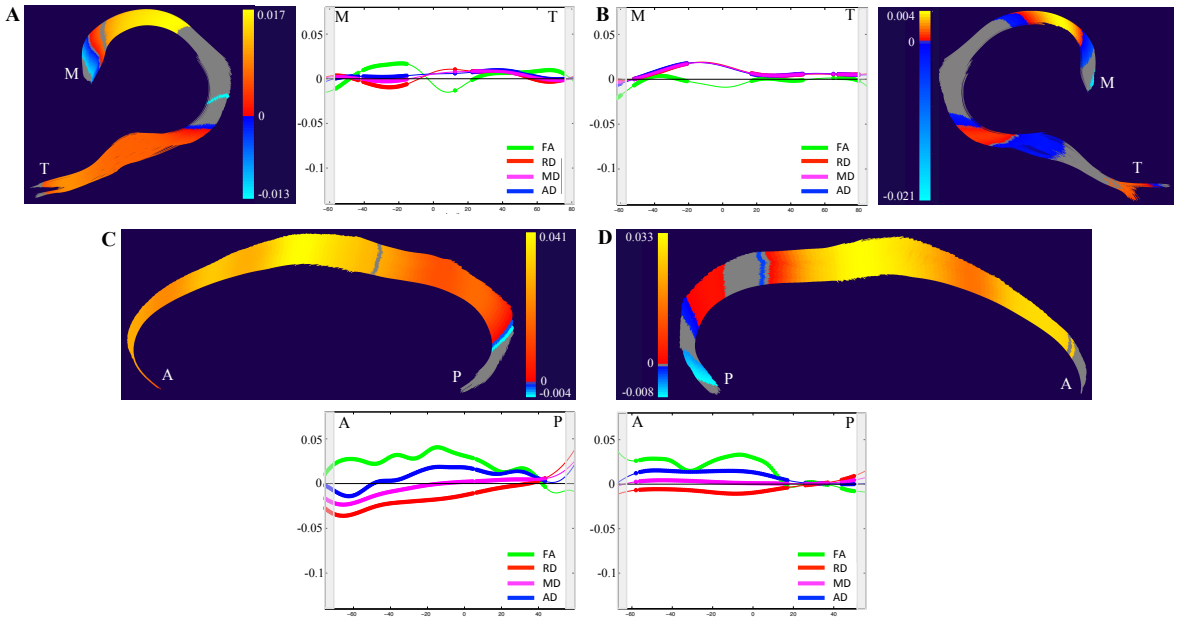

Figure 3.6: White matter integrity in smokers positively correlates with exhaled carbon monoxide (CO). Effect of CO on white matter integrity in the left fornix (A), right fornix (B), left superior cingulum (C), and right superior cingulum (D). Plots depict diffusion parameter beta values for the effect of CO. A positive beta indicates a positive correlation between CO and diffusion property, a negative beta indicates a negative correlation. Significant correlations are indicated by filled circles. The figures map the respective significant beta locations for FA. Coloration for the figures is by relative FA beta magnitude and effect direction. Cool colors indicate a negative correlation; warm colors indicate a positive correlation. FA− fractional anisotropy, RD− radial diffusivity, AD− axial diffusivity, MD− mean diffusivity, M− medial, T− temporal, A− anterior, P− posterior.

WM and a biological measure of consumption: exhaled CO

While self−reported cigarettes per day provides a widely employed and useful measure of smoking habit intensity, variations in the type of cigarettes are smoked and the manner in which they are smoked can introduce significant variation between individuals reporting identical numbers of cigarettes smoked per day [140]. We therefore also assessed the relationship between measures of WM integrity and exhaled CO levels among smokers. We found that exhaled CO positively correlated with WM microstructure integrity in the left fornix body and fimbria (Figure 3.6A), as well as in the left

and right cingulum anterior and body (Figure 3.6C, D). In other words, those with higher biological measures of smoking intensity on the day of the scan had increased WM tract integrity in these locations. Notably, we did not observed a significant relationship between WM integrity and exhaled CO in either the left or right fornix crus, with betas suggesting the opposite relationship between WM integrity and exhaled CO, compared to cigarettes/day, in these regions.

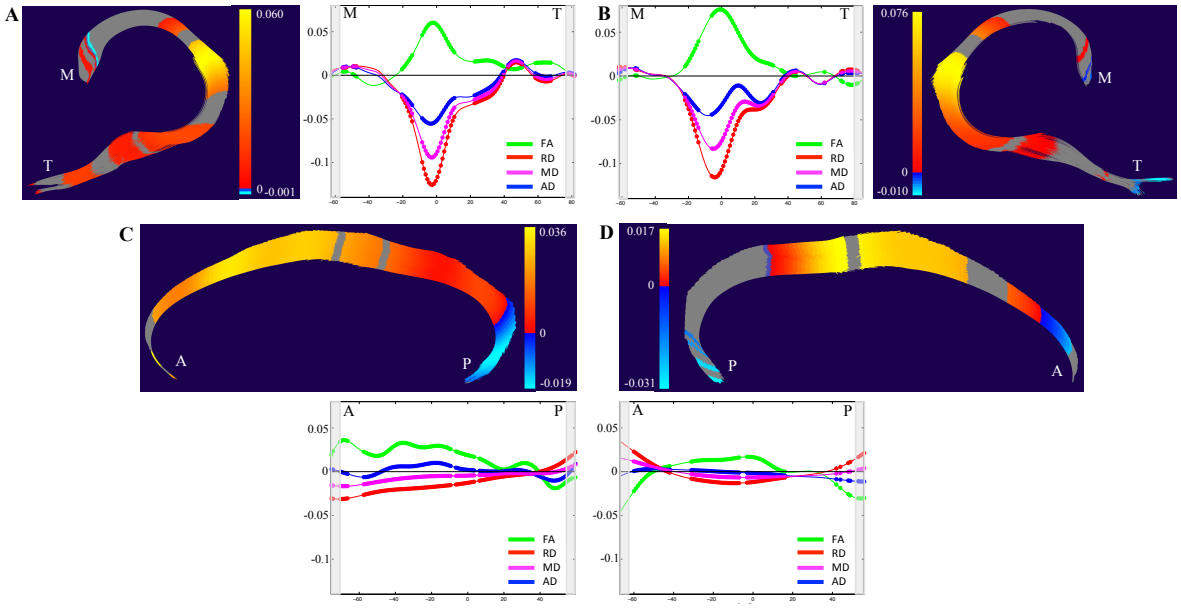

Figure 3.7: White matter integrity in smokers positively correlates with Cigarette Dependence Scale (CDS). Effect of CDS on white matter integrity in the left fornix (A), right fornix (B), left superior cingulum (C), and right superior cingulum (D). Plots depict diffusion parameter beta values for the effect of CDS. A positive beta indicates a positive correlation between CDS and diffusion property, a negative beta indicates a negative correlation. Significant correlations are indicated by filled circles. The figures map the respective significant beta locations for FA. Coloration for the figures is by relative FA beta magnitude and effect direction. Cool colors indicate a negative correlation; warm colors indicate a positive correlation. FA− fractional anisotropy, RD− radial diffusivity, AD− axial diffusivity, MD− mean diffusivity, M− medial, T− temporal, A− anterior, P− posterior.

3.3.3 WM and cigarette dependence

While self−reported cigarettes per day and exhaled CO each provide quantitative measures of heaviness of smoking, which is related to cigarette dependence, heaviness and dependence (or addiction) are not perfectly correlated. As such we also investigated the relationship between WM microstructure integrity and a quantitative measure of cigarette addiction: Cigarette Dependence Scale (CDS) scores. We observed positive correlations between WM integrity and CDS scores within the left and right fornix crus and fimbria, the bilateral cingulum body, and the left anterior cingulum (Figure 3.7). These findings showed better correspondence with the self−reported cigarettes per day associations with WM than did WM associations with CO, and supports the interpretation that among smokers more severe cigarette addiction is associated with more intact WM microstructure.

3.3.4 Summary of Findings

White matter integrity is decreased in smokers compared to nonsmokers in the fornix crus and body bilaterally. Within smokers, white matter integrity of the fornix crus and body bilaterally positively correlates with cigarettes smoked per day and CDS scores. Within smokers, white matter integrity of the cingulum anterior and body bilaterally positively correlates with cigarettes smoked per day, exhaled carbon monoxide concentration, and CDS scores. Results for the uncinate were of minimal effect size and contained multiple sign reversals inhibiting robust interpretation for both between group and within smokers analyses.

3.4 Discussion

3.4.1 Differences between smokers and nonsmokers

To our knowledge, this is the first investigation of WM diffusion parameters comparing cigarette smokers and non−smokers that allows localization of effects along specific fiber tracts. Previous DTI studies in cigarette smokers relied upon voxelwise or ROI based analyses; these less specific techniques may have contributed to the mixed findings in the literature. As can be seen in Figure 3.3, group effects on diffusion properties vary along the length of the tracts, underlining the utility of a more localized and specific form of DTI tractography analysis.

While most previous studies of smokers have found increased WM integrity, as measured by FA, in smokers compared to non−smokers, here we found smokers to have decreased WM integrity in bilateral fornix body and crus compared to nonsmokers. It is important to note, however, that this is the first published report comparing WM microstructural integrity in the fornix between smokers and nonsmokers. We also note that although the omnibus tests of group differences in diffusion parameters within the fornix crus and body were significant, large magnitude effects, the posthoc analysis of independent diffusion parameters did not identify significant group effects, indicating that the omnibus group effects were not driven by an individual diffusion parameter, but by collective effects across parameters. Thus, the group differences in WM integrity reported here may reflect a combination of changes in myelination, cell death, inflammation, and fiber bundle organization.

Theoretical role for the fornix in cigarette addiction

The fornix is a part of the limbic circuitry and is implicated in episodic memory, networks that may play an important role in addiction [141**?** ; 83]. Previous work has found episodic memory to be disrupted in deprived smokers [82], and the same

circuit used in episodic memory is utilized in episodic prospection. The ability to vividly imagine future outcomes in a detail rich manner is known to impact decisions between alternate outcomes [80; 81], a process crucial to the behavioral change necessary for addiction cessation. As such, abnormalities in the circuitry supporting episodic prospection could theoretically hinder smoking cessation and undermine certain behavioral cessation therapies. Further, the fornix plays a role in addiction as it connects the hippocampus to the nucleus accumbens, a structure well documented for its role in the reward processing of addiction [142; 143]. Additionally, it has been documented that smokers have decreased hippocampal volumes bilaterally compared to nonsmokers, and that hippocampal volumes decreased with increased pack/yrs [115]. As the fornix is the main projection of the hippocampus, it is within reason to think there may also be a difference in the fornix of smokers and nonsmokers.

3.4.2 Findings within smokers

As the primary difference between groups was in the fornix body and crus bilaterally, it is this location that was focused on initially in our within smokers investigation. Additional examination of the cingulum and uncinate bilaterally were also pursued. It is noteworthy, that this is the first study to perform correlational analysis between white matter microstructural integrity and addiction severity measured with the CDS. All prior DTI studies have used the FTND to assess addiction severity; a measure with reduced validity regarding construct and prediction when compared to the CDS [55; 53; 54]. Further, only one prior study has found a positive correlation between white matter integrity in smokers and cigarette consumption as measured by pack/years [103]. Most other studies find either a negative correlation [104; 110; 106; 107], or no correlation at all [105; 109].

Fornix body and crus integrity positively correlate with cigarette consumption and addiction severity

Both cigarettes/day and CDS scores positively correlated with white matter integrity in the fornix body and crus. The relationship between CDS scores and WM integrity best matched the location the between groups results were found in, and had the greatest magnitude effect of all analyses performed. This suggests that this increase in white matter integrity with increasing addiction severity is more a function of the addiction process overall and not just a reflection of consumption. This is supported by the fact that the biological measure of consumption, CO, showed little to no relationship with white matter integrity in the fornix crus bilaterally for smokers.

One prior study has found smokers who relapsed had larger bilateral hippocampi compared to those smokers who maintained abstinence [144]. This may suggest that the more addicted smokers have larger hippocampi, and this may translate to an increase in integrity in the fornix of the most addicted smokers.

Cingulum anterior and body integrity positively correlate with cigarette consumption and addiction severity

In the cingulum bilaterally, white matter microstructural integrity positively correlated with both measures of consumption (cigarettes/day and CO) and the measure of addiction severity (CDS). These relationships occurred in the cingulum body and anterior, and were of greatest magnitude in the left cingulum. Unlike findings in the fornix of smokers, the cingulum findings are all of similar magnitude, but the largest bilateral effect is that of CO. The anterior cingulate cortex has one of the highest densities of nicotinic acetylcholine receptors (nAChRs) in the brain, and maybe this receptor density could cause this region of the cingulum to be particularly sensitive to the effects of recent cigarette consumption as measured by CO concentration [145].

Our results in the cingulum are in conflict with prior DTI literature where smokers were found to have higher white matter integrity (FA) in the anterior cingulum when compared to nonsmokers [106; 107]. Further, both of these studies found negative correlations between white matter integrity and addiction severity. Hudkins 2012 found a negative correlation between FA and addiction severity as measured by FTND, cigs/day, and pack years [106], while Huang 2013 a negative correlation between FA and physical dependence, hooked on nicotine checklist scores, and FTND (trending) [107]. We find a positive correlation between cigarette dependence and white matter integrity along the length of the cingulum anterior and body within smokers.

Prior fMRI studies have shown the anterior cingulate to be reactive to cigarette smoking cues [146; 147; 148], affiliated with craving for cigarettes [148], and increased craving has been related to increased potential for relapse. As our participants were active smokers with no intent of cessation, perhaps this link to craving and continuation to smoke could explain the findings in the anterior cingulum. Further, in this same study those smokers that slipped from abstinence had decreased functional connectivity between insula and dACC [148]. The authors suggested that this could potentially reflect reduced top down control after exposure to smoking cues. Perhaps, the increased structural integrity we see in our data reflects a compensatory effort in order to combat this reduced functional connectivity with increased addiction severity.

3.4.3 Limitations

The small sample size of this study limited our power to detect significant effects of either group or cigarette addiction severity. This limitation may, for example, explain the lack of observed significant effects in the uncinate. Moreover, we were unable to assess whether age, sex, ethnicity, or socioeconomic status moderated any of the effects of smoking, as might be expected. Another limitation is the lack of information

regarding other substance use among these participants. As such, cigarette smoking *per se* may not entirely account for the effects that we observed. This issue is of particular concern with regard to alcohol use, as heavy alcohol use is frequently associated with heavy smoking [149], and heavy alcohol use is known to damage WM integrity in the brain [150]. Knowing the alcohol consumption of our participants would have allowed us to control for this potential confound.

3.4.4 Open questions

While we have documented WM integrity differences between smokers and nonsmokers, as well as differences among smokers that co−vary with addiction severity and heaviness of smoking, whether these structural differences are consequences of cigarette dependence or use, or preexisting features remains unknown. Prospective longitudinal studies would shed light on this issue and will be essential for identifying anomalies in brain structure that contribute to risk for cigarette dependence. Furthermore, while we specifically investigated tracts implicated in episodic prospection, we did not explicitly test episodic prospection, or its ability to modulate decision−making, in these participants. Future studies that investigate the relationship between WM structural integrity in these tracts and the latter behavioral phenomenon may prove informative.

3.5 Conclusions

Consistent with our hypothesis, we found that smokers have decreased WM integrity compared to nonsmokers in fiber tracts linking the medial temporal and frontal lobes, specifically the bilateral fornix body and crus. Surprisingly, among smokers we found a positive correlation between WM integrity and measurements of cigarette consumption and addiction severity in the fornix, as well as in the cingulum, bilaterally. To our knowledge, this is the first study in the field of cigarette dependence to use a DTI

tractography analysis framework that provides tract specific and localizable results along the length of a tract. Perhaps with specific and localizable results, we can begin to clarify the mixed results from prior literature as to the relationship between cigarette smoking and WM integrity. Further, a better understanding the role of the fornix and cingulum in cigarette dependence may facilitate the development of novel therapies for cigarette cessation. Prospective longitudinal studies are needed to determine if these localized findings of white matter integrity are a result of cigarette dependence or if they are pre−existing risk factors for cigarette addiction.

CHAPTER 4

STRUCTURAL ALTERATIONS IN CIGARETTE SMOKERS: IMPLICATIONS FOR COGNITIVE CONTROL, EPISODIC PROSPECTION, AND DECISION–MAKING

[1]

4.1 Introduction

Cigarette smoking is the number one preventable cause of death, responsible for one in five deaths in the US [3; 5] and one in ten deaths worldwide [1]. While it receives less attention than other mortality factors, cigarettes cause more deaths than alcohol use, illegal drug use, human immunodeficiency virus (HIV), motor vehicle accidents, murders, and suicides combined [4; 5]. In addition to mortality, cigarettes induce significant morbidity increasing the risk for coronary heart disease, stroke, chronic obstructive lung diseases, and multiple forms of cancer [3; 5]. Along with the clear effect of cigarettes on the body, the 7000 chemicals in cigarette smoke also impacts the brains biology and function [151; 152; 153]. Moreover, the binding of nicotine to acetylcholine receptors secondarily causes alterations in nearly all other neurotransmitter systems in the brain [49], which in turn affects behavior and may contribute to the formation cigarette dependence and addiction.

In the past decade, neuroimaging has been used to precisely assess living brain

[1]This chapter is in preparation for submission to NeuroImage Clinical

structure in cigarette smokers. This work has demonstrated that compared to nonsmokers, smokers have decreased total brain grey matter volume and density, this gray matter decrease has been localized to the frontal lobe, temporal lobe, insula, thalamus, and substantia nigra. Moreover, finer−grained investigations have identified less grey matter among smokers in the anterior cingulate, prefrontal cortex (PFC), orbital frontal cortex (OFC), parahippocampal gyrus, hippocampus, or hippocampus subfields [113; 114; 110; 115; 116]. These decreases in gray matter volume/density in the frontal lobe, temporal lobe, left PFC, hippocampus, subiculum, and presubiculum negatively correlate with pack years [113; 110; 115]. Decreased cortical thickness was also found in the anterior cingulate cortex, insula, total brain reward system, total frontal cortex, and medial OFC, with the decrease in the OFC cortical thickness correlating with cigarettes per day and pack years [117; 118].

Many of these areas altered in volume or thickness in cigarette smokers are a part of the circuitry implicated in episodic prospection and decision−making, a circuit thought to be important for addiction as a whole and cigarette addiction specifically. Previously, we found that white matter integrity of tracts involved in the episodic prospection circuitry (cingulum, fornix and uncinate fasciculus) are abnormal in the brains of smokers compared to nonsmokers, and within smokers white matter tract integrity changed as a function of cigarette dependence severity and cigarette consumption (Chapter 3). In this paper, we follow up these white matter findings with results on gray matter morphometry via volume and thickness measurements in cortical and subcortical regions served by the cingulum, fornix and uncinate tracts to see if they differ between smokers and nonsmokers, and if the volumes and cortical thickness vary as a function of smoking measures. Specifically we utilized FreeSurfer to analyze the cingulate cortex, orbital frontal cortex, inferior frontal cortex, parahippocampal gyrus, hippocampus, thalamus,

and amygdala. We hypothesized that the volume and thickness of our regions of interest would be decreased in smokers compared to nonsmokers, and that within smokers the volume and thickness would negatively correlate with measurements on cigarette consumption (cigarettes per day and breath carbon monoxide (CO)) and cigarette addiction severity as determined by the Cigarette Dependence Scale.

Participants	Smokers (n=11)			Nonsmokers (n=15)			
	Mean / %	SD	(Range)	Mean / %	SD	(Range)	p-value
Age (years)	25.2	7.1	(19-40)	23.4	3.6	(19-29)	0.408
Sex (% Female)	55%			40%			0.692
Ethnicity (% Caucasian)	73%			47%			0.246
Education (years)	14.9	2	(12-18)	16.6	2.5	(12-21)	0.058
Smoking Measures:							
Average Cigarettes/Day	13.2	6.5	(5-25)				
CO concentration (parts/million)	12.5	11.3	(0-34)				
Cigarette Dependence Scale	42.6	10.6	(27-59)				
Age of Onset	17.5	2.4	(13-22)				
Years Smoking	7.6	7.2	(1-25)				

Table 4.1: Participant demographics and smoking measures. CO = carbon monoxide, SD = standard deviation.

4.2 Methods

4.2.1 Participants

Participants were recruited from the University of North Carolina at Chapel Hill (UNC) and surrounding areas by advertisement. Participants were healthy, right−handed, native English speakers, 18−40 years old, without history of disorders of the nervous system, current psychoactive medication use, or contraindications to magnetic resonance imaging (MRI). Non−smokers reported no lifetime regular smoking; smokers self−reported smoking $\geq$5 cigarettes per day. Participants provided written informed consent as approved by the UNC Office of Human Research Ethics, and received monetary compensation for participating.

We acquired high resolution magnetization prepared rapid gradient echo (MPRAGE) T1−weighted images from 29 participants, 15 non−smokers and 14 smokers. Data from n=3 smokers were excluded due to artifacts and low signal to noise ratio. Thus, all

analyses reported here derive from 26 participants (15 non−smokers, 11 smokers). The groups did not differ significantly by age, sex, ethnicity, or years of education (Table 4.1).

4.2.2 Measures

Smokers were instructed to smoke as usual on the day of the scan. Prior to scan acquisition, participants completed questionnaires, and provided a breath carbon monoxide (CO) measurement. The questionnaires included a lab developed questionnaire about smoking habits [138], and the Cigarette Dependence Scale (CDS, [55]). We chose the CDS over the more frequently employed Fagerstrm Test for Nicotine Dependence (FTND) as evidence demonstrates that the CDS performs better than the FTND on measures of construct and predictive validity [53; 54].

4.2.3 Image Acquisition

Data were acquired on a 3T Siemens Allegra head−only MRI scanner (Siemens Medical System, Erlangen, Germany) with a standard Siemens 8−channel phased array head coil. A whole−head, high−resolution T1−weighted MPRAGE images was obtained from each participant (TR/TE/T1=1750/4.38/900 ms; flip angle=8°; 25.6 cm FoV; 256 208 in-plane matrix, 160 axial slices, voxel resolution = 1.0 mm^3).

4.2.4 Image processing

The publicly available FreeSurfer version 5.3 (`http://surfer.nmr.mgh.harvard.edu/`) was utilized to assess bilateral regional cortical and subcortical volumes, and regional cortical thickness [85; 86; 87; 88; 89; 90; 91; 92; 93; 94; 95; 96; 97]. Measurements were acquired from the 2009 Destrieux Atlas in FreeSurfer for regions important for episodic prospection decision−making (Figure 4.1). Specifically we analyzed the 42 cortical and 6 subcortical regions composing the cingulate cortex, orbital frontal cortex,

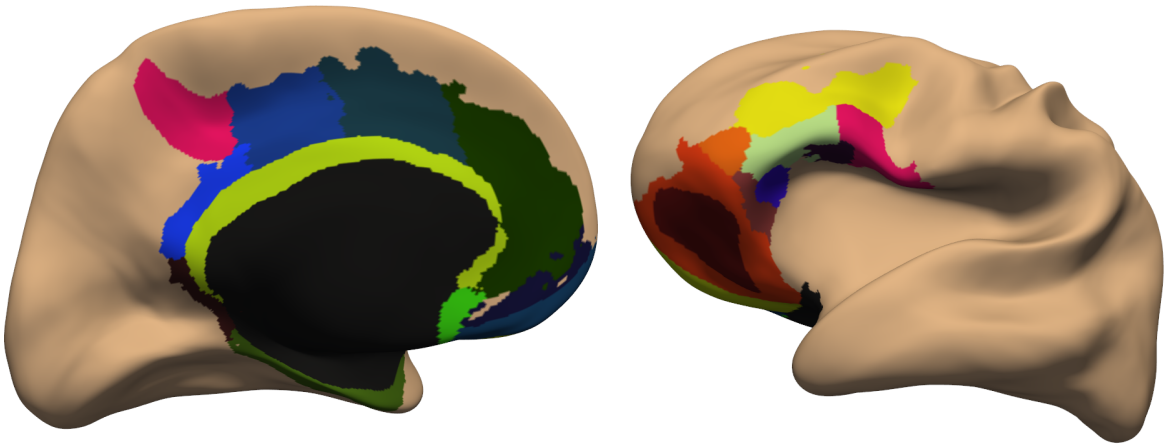

Figure 4.1: Cortical regions investigated that are implicated in episodic prospection and decision−making. Regions from the 2009 Destrieux atlas composing the cingulate, the inferior frontal gyrus, and the orbital frontal cortex projected on an average inflated brain created from our participant sample. Tan areas were not investigated, and the black region represents the medial wall. These cortical regions, and subcortical regions consisting of the hippocampus, thalamus, and amygdala were investigated bilaterally.

inferior frontal cortex, parahippocampal gyrus, hippocampus, thalamus, and amygdala bilaterally. Right and left structures were tested separately for cortical volume (ml) and cortical thickness (mm). Cortical measurements from the temporal lobe were not considered due to the poor surface construction in this location resulting from low T1 intensities.

4.2.5 Statistics

For between group comparisons, we used Students t−tests for continuous measures, and χ^2 tests for dichotomous variables. Volume and thickness estimates were exported to SPSS (version 21; SPSS Inc., Chicago, IL, USA) and analyzed via multiple regression with the first model evaluating the effect of total intracranial volume (ICV) and age, and the second group evaluating total intracranial volume, age, and group (smokers vs non−smokers). There was no difference in ICV between smokers and non−smokers. For within smokers analysis we calculated partial correlation Pearson

Group Analysis (n = 26)				
ROI	p	β	95% C.I.	
Left Hippocampus	0.021	-331.149	-588.315	-76.193
Left Posterior Ventral Cingulate Gyrus Thickness	0.020	-0.226	-0.389	-0.060
Right Middle Posterior Cingulate Volume	0.043	400.788	37.342	743.837

Smoker Analysis (n = 11)				
ROI				
Cigarettes/Day	p	r	95% C.I.	
Left Amygdala	0.023	-0.74	-0.977	0.011
Right Pars Orbitalis Gyrus Thickness	0.018	-0.757	-0.984	-0.121
Right Pars Triangularis Gyrus Thickness	0.001*	-0.889	-0.994	0.277
CO	p	r	95% C.I.	
Right Pars Orbitalis Gyrus Volume	0.042	-0.685	-0.972	0.119
Right Pars Orbitalis Gyrus Thickness	0.001*	-0.895	-0.991	-0.629
Right Pars Triangularis Gyrus Thickness	0.035	-0.702	-0.973	0.755
Right Orbital Lateral Sulcus Thickness	0.015	-0.77	-0.977	-0.515
CDS	p	r	95% C.I.	
Right Pars Triangularis Gyrus Thickness	0.019	-0.753	-0.99	0.558
Left Pars Triangularis Gyrus Thickness	0.004	-0.841	-0.98	-0.15
Left Middle Anterior Cingulate Thickness	0.013	-0.782	-0.979	-0.499

Table 4.2: Significant results from cortical and subcortical volume, and cortical thickness analysis. Significant results split by between group and within smokers findings. with the smokers analysis divided by measurement of cigarette consumption or dependence. P−values presented here are the non−FDR adjusted figures, with the * designating the two results that survived correction. ROI = region of interest, C.I. = confidence interval, CO = carbon monoxide, CDS = cigarette dependence scale.

coefficients in models for demographic factors, smoking habit intensity measures and FreeSurfer measurements, as implemented in SPSS. To eliminate concerns regarding violation of parametric test assumptions, bootstrapping procedures (n = 10,000 resamples) were used in tests of statistical significance. Correction of p−values for multiple comparisons using the false discovery rate (FDR) procedure [154] was carried out in R (`http://www.R-project.org`). The threshold for statistical significance was $p < .05$.

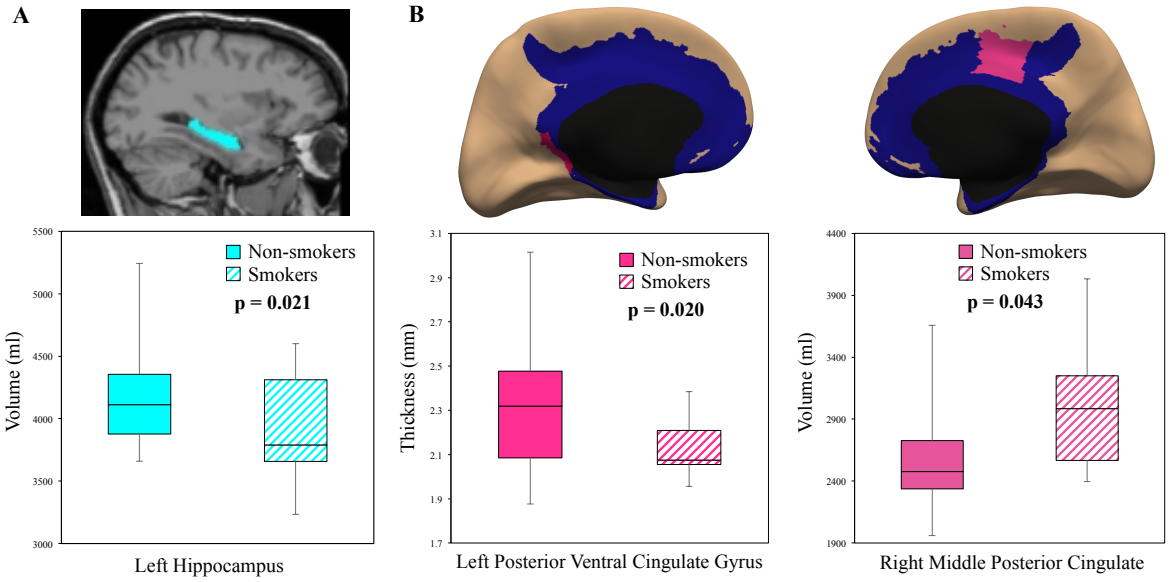

Figure 4.2: Significant findings when comparing smokers to non−smokers. A. In subcortical regions, smokers were found to have decreased volume of the left hippocampus compared to nonsmokers. B. Cortical thickness/volume findings portrayed on an average inflated brain created from our sample population. Brain images relate to the plot positioned directly below. Smokers were found to have a thinner cortex in the left posterior ventral cingulate than nonsmokers, and a greater cortical volume than nonsmokers for the right middle posterior cingulate. Plots demonstrate the range of volumes for each group, the median, and the first and third quartile. Tan areas were not investigated, dark blue areas were investigated but non−significant, significant areas are shades of pink.

4.3 Results

Visualization of all regions analyzed can be seen in Figure 4.1. Significant results from all analyses are located in Table 4.2. Those p−values that survived FDR correction at a 0.05 threshold are indicated with an asterisk. For result visualizations, brain regions that are dark blue indicate investigated regions that were not significant. Significant regions are represented by different shades of warm colors (pink, red, orange, yellow).

4.3.1 Comparison of smokers to non−smokers

Smokers were found to have decreased volume in the left hippocampus (Figure 4.2A), and decreased cortical thickness in the left posterior ventral cingulate gyrus compared to nonsmokers (Figure 4.2B left). However, the right middle posterior gyrus and sulcal volume was greater in smokers than nonsmokers (Figure 4.2B right).

4.3.2 Within smokers analysis

Findings within smokers by smoking variable of interest can be seen in Figure 4.3. For all smoking variables investigated, negative correlations were found with regional volumes and thicknesses as displayed on an inflated average brain in Figure 4.3A.

Cigarettes per day

Right inferior frontal gyrus regions, the pars triangularis and pars orbitalis, are decreased in thickness with increasing numbers of cigarettes per day. The left amygdala volume also shows a negative correlation with cigarettes consumed daily (Figure 4.3B).

Breath carbon monoxide concentration

Inverse correlations are also found when looking at the effect of carbon monoxide (CO) concentration. Cortical thickness decreases as a function of increasing CO in the right pars triangularis gyrus, right pars orbitalis gyrus, and right lateral orbital sulcus. Cortical volume also negatively correlated with CO in the right pars orbitalis gyrus (Figure 4.3C).

Cigarettes Dependence Scale scores

With increasing addiction severity as measured via the CDS, cortical thickness decreased in the right pars triangularis gyrus, left pars triangularis gyrus, and left middle anterior cingulate gyrus and sulcus (Figure 4.3D).

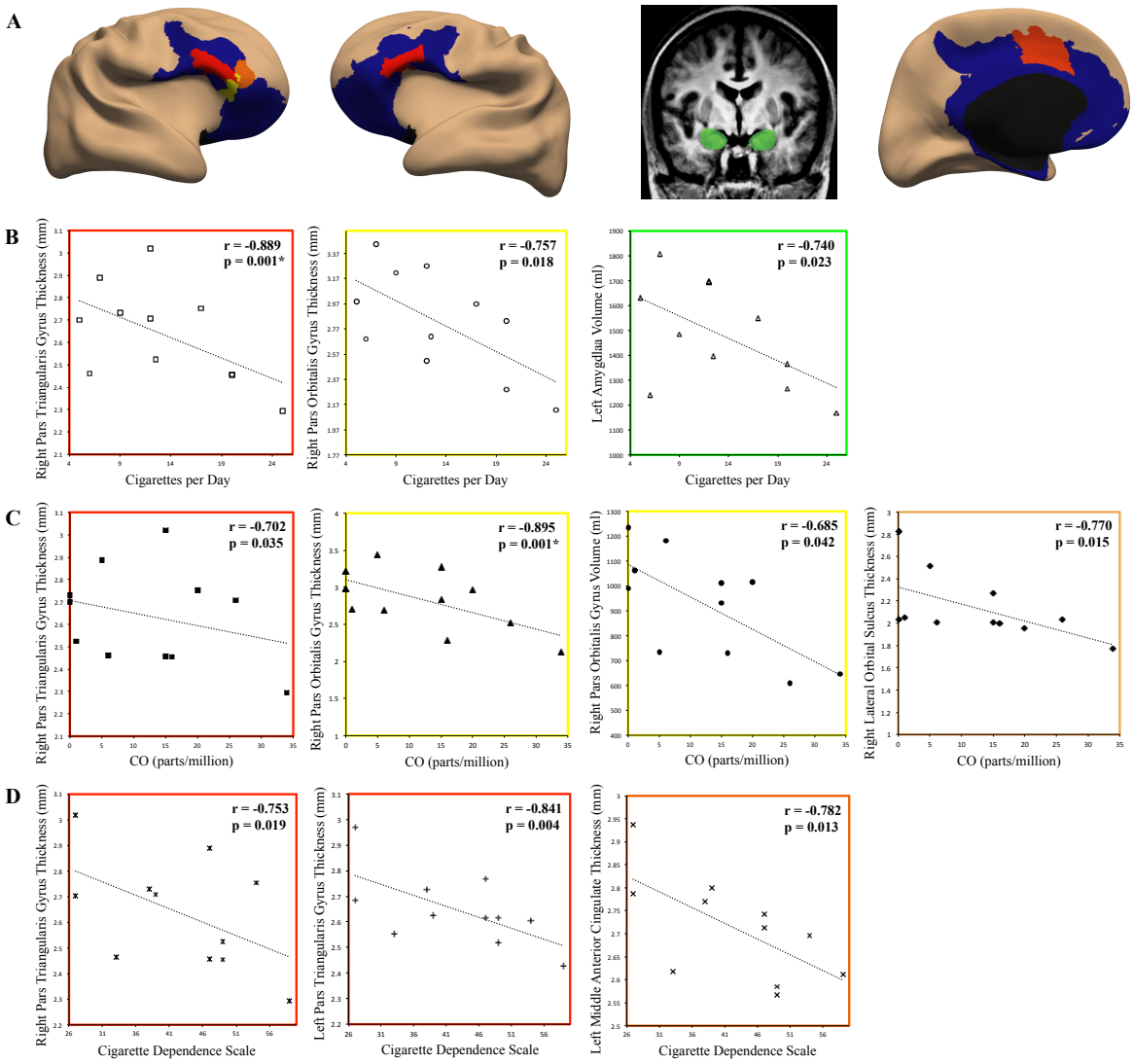

Figure 4.3: Volume and thickness findings within smokers and how they correlate with measurements of cigarette consumption and cigarette dependence severity. A. Cortical thickness and volume findings in smokers projected on an inflated average brain created from the sample population. Left most brain displays the right pars triangularis (red), pars orbitalis (yellow), and lateral orbital sulcus (bright orange). The second brain shows the left pars triangularis in red. The third image is an anatomical MRI highlighting the amygdala. The right most brain displays the left middle anterior cingulate in dark orange. B. Correlations between cortical thickness/volume and subcortical volumes, and cigarettes per day. C. Correlations between cortical thickness/volume and breath carbon monoxide (CO). D. Correlations between cortical thickness/volume and Cigarette Dependence Scale scores. All plot outlines are colored to match their corresponding cortical or subcortical brain region. The correlation coefficients and p−values displayed are from the partial correlation analysis with bootstrapping.

4.4 Discussion

Overall, smokers were found to have decreased volume and thickness in regions important for episodic prospection and decision-making than non−smokers, and within smokers cortical thickness and volume was found to decrease with increasing cigarette consumption and dependence.

4.4.1 Structural differences between cigarette smokers and non−smokers

Consistent with our hypothesis, smokers had decreased volume in the left hippocampus and decreased cortical thickness in the left posterior ventral cingulate gyrus compared to nonsmokers. Both the hippocampus and cingulate are part of the circuitry required for episodic prospection and decision−making. Decreased volumes and cortical thickness in these areas could translate to reduced functionality of these areas, rendering smokers with an inability to truly prospect and appreciate how choosing delayed reward could be better than the instant gratification of smoking now. Decreased hippocampal volume has been previously documented in cigarette smokers, and this decrease in volume likely plays a role in the cycle of cigarette addiction [115]. Contrary to our hypothesis and adding breadth to the literature, we also found an increase in volume in the right middle posterior cingulate cortex of smokers compared to nonsmokers, a region important for emotional awareness. Increases in volume could result from increased neuronal connections, increased astrocytes, inflammation, and edema. However, as this finding was barely significant it is likely that with a larger sample size this effect would not have been observed, and thus it should be interpreted with caution.

4.4.2 Grey matter thickness and volume negatively correlates with cigarette consumption and addiction severity

Within smokers, most of the findings reside in the right hemisphere and particularly within the right inferior frontal gyrus (IFG) regions, the pars triangularis and pars orbitalis. While we did not detect a difference by group for inferior frontal gyrus regions, a recent study with a larger sample size did detect this effect of group [113]. Of the regions displaying inverse relationships with measures of cigarette dependence, only the right pars triangularis cortical thickness negatively correlated with all three smoking measures. This region showed decreased cortical thickness with increasing number of cigarettes, increasing CO concentration, and with increasing addiction severity as measured with the CDS. The left pars triangularis cortical thickness also correlated negatively with Cigarette Dependence Scale scores. This is the first study to show cortical thickness measurements within smokers to correlate with scores on the CDS, as most other smoking studies default to the FTND to measure cigarette addiction severity.

The region with the second most number of relationships was the right pars orbitalis, whose cortical thickness negatively correlated with cigarettes per day and CO, and its volume with CO. In addition to these two regions of the inferior frontal gyrus, other regions found to have significant negative correlations were the left amygdala volume (cigs/day), right lateral orbital sulcus thickness (CO), and left middle anterior cingulate thickness (CDS). Together, all of these regions are important for cognitive control, resisting the desire to make impulsive choices, processing of emotional stimuli, episodic retrieval, and decision−making [155; 156; 157; 158; 159; 160; 161; 162].

Decreased cortical thicknesses and volumes in these areas may lead to decreased ability of these regions to perform their functions, leading to more impulsive choices and impaired decision making. Functional studies where smokers are asked to purposefully

resist an immediate reward for a delayed reward show hyperactivity, or increased recruitment in these areas compared to normal controls [160]. This increased recruitment suggests a deficit in function, where more neurons are required to perform the same cognitive task that normal individuals require less neurons to do. Impaired function in these regions is also supported by the definition of cigarette addiction, where behavior is characterized by the continued preference for immediate gratification of continuing to smoke even in the face of negative consequences. Additionally, reduced functionality of these regions was also shown through hypoactivity of the anterior cingulate (ACC), inferior frontal gyrus, and posterior cingulate (PCC) on an affective stroop task measuring reactivity to negative emotional cues [163]. The authors deduced that this hypoactivity in the ACC, IFG, and PCC supported the notion that chronic cigarette use may handicap inhibitory control and conflict resolution of emotionally salient distractors, and that this reduction may lead to the recruitment of additional brain regions during negative emotional decision making. Further, the direction of the effect suggested that smokers were biasing their attention away from negative cues, thereby reinforcing the use of cigarette through increased affect.

While most findings within smokers also did not survive FDR correction, the consistency of the findings across measures of cigarette consumption and addiction severity makes these effects more believable and likely to be found in the case of a larger sample size. Some relationships within smokers also trended towards significance such as the left hippocampus volume (CO, $p = 0.052$, r $= -0.662$), right pars opercularis thickness (CDS, $p = 0.052$, r $= -0.662$), and right fontal inferior sulcus thickness (CO, $p = 0.052$, r $= -0.661$). Areas found to be different in smokers and nonsmokers, the left posterior ventral cingulate gyrus thickness and right middle posterior cingulate volume did not significantly correlate with cigs/day, CO or CDS in smokers, which means other smoking variables must contribute to the difference between groups.

4.4.3 Limitations

With a small sample size, this study has clear limitations in terms of the generalizability of the findings. The results reported here will serve as hypotheses for future larger imaging studies. Further, analysis of cortical regions within the temporal lobe was impaired due to low signal contrast, prohibiting from investigating all cortical regions important for this circuitry of episodic prospection and decision making. Also as a cross sectional analysis, we can not know whether the findings reported here are caused by cigarette smoking, or are pre−existing differences in the brain structure of individuals that make them more likely to become dependent on cigarettes. However, animal literature demonstrates that exposure to the components of cigarette smoke causes neuronal cell death through direct toxicity, oxidative stress, and increased inflammation [151; 152; 153]. While this study specifically examines regions important for episodic prospection and decision−making, it does not explicitly test whether episodic prospection is impaired in cigarette smokers and whether an impairment correlates with cigarette consumption and addiction severity. Results from this study should be used as hypotheses in a larger imaging study directly investigating these questions.

4.4.4 Conclusions

The present findings are in line with the existing body of literature looking not only between smokers and non−smokers, but within smokers as a function of addiction severity. Overall our findings support the hypothesis that gray matter in brain regions implicated in episodic prospection and decision−making are decreased in smokers compared to non−smokers, with regional gray matter thicknesses and volumes negatively correlating with measures of cigarette habit intensity.

CHAPTER 5

DISCUSSION

5.1 Aim of this dissertation

Through this study we sought to determine if there are any structural differences between cigarette smokers and non−smokers in the circuitry important for episodic prospection and decision making through the use of DTI and sMRI analysis. Further, we investigated within smokers whether there were any structural changes in this circuitry that correlated with measurements of cigarette consumption (cigarettes per day and breath carbon monoxide), and addiction severity as measured with the cigarette dependence scale (CDS). Specifically we studied the white matter tracts the cingulum, fornix, and uncinate, and the grey matter regions that these tracts connect, namely regions of the medial temporal lobe and the prefrontal cortex. Our hypotheses were that smokers would have decreased white matter structural integrity in the tracts bilaterally compared to nonsmokers, and that the brain regions served by these tracts would have decreased volume and thickness in smokers compared to non−smokers. Within smokers, we hypothesized that with increasing cigarette consumption and addiction severity there would be decreased white matter integrity, and decreased regional grey matter volume and thickness.

5.2 Brief results summary

DTI analysis provided findings within the fornix and cingulum, while sMRI analysis complemented the DTI investigation with results in the hippocampus, cingulate, amygdala, OFC, and inferior frontal gyrus. All of these regions are implicated in the circuitry important for episodic prospection, cognitive control, and conflict resolution in decision−making [155; 156; 157; 158; 159; 160; 161; 162].

Group differences were found between the two methods that provide strong evidence supporting the assertion that cigarette smokers have altered circuitry important for episodic prospection, and decision−making. While findings of decreased white matter integrity in the fornix crus and body of smokers is new for the field studying cigarette dependence, the result showing decreased left hippocampal volume in smokers compared to non−smokers falls in line with prior studies [115]. Both group results are in line with our hypothesis that smokers would demonstrate white matter of lower integrity and decreased grey matter volume.

However, findings within smokers provide an interesting story for how white and grey matter integrity relate to measurements of cigarette consumption and addiction severity. Within smokers, with increasing cigarette consumption and dependence we measured increased white matter integrity or organization within the fornix and cingulum bilaterally. Both of these findings are new for the field, and are contrary to our hypothesis for the effect of smoking variables on white matter integrity. While prior DTI literature provides mixed results as to the direction of group effect on white matter integrity, almost all studies to find a relationship between white mater integrity and measurements of smoking consumption and dependence have demonstrated a negative relationship [104; 110; 106; 107]. However, as pointed out in the Smoking DTI Chapter, all prior DTI smoking literature has relied on less specific and localized analysis techniques for the measurement of diffusion parameters than what was employed in

this dissertation. With along the tract analysis of diffusion becoming the gold standard for DTI investigation, hopefully these positive correlations will be replicated by future studies. Either way, along the tract analysis provides a more realistic picture of diffusion in individual fiber tracts, and a better insight to the potential differences in neurobiology among smokers. These findings provide interesting hypotheses to follow up on in future work.

While DTI analysis found a positive correlation between white matter integrity and measurements of cigarette consumption and addiction severity, sMRI analysis found negative correlations between these same measures and findings of brain region cortical thickness and volume within smokers. Structures demonstrating decreased volume and thickness were two regions of the inferior frontal gyrus (pars triangularis and pars orbitalis), lateral orbital frontal sulcus, middle anterior cingulate, and amygdala. These regions are all functionally related to the weighing of emotional features of a decision, impulse inhibition, and cognitive control [155; 156; 157; 158; 159; 160; 161; 162]. A previous study found that chronic cigarette smoking is associated with reduced functionality of the inferior frontal gyrus in inhibitory control, and the anterior cingulate in conflict resolution when an emotional distractor is present [163]. A separate study also came to the same conclusion that the inferior frontal gyrus showed decreased functionality in cigarette smokers compared to nonsmokers, and it demonstrated this decrease in function through increased activation when smokers tried to resist an immediate small reward to hold out for a delayed larger reward [160]. The authors suggested that this increase in activation could reflect the need for increased neuronal recruitment to perform the same task a non−addicted individual would require less neuronal activity to perform.

Decreased cortical thickness and volumes in these regions with increasing cigarette use, as well as addiction severity suggests that cigarette smoking may cause damage to

neurons and result in cell death. Cigarette smoke is composed of over 7000 chemicals, many of which are known carcinogens and toxins [3]. Besides through direct toxicity of cells from the many chemicals in cigarette smoke, this chemical milieu also leads to increased leakiness of the blood brain barrier, oxidative stress, and upregulation of inflammatory cytokines, all of which can cause further secondary damage to neurons [153; 152; 151]. There is work showing that those with a history of cigarette smoking lose volume in the pars triangularis, pars orbitalis, lateral orbitofrontal cortex, posterior cingulate gyrus, and isthmus of the cingulate gyrus at an increased rate compared to non−smokers [164]. Indicating, that just a history, not even current smoking, is associated with long term changes in the brain that lead to increased rate of cortical atrophy in regions important for memory, impulse control, and decision−making.

Thus, what our results may imply is that as cigarette consumption and dependence increase, the exposure to the components of cigarette smoke may cause cellular damage and ultimately neuronal cell death as visualized by the decrease in gray matter thickness and volume. This cell death would lead to a loss of axons composing the white matter tracts that serve to connect this circuitry for episodic prospection and decision−making. With a loss of cells, there are less cells in these regions to perform their necessary function, likely resulting in a functional deficit. As this insult likely is chronic and occurs over a long period of time, the brain may try to structurally compensate for this loss of cells by strengthening or reorganizing the connectivity between these brain regions, thus enhancing the white matter integrity of these fiber bundles in hopes to rescue some functionality and ultimately behavior. Alternatively, these differences in brain region thickness and volume could equally indicate structural aberrations that predispose individuals to become cigarette dependent and to smoke to a certain extent, or a mixture of structural predisposition and damage caused by smoking.

5.3 Circuit components with significant results in both DTI and sMRI analysis

5.3.1 Group differences in the fornix and hippocampus

In the DTI analysis, smokers were found to have decreased structural integrity in the fornix crus and body bilaterally compared to nonsmokers. This finding relates to the sMRI result that smokers have smaller left hippocampal volume than non−smokers. While the hippocampus is composed of much more than the cells that create the fornix, the fornix is the white matter projection of the hippocampus that allows it to communicate with other regions of the brain as it orchestrates the formation and recall of memory. Decreased volume in the hippocampus is typically taken to represent the loss of neurons through cell death, or a loss of neuropil. With loss of neuron cell bodies, the fiber tract of the fornix could be affected and the integrity decreased if the cells lost were those that form the fornix. If this is the case though, the question is then why is the decrease in white matter integrity only in the fornix crura and body? Specifically, why is it not also in the fimbria, the part of the fornix still housed in the hippocampus?

The crura is the location on the fornix where there are commissural fibers that form a web between the two fornix crus, serving as the main form of communication between the left and right hippocampi, and the fornix body is the only section of the fornix where the left and right are together as one tract. Whether this anatomical feature could have something to do with the decreased white matter integrity is unknown. Perhaps these fibers that allow for inter−hemispheric communication are particularly vulnerable to possible insult that may be caused by cigarette smoking, or this region could represent a structural difference that makes individuals more likely to become smokers. Perhaps a decreased structural integrity in this region of the fornix impairs cross referencing between hippocampi and thus leads to cigarette smokers only best appreciating the now with a decreased ability to access the past or to prospect into the future.

To our knowledge this is the first time that the fornix has been analyzed in cigarette smokers. However, previous work has found decreased hippocampal volume in smokers compared to non−smokers, backing up the validity of our data and suggesting that this finding in the fornix is worth following up on in future investigations [115]. This paper also found that increased hippocampal volume, particularly on the left, corresponded to better learning and memory. This would make sense since smokers are known to perform more poorly on tasks assessing learning and memory [165; 166]. Damage to either the fornix or hippocampus would impair the use of memory in decision−making, a process important for daily life and specifically behavioral choices such as the choice between smoking now or abstaining for future improved health.

5.3.2 How measurements of smoking consumption and severity affect the cingulum and cingulate

For both measures of cigarette consumption (cigarettes/day and exhaled CO) and cigarette dependence scale scores, positive relationships were found with white matter integrity bilaterally. Unlike findings in the fornix, for the cingulum, the largest bilateral effect is found with exhaled CO, particularly for the anterior cingulum. This may be due to the fact that the cingulum may be more affected by the biological cascade of neurotransmitters caused by the main addictive component in cigarettes, nicotine. The cingulate cortex, particularly the anterior cingulate, has a large amount of nAChRs which nicotine can bind and alter behavior via long term potentiation of glutamate signaling, which would could contribute to increased tract stability or organization with increased smoking.

While the white matter tract findings in the cingulum related positively with measures of cigarette consumption and addiction severity, grey matter cortical thickness of the left middle anterior cingulate thickness negatively correlated with CDS scores. Here

this decrease in thickness could represent cell death, and the increased white matter integrity of the cingulum feeding this region of the cortex may represent a reorganization of the tract in order to functionally compensate for the decrease in neurons available to perform the same function. Much of the fMRI literature in smokers focuses on the anterior aspect of the cingulate cortex and its involvement in responses to cigarette and smoking cues. This misallocated attention to cigarettes cues is thought to play a role in cigarette craving, and to ultimately be what leads to relapse during a quit attempt. The role of the anterior cingulate in emotional valuation of cues, and top−down inhibition is altered in cigarette smokers. The structural changes in cortical thickness and a restructuring of the white matter bundle for compensation, may lead to this altered behavior.

5.4 Implications of findings on clinical practice

Knowing that these areas necessary for episodic memory and prospection are structurally deficient in smokers compared to non−smokers is important and has potential implications for behavior and treatment. The ability to draw upon past experiences and to realistically weigh the future consequences of choices are skills utilized every day when making decisions about how to lead our life. Smokers have already been shown to perform less well than non−smokers on measures of episodic memory, and our findings provide possible structural explanations for this behavioral difference [165]. The ability to think in a detailed manner about yourself in the past and future is particularly pertinent when enrolled in cognitive behavioral therapy, one of the main strategies of treatment available to cigarette users when looking for help in quitting smoking. If the circuit required to perform the tasks in therapy are damaged in cigarette smokers either prior to smoking or as a result of smoking, then it is no surprise that the success rate of cessation is so low when long term end points are evaluated (a year or more). Perhaps

strategies or exercises to improve episodic prospection could be beneficial before the initiation of cognitive behavioral therapy. Although, since individuals with cigarette dependence also demonstrate low self−control, it is unlikely that they will stick with a training regimen prior to starting treatment.

Which leads into our findings within smokers that let us know that regions of the brain required for impulse control, emotional salience of cues, and conflict resolution in decision−making are important for and have strong relationships to the heaviness of smoking, as well as the severity of the addiction. These results give structural support to behavioral findings demonstrating that cigarette smokers behave more impulsively than normal controls on measures of impulsivity, such as the delay discounting (DD) task [167; 168; 169; 170; 171; 56; 172]. Further, the level of impulsivity within smokers on the DD task has been shown previously to positively correlate with higher smoking rates [173; 174; 131; 171], an earlier age of smoking onset [175], and a shorter time to relapse after a quit attempt [176; 177].

5.5 How our findings in cigarette smokers relate to other forms of addiction

It is cautionary to compare structural brain alterations across addictions, because each substance will likely affect the brain differently. However, while some of our results could reflect the brains exposure to cigarette smoke specifically, it is likely that our findings are also in part a result of the process of addiction formation and maintenance, or biological predisposition to addiction disorders. These latter two components may have shared features between addiction disorders. Some of these shared features could represent genetic predispositions, as most addiction disorders have some genetic influence. While the level of heredity will vary between substances and ethnic groups, it is likely that the heredity will manifest in several domains. For cigarette dependence, the overall heredity is 59%, but the smoking initiation (50%) and cigarette addiction

maintenance likely have separate heritability [178]. Prior studies in alcoholism have consistently found decreased FA in alcoholics, and decreased grey matter volumes [179]. DTI analysis is new in gambling, but a recent study did show decreased FA in the corpus callosum compared to controls [180], however this effect may in part be due to alcohol consumption. This highlights the important point that most addiction disorders are comorbid with other addiction disorders, and with psychiatric disorders. Care must be taken in the data acquisition and analysis to fully control for these confounds.

5.6 All things considered

Together, both the DTI and sMRI analysis performed in this dissertation found results that support the hypothesis that the circuitry implicated in episodic prospection and decision−making is structurally altered in individuals that are cigarette dependent. These structural alterations may contribute to the behavioral impulsivity displayed by cigarette smokers, both in their performance on the delay discounting task and in the real life decision to continue smoking.

The utilization of along the tract DTI analysis furthers our understanding of the neurobiology of this disease. Unlike in prior literature where broad statements were made about entire tracts, using along the tract analysis plainly shows us that changes are not uniform in direction or magnitude along the length of the tract. This makes biological sense as the tracts traverse the brain and connect various cortical and subcortical regions, they enter and are involved in multiple microenvironments that will differ in vulnerability to damage from cigarette smoking.

5.7 Novel components of this study

The analyses performed for this dissertation have several novel components that add to the field study cigarette dependence. The prior DTI literature investigating cigarette

smokers has reported inconsistent results. One reason for these inconsistencies may be the analysis methods used which make it impossible to have localized, tract specific results. In hopes of providing clarity, this study is the first in the cigarette smoking field of research to use an along the tract tractography based DTI analysis. This style of analysis makes it possible for the first time in the smoking literature to analyze diffusion at each millimeter along a singular fiber bundle. This study is also the first to use our along the tract UNC−Utah NA−MIC DTI Fiber Analysis Framework in an adult study sample. While this framework existed prior to my completion of 2 of this dissertation, it was present in separate scripts available for use only in command line format. Now, there are graphical user interfaces for each step of the process, allowing for a smooth analysis of diffusion data for any non−technical user. Further, prior to this study, all of previous application of the tools in our framework were in neonate and infant brain development studies. This study demonstrates that this workflow can be used for the study of adult data, and the framework is now freely available to the entire neuroscience field.

As along the tract analysis of DTI data is a new technique, we are also the first in the cigarette dependence field to pair this DTI analysis style with sMRI analysis. Combining imaging modalities is a powerful technique that enables a more clear perspective as to the biology being observed in the brain, by collecting information on both the white and gray matter. While the DTI and sMRI analysis provide different kinds of information on brain structure, looking at the two information types together helps in determining the full picture. Through multimodal analysis, we were able to uncover a new interesting story that may provide structural evidence for known behavioral differences between smokers and non−smokers, and among those who are cigarette dependent.

Within the cigarette dependence literature, this is the first study to investigate the

fornix, and thus our findings in this tract adds breadth to the literature and provides a new region of the brain worthy of further investigation in cigarette dependence. Lastly, this is the first study to our knowledge to correlate white and grey matter structural findings with the Cigarette Dependence Scale as a measurement of cigarette addiction severity. Most prior studies rely upon the FTND to measure addiction severity, so these analyses provide support for the use of the CDS in future studies.

5.8 Limitations

The limitations to this dissertation are many. The first and largest limitation being the small sample size for analysis that limits the generalizability of the results, and requires replication. While our sample size is similar to other studies published in the literature, we acknowledge that there are many factors involved in cigarette dependence that were not investigated directly, or controlled for in this study due to limited power. Ideally we would like to have considered family history of cigarette dependence, common polymorphisms in important enzyme genes that regulate dopamine levels such as DAT and COMT, as well as nAChR SNPs that could contribute to addiction disorders. We did not collect information on the use of other legal and illegal substances, which is an important detail to consider in cigarette smokers as alcohol consumption and the use of other drugs is often comorbid with cigarette dependence. Other studies also often look at how age of onset affects cigarette addiction severity, and have found those who start smoking at an earlier age to be more impaired on measures of working memory [**?**]. While we did not look at age of onset in our study, we did control for participant age, which positively correlated with age of onset for the DTI study, but not the sMRI analysis. Age of onset did however negatively correlate with craving prior to the scan, which highlights yet another facet of addiction (craving) that we would like to further investigate. Due to these limitations, our results are preliminary and will form the basis

for future scientific inquiry within the lab.

Further, the data analyzed here were collected within a study thats main focus was fMRI analysis, thus the DTI and sMRI acquisition sequences, and field of views were not optimal for these methods of analysis. For example, there were several regions of the brain that could not be analyzed in the structural analysis with FreeSurfer as the signal intensity was too low in regions of the temporal pole and superior frontal and parietal cortices. This limited our analysis of the circuitry involved in episodic prospection and decision−making as we could not interrogate the temporal lobe cortical regions for effect of group or cigarette consumption and dependence. While this limited the analysis in this dissertation, it did allow us to recognize the situation, and to adjust our DTI and sMRI protocols for other studies in the lab where data acquisition was ongoing or still in the planning stages. So through this dissertation, our lab will now have better DTI and sMRI acquisition sequences going forward, and frameworks with which to analyze the data.

5.9 Remaining questions and future studies in an ideal world

What is not known, and what has not been shown in the literature is whether these deficits and deviations from normal structure and function are prior existing differences in individuals that make them more susceptible to trying and becoming dependent on cigarettes, or are these deviations in structure and function caused by the addiction to cigarettes either through insult or by altering the neurobiology and connectivity landscape, or both? In order to know the answer to this question, longitudinal studies are needed to analyze the brains of individuals before they begin smoking, see which individuals choose to smoke, which ones become dependent, and how the amount and time of smoking changes the structural and functional integrity of their brain.

Cognitive behavioral therapy may help in deflecting impulsive choice by distracting

attention from the immediate reward and purposefully placing attention on the delayed reward. Episodic prospection is a key component of cognitive behavioral therapy. Thus, while this study was motivated by two papers demonstrating that the use of episodic prospection during the delayed reward discounting tasks could decrease delay discounting/impulsive choice in healthy controls, this hypothesis remains to be tested in cigarette smokers.

An ideal cross sectional study would be to recruit a large number of cigarette dependent individuals, and an age and sex matched group of never−smokers ages 18−40. Participants should be right handed, non−pregnant, have no contraindications to MRI, no psychoactive medication use, or any serious medical illness. Non−smokers should be defined as never−smokers, and smokers would be defined as consuming 15 or more cigarettes per day for the past year. there would be two study sessions, where in the first session participants will come to the lab and fill out questionnaires and self−report measures assessing cigarette consumption, dependence and other variables often comorbid with smoking. These measures would include the Cigarette Dependence Scale, the Fagerstrm Test for Nicotine Dependence, Minnesota Nicotine Withdrawal Questionnaire, a cigarette craving questionnaire, a family history of smoking questionnaire, an IQ measurement, Barratt Impulsivity Scale, AUDIT, Drug Use Inventory, Beck Depression Inventory, State−Trait Anxiety Inventory, BMI, and Hollingshead Socioeconomic Status. Importantly, also during this first session they will fill out a calendar of important events coming up in their life for the next year and rate each event on personal relevance, arousal, and valence. It is from these events that we will construct an episodic prospection version of the delayed discounting task. This first session will conclude with a training session in the mock scanner where participants can be exposed to the normal delay discounting task, and their personal discounting rate will be assessed. A saliva sample will be collected at both visits to ensure at least one quality

sample and ample amount of material for genetic analysis of various COMT, VAT, DA receptor, and nAChR SNPs implicated in cigarette dependence. The second session will require an exhaled CO measurement prior to scanning, a practice round of the normal delay discounting task, and then performance of the experimental trials while within the scanner. The experimental delay discounting task will include the normal condition trials of Want, Dont Want, Sooner, and Larger, as well as an Episodic Want condition. The normal and episodic want conditions will occur for the same number of trials. The episodic want conditions will appear the same as the want condition options with the addition of an episodic tag from that participants calendar of events for the appropriate timing of the delay option. This experiment would allow us to explicitly test whether episodic prospection changes the delay discounting behavior of smokers compared to non−smokers, and if the behavior within smokers varies by any of the collected questionnaires relevant for cigarette dependence.

This ideal study could be adjusted for the gold standard of longitudinal analysis if recruitment of participants occurred at about age 10, prior to the development of cigarette dependence. Recruitment would be established on baseline behavioral impulsivity as measured by the normal delay discounting task. We would want an even amount of low and high discounters to assess whether this measure of behavioral impulsivity is something that exists prior to cigarette dependence, and that predisposes individuals to trying cigarettes and becoming dependent. We would also want an even split of individuals with and without family history of cigarette smoking. Cigarette dependence has been show to be 75% heritable, thus having an equal representation of the genetically predisposed and normal individuals will allow us to make statements of heritability and how it interacts with the use of episodic prospection to alter behavioral impulsivity [181]. Anatomical, DTI, resting state functional, and delay discounting task fMRI imaging would be acquired at each test visit, along with the questionnaires.

These acquisition sequences would be optimized for high quality data for each type of image, and include a field of view containing the entire head of each participant. The state of each participants acquisition would also be quality controlled in real time to ensure that each acquisition meets the standard of an acceptable image. This would require a lengthy scan time, but in this fantasy, funds are limitless and participants stay still for long periods of time. Visits would be at intake (10 yrs old) and then every five years afterward until age 60, with a total 11 visits. This span of time aims to catch individuals before exposure to cigarettes, during the years of cigarette experimentation, the transition to dependence, the years where quit attempts occur and fail, the time around 40 yrs old when quit attempts start to achieve a better rate of success, and then twenty years post quit to see if any structural or functional insults from cigarette smoking resolve with cessation.

5.10 In conclusion

Through the study of both DTI and sMRI data we found smokers to have decreased integrity in brain regions implicated in episodic prospection, decision making, and impulse control. These findings give structural support to behavioral literature documenting that smokers show decreased impulse control, perform impulsively in decision making tasks, and perform poorly on measures of episodic memory. Prospective studies are needed to know what comes first, the structural aberration or the addiction, but using our new method for DTI analysis can help provide more detailed results for diffusion along individual fiber bundles. These more specific and localizable results will help in better understanding the neurobiology of cigarette dependence. Through a better understanding of the neurobiology of cigarette addiction, we can create more effective therapies that smokers would want to use to aid in their cessation attempts.

BIBLIOGRAPHY

[1] W. H. Organization, "Who tobacco fact sheet n339," July 2013.

[2] W. H. Organization, "Who report on the global tobacco epidemic, 2011," report, World Health Organization, 2011.

[3] U. D. of Health and H. Services, "How tobacco smoke causes disease: What it means to you," Atlanta, 2010.

[4] A. Mokdad, J. Marks, D. Stroup, and J. Gerberding, "Actual causes of death in the united states, 2000," *JAMA: Journal of the American Medical Association*, vol. 291, no. 10, pp. 1238–45, 2004.

[5] C. for Disease Control and Prevention, "Annual smoking-attributable mortality, years of potential life lost, and productivity losses - united states, 2000 - 2004," report, 2008.

[6] U. D. of Health and H. Services, "The health consequences of smoking: A report of the surgeon general," report, U.S. Department of Health and Human Services, CDC, 2004.

[7] C. for Disease Control and Preventions, "Current cigarette smoking among adults - united states 2011," report, 2012.

[8] J. Anthony, L. Warner, and R. Kessler, "Comparitive epidemiology of dependence on tobacco, alcohol, controlled substances, and inhalants: Basic findings from the national comorbidity survey," *Experimental and Clinical Psychopharmacology*, vol. 2, pp. 244–268, 1994.

[9] M. C. Fiore, "Treating tobacco use and dependence: 2008 update. u.s. public health service clinical practice guideline executive summary.," *Respiratory Care*, vol. 53, no. 9, pp. 1217–1222, 2008.

[10] C. for Disease Control and Prevention, "Quitting smoking among adults - united states, 2001-2010," report, 2011.

[11] T. M. Piasecki, "Relapse to smoking," *Clin Psychol Rev*, vol. 26, no. 2, pp. 196–215, 2006.

[12] S. Muehlig, *Tobacco Addiction*, pp. 403–428. InTech, 2011.

[13] K. Messer, D. R. Trinidad, W. K. Al-Delaimy, and J. P. Pierce, "Smoking cessation rates in the united states: a comparison of young adult and older smokers," *Am J Public Health*, vol. 98, no. 2, pp. 317–22, 2008.

[14] C. for Disease Control and Prevention, "Best practices for comprehensive tobacco control programs - 2014," report, 2014.

[15] R. Doll, R. Peto, J. Boreham, and I. Sutherland, "Mortality in relation to smoking: 50 years' observations on male british doctors," *BMJ*, vol. 328, no. 7455, p. 1519, 2004.

[16] S. I. Rennard and D. M. Daughton, "Smoking cessation," *Clin Chest Med*, vol. 35, no. 1, pp. 165–176, 2014.

[17] L. F. Stead, R. Perera, C. Bullen, D. Mant, and T. Lancaster, "Nicotine replacement therapy for smoking cessation," *Cochrane Database Syst Rev*, no. 1, p. CD000146, 2008.

[18] S. Shiffman, C. M. Dresler, P. Hajek, S. J. Gilburt, D. A. Targett, and K. R. Strahs, "Efficacy of a nicotine lozenge for smoking cessation," *Arch Intern Med*, vol. 162, no. 11, pp. 1267–76, 2002.

[19] C. Lerman, V. Kaufmann, M. Rukstalis, F. Patterson, K. Perkins, J. Audrain-McGovern, and N. Benowitz, "Individualizing nicotine replacement therapy for the treatment of tobacco dependence: a randomized trial," *Ann Intern Med*, vol. 140, no. 6, pp. 426–33, 2004.

[20] D. P. Sachs, "Effectiveness of the 4-mg dose of nicotine polacrilex for the initial treatment of high-dependent smokers," *Arch Intern Med*, vol. 155, no. 18, pp. 1973–80, 1995.

[21] R. West, P. Hajek, F. Nilsson, J. Foulds, S. May, and A. Meadows, "Individual differences in preferences for and responses to four nicotine replacement products," *Psychopharmacology (Berl)*, vol. 153, no. 2, pp. 225–30, 2001.

[22] A. Cepeda-Benito, J. T. Reynoso, and S. Erath, "Meta-analysis of the efficacy of nicotine replacement therapy for smoking cessation: differences between men and women," *J Consult Clin Psychol*, vol. 72, no. 4, pp. 712–22, 2004.

[23] C. Lerman, R. Tyndale, F. Patterson, E. P. Wileyto, P. G. Shields, A. Pinto, and N. Benowitz, "Nicotine metabolite ratio predicts efficacy of transdermal nicotine for smoking cessation," *Clin Pharmacol Ther*, vol. 79, no. 6, pp. 600–8, 2006.

[24] R. Ray, R. A. Schnoll, and C. Lerman, "Nicotine dependence: biology, behavior, and treatment," *Annu Rev Med*, vol. 60, pp. 247–60, 2009.

[25] K. Cahill, S. Stevens, and T. Lancaster, "Pharmacological treatments for smoking cessation," *JAMA*, vol. 311, no. 2, pp. 193–4, 2014.

[26] J. W. Coe, P. R. Brooks, M. G. Vetelino, M. C. Wirtz, E. P. Arnold, J. Huang, S. B. Sands, T. I. Davis, L. A. Lebel, C. B. Fox, A. Shrikhande, J. H. Heym, E. Schaeffer, H. Rollema, Y. Lu, R. S. Mansbach, L. K. Chambers, C. C. Rovetti, D. W. Schulz, r. Tingley, F. D., and B. T. O'Neill, "Varenicline: an alpha4beta2 nicotinic receptor partial agonist for smoking cessation," *J Med Chem*, vol. 48, no. 10, pp. 3474–7, 2005.

[27] K. Cahill, L. F. Stead, and T. Lancaster, "Nicotine receptor partial agonists for smoking cessation," *Cochrane Database Syst Rev*, no. 1, p. CD006103, 2007.

[28] S. G. Gourlay, L. F. Stead, and N. L. Benowitz, "Clonidine for smoking cessation," *Cochrane Database Syst Rev*, no. 3, p. CD000058, 2004.

[29] J. R. Hughes, L. F. Stead, and T. Lancaster, "Antidepressants for smoking cessation," *Cochrane Database Syst Rev*, no. 1, p. CD000031, 2007.

[30] S. David, T. Lancaster, L. F. Stead, and A. E. Evins, "Opioid antagonists for smoking cessation," *Cochrane Database Syst Rev*, no. 4, p. CD003086, 2006.

[31] R. A. Schnoll and C. Lerman, "Current and emerging pharmacotherapies for treating tobacco dependence," *Expert Opin Emerg Drugs*, vol. 11, no. 3, pp. 429–44, 2006.

[32] I. Esterlis, J. O. Hannestad, E. Perkins, F. Bois, D. C. D'Souza, R. F. Tyndale, J. P. Seibyl, D. M. Hatsukami, K. P. Cosgrove, and S. S. O'Malley, "Effect of a nicotine vaccine on nicotine binding to beta2*-nicotinic acetylcholine receptors in vivo in human tobacco smokers," *Am J Psychiatry*, vol. 170, no. 4, pp. 399–407, 2013.

[33] A. A. Feduccia, S. Chatterjee, and S. E. Bartlett, "Neuronal nicotinic acetylcholine receptors: neuroplastic changes underlying alcohol and nicotine addictions," *Front Mol Neurosci*, vol. 5, p. 83, 2012.

[34] C. Gotti and F. Clementi, "Neuronal nicotinic receptors: from structure to pathology," *Prog Neurobiol*, vol. 74, no. 6, pp. 363–96, 2004.

[35] C. Gotti, M. Moretti, A. Gaimarri, A. Zanardi, F. Clementi, and M. Zoli, "Heterogeneity and complexity of native brain nicotinic receptors," *Biochem Pharmacol*, vol. 74, no. 8, pp. 1102–11, 2007.

[36] C. Gotti, F. Clementi, A. Fornari, A. Gaimarri, S. Guiducci, I. Manfredi, M. Moretti, P. Pedrazzi, L. Pucci, and M. Zoli, "Structural and functional diversity of native brain neuronal nicotinic receptors," *Biochem Pharmacol*, vol. 78, no. 7, pp. 703–11, 2009.

[37] E. X. Albuquerque, E. F. Pereira, M. Alkondon, and S. W. Rogers, "Mammalian nicotinic acetylcholine receptors: from structure to function," *Physiol Rev*, vol. 89, no. 1, pp. 73–120, 2009.

[38] S. Wonnacott, J. Irons, C. Rapier, B. Thorne, and G. G. Lunt, "Presynaptic modulation of transmitter release by nicotinic receptors," *Prog Brain Res*, vol. 79, pp. 157–63, 1989.

[39] E. X. Albuquerque, E. F. Pereira, N. G. Castro, M. Alkondon, S. Reinhardt, H. Schroder, and A. Maelicke, "Nicotinic receptor function in the mammalian central nervous system," *Ann N Y Acad Sci*, vol. 757, pp. 48–72, 1995.

[40] W. A. Corrigall, K. M. Coen, and K. L. Adamson, "Self-administered nicotine activates the mesolimbic dopamine system through the ventral tegmental area," *Brain Res*, vol. 653, no. 1-2, pp. 278–84, 1994.

[41] M. Nisell, G. G. Nomikos, and T. H. Svensson, "Infusion of nicotine in the ventral tegmental area or the nucleus accumbens of the rat differentially affects accumbal dopamine release," *Pharmacol Toxicol*, vol. 75, no. 6, pp. 348–52, 1994.

[42] B. Schilstrom, M. V. Fagerquist, X. Zhang, P. Hertel, G. Panagis, G. G. Nomikos, and T. H. Svensson, "Putative role of presynaptic alpha7* nicotinic receptors in nicotine stimulated increases of extracellular levels of glutamate and aspartate in the ventral tegmental area," *Synapse*, vol. 38, no. 4, pp. 375–83, 2000.

[43] V. I. Pidoplichko, J. Noguchi, O. O. Areola, Y. Liang, J. Peterson, T. Zhang, and J. A. Dani, "Nicotinic cholinergic synaptic mechanisms in the ventral tegmental area contribute to nicotine addiction," *Learn Mem*, vol. 11, no. 1, pp. 60–9, 2004.

[44] H. D. Mansvelder and D. S. McGehee, "Cellular and synaptic mechanisms of nicotine addiction," *J Neurobiol*, vol. 53, no. 4, pp. 606–17, 2002.

[45] M. W. Quick and R. A. Lester, "Desensitization of neuronal nicotinic receptors," *J Neurobiol*, vol. 53, no. 4, pp. 457–78, 2002.

[46] J. R. Wooltorton, V. I. Pidoplichko, R. S. Broide, and J. A. Dani, "Differential desensitization and distribution of nicotinic acetylcholine receptor subtypes in midbrain dopamine areas," *J Neurosci*, vol. 23, no. 8, pp. 3176–85, 2003.

[47] R. Nashmi, C. Xiao, P. Deshpande, S. McKinney, S. R. Grady, P. Whiteaker, Q. Huang, T. McClure-Begley, J. M. Lindstrom, C. Labarca, A. C. Collins, M. J. Marks, and H. A. Lester, "Chronic nicotine cell specifically upregulates functional alpha 4* nicotinic receptors: basis for both tolerance in midbrain and enhanced long-term potentiation in perforant path," *J Neurosci*, vol. 27, no. 31, pp. 8202–18, 2007.

[48] M. E. Nelson, A. Kuryatov, C. H. Choi, Y. Zhou, and J. Lindstrom, "Alternate stoichiometries of alpha4beta2 nicotinic acetylcholine receptors," *Mol Pharmacol*, vol. 63, no. 2, pp. 332–41, 2003.

[49] N. L. Benowitz, "Neurobiology of nicotine addiction: implications for smoking cessation treatment," *Am J Med*, vol. 121, no. 4 Suppl 1, pp. S3–10, 2008.

[50] C. R. Breese, M. J. Marks, J. Logel, C. E. Adams, B. Sullivan, A. C. Collins, and S. Leonard, "Effect of smoking history on [3h]nicotine binding in human postmortem brain," *J Pharmacol Exp Ther*, vol. 282, no. 1, pp. 7–13, 1997.

[51] N. Benowitz, P. Jacob, K. Ahijevych, M. Jarvis, S. Hall, J. LeHouezec, A. Hansson, E. Lichtenstein, J. Henningfield, J. Tsoh, R. Hurt, and W. Velicer, "Biochemical verification of tobacco use and cessation.," *Nicotine and Tobacco Reesearch*, vol. 4, pp. 149–159, 2002.

[52] T. F. Heatherton, L. T. Kozlowski, R. C. Frecker, and K. O. Fagerstrom, "The fagerstrom test for nicotine dependence: a revision of the fagerstrom tolerance questionnaire," *Br J Addict*, vol. 86, no. 9, pp. 1119–27, 1991.

[53] J. F. Etter, "A comparison of the content-, construct- and predictive validity of the cigarette dependence scale and the fagerstrom test for nicotine dependence," *Drug Alcohol Depend*, vol. 77, no. 3, pp. 259–68, 2005.

[54] J. F. Etter, "Comparing the validity of the cigarette dependence scale and the fagerstrom test for nicotine dependence," *Drug Alcohol Depend*, vol. 95, no. 1-2, pp. 152–9, 2008.

[55] J. F. Etter, J. Le Houezec, and T. V. Perneger, "A self-administered questionnaire to measure dependence on cigarettes: the cigarette dependence scale," *Neuropsychopharmacology*, vol. 28, no. 2, pp. 359–70, 2003.

[56] B. Reynolds, "A review of delay-discounting research with humans: relations to drug use and gambling," *Behavioural Pharmacology*, vol. 17, no. 8, pp. 651–667, 2006.

[57] J. MacKillop, M. T. Amlung, L. R. Few, L. A. Ray, L. H. Sweet, and M. R. Munafo, "Delayed reward discounting and addictive behavior: a meta-analysis," *Psychopharmacology (Berl)*, vol. 216, no. 3, pp. 305–21, 2011.

[58] S. H. Mitchell and V. B. Wilson, "Differences in delay discounting between smokers and nonsmokers remain when both rewards are delayed," *Psychopharmacology (Berl)*, vol. 219, no. 2, pp. 549–62, 2012.

[59] J. M. Mitchell, H. L. Fields, M. D'Esposito, and C. A. Boettiger, "Impulsive responding in alcoholics," *Alcoholism, clinical and experimental research*, vol. 29, no. 12, pp. 2158–69, 2005.

[60] M. E. Hasselmo, "A model of episodic memory: mental time travel along encoded trajectories using grid cells," *Neurobiology of learning and memory*, vol. 92, no. 4, pp. 559–73, 2009.

[61] M. E. Hasselmo, L. M. Giocomo, M. P. Brandon, and M. Yoshida, "Cellular dynamical mechanisms for encoding the time and place of events along spatiotemporal trajectories in episodic memory," *Behavioural brain research*, vol. 215, no. 2, pp. 261–74, 2010.

[62] K. B. McDermott, K. K. Szpunar, and S. E. Christ, "Laboratory-based and autobiographical retrieval tasks differ substantially in their neural substrates," *Neuropsychologia*, vol. 47, no. 11, pp. 2290–8, 2009.

[63] S. M. Daselaar, H. J. Rice, D. L. Greenberg, R. Cabeza, K. S. LaBar, and D. C. Rubin, "The spatiotemporal dynamics of autobiographical memory: neural correlates of recall, emotional intensity, and reliving," *Cerebral cortex*, vol. 18, no. 1, pp. 217–29, 2008.

[64] R. Cabeza and P. St Jacques, "Functional neuroimaging of autobiographical memory," *Trends in cognitive sciences*, vol. 11, no. 5, pp. 219–27, 2007.

[65] E. A. Kensinger, "Remembering the details: Effects of emotion," *Emotion review*, vol. 1, no. 2, pp. 99–113, 2009.

[66] E. Svoboda, M. C. McKinnon, and B. Levine, "The functional neuroanatomy of autobiographical memory: a meta-analysis," *Neuropsychologia*, vol. 44, no. 12, pp. 2189–208, 2006.

[67] M. St-Laurent, H. Abdi, H. Burianova, and C. L. Grady, "Influence of aging on the neural correlates of autobiographical, episodic, and semantic memory retrieval," *Journal of cognitive neuroscience*, 2011.

[68] D. R. Addis, A. T. Wong, and D. L. Schacter, "Remembering the past and imagining the future: common and distinct neural substrates during event construction and elaboration," *Neuropsychologia*, vol. 45, no. 7, pp. 1363–77, 2007.

[69] Y. D. Van der Werf, J. Jolles, M. P. Witter, and H. B. Uylings, "Contributions of thalamic nuclei to declarative memory functioning," *Cortex; a journal devoted to the study of the nervous system and behavior*, vol. 39, no. 4-5, pp. 1047–62, 2003.

[70] A. Ben-Yakov and Y. Dudai, "Constructing realistic engrams: poststimulus activity of hippocampus and dorsal striatum predicts subsequent episodic memory," *The Journal of neuroscience : the official journal of the Society for Neuroscience*, vol. 31, no. 24, pp. 9032–42, 2011.

[71] K. K. Szpunar, J. C. Chan, and K. B. McDermott, "Contextual processing in episodic future thought," *Cerebral cortex*, vol. 19, no. 7, pp. 1539–48, 2009.

[72] J. J. Summerfield, D. Hassabis, and E. A. Maguire, "Cortical midline involvement in autobiographical memory," *NeuroImage*, vol. 44, no. 3, pp. 1188–200, 2009.

[73] B. H. Schott, C. Niklas, J. Kaufmann, N. C. Bodammer, J. Machts, H. Schutze, and E. Duzel, "Fiber density between rhinal cortex and activated ventrolateral prefrontal regions predicts episodic memory performance in humans," *Proceedings of the National Academy of Sciences of the United States of America*, vol. 108, no. 13, pp. 5408–13, 2011.

[74] E. Svoboda and B. Levine, "The effects of rehearsal on the functional neuroanatomy of episodic autobiographical and semantic remembering: a functional magnetic resonance imaging study," *The Journal of neuroscience : the official journal of the Society for Neuroscience*, vol. 29, no. 10, pp. 3073–82, 2009.

[75] A. Abraham, R. I. Schubotz, and D. Y. von Cramon, "Thinking about the future versus the past in personal and non-personal contexts," *Brain research*, vol. 1233, pp. 106–19, 2008.

[76] C. Metzler-Baddeley, D. K. Jones, B. Belaroussi, J. P. Aggleton, and M. J. O'Sullivan, "Frontotemporal connections in episodic memory and aging: a diffusion mri tractography study," *The Journal of neuroscience : the official journal of the Society for Neuroscience*, vol. 31, no. 37, pp. 13236–45, 2011.

[77] S. R. Rudebeck, J. Scholz, R. Millington, G. Rohenkohl, H. Johansen-Berg, and A. C. Lee, "Fornix microstructure correlates with recollection but not familiarity memory," *The Journal of neuroscience : the official journal of the Society for Neuroscience*, vol. 29, no. 47, pp. 14987–92, 2009.

[78] D. L. Schacter, D. R. Addis, and R. L. Buckner, "Episodic simulation of future events: concepts, data, and applications," *Annals of the New York Academy of Sciences*, vol. 1124, pp. 39–60, 2008.

[79] D. C. M. Suddendorf, T.; Addis, "Mental time travel and the shaping of the human mind," *Philosophical transactions of the Royal Society B*, vol. 364, pp. 1317–1324, 2009.

[80] J. Peters and C. Bchel, "Episodic future thinking reduces reward delay discounting through an enhancement of prefrontal-mediotemporal interactions," *Neuron*, vol. 66, no. 1, pp. 138–48, 2010.

[81] R. G. Benoit, S. J. Gilbert, and P. W. Burgess, "A neural mechanism mediating the impact of episodic prospection on farsighted decisions," *The Journal of*

neuroscience : the official journal of the Society for Neuroscience, vol. 31, no. 18, pp. 6771–9, 2011.

[82] P. S. Merritt, A. R. Cobb, L. Moissinac, and E. Hirshman, "Evidence that episodic memory impairment during tobacco abstinence is independent of attentional mechanisms," *The Journal of general psychology*, vol. 137, no. 4, pp. 331–42, 2010.

[83] J. A. Boening, "Neurobiology of an addiction memory," *J Neural Transm*, vol. 108, no. 6, pp. 755–65, 2001.

[84] A. R. Verde, F. Budin, J. B. Berger, A. Gupta, M. Farzinfar, A. Kaiser, M. Ahn, H. Johnson, J. Matsui, H. C. Hazlett, A. Sharma, C. Goodlett, Y. Shi, S. Gouttard, C. Vachet, J. Piven, H. Zhu, G. Gerig, and M. Styner, "Unc-utah na-mic framework for dti fiber tract analysis," *Front Neuroinform*, vol. 7, p. 51, 2014.

[85] A. Dale, B. Fischl, and M. Sereno, "Cortical surface-based analysis. i. segmentation and surface reconstruction.," *Neuroimage*, vol. 9, pp. 179–194, 1999.

[86] F. Segonne, A. Dale, E. Busa, M. Glessner, D. Salat, H. Hahn, and B. Fischl, "A hybrid approach to the skull stripping problem in mri," *Neuroimage*, vol. 22, no. 1060-1075, 2004.

[87] B. Fischl, D. Salat, E. Busa, M. Albert, M. Dieterich, C. Haselgrove, A. van der Kouwe, R. Killiany, D. Kennedy, S. Klaveness, A. Montillo, N. Makris, B. Rosen, and A. Dale, "Whole brain segmentation: automated labeling of neuroanatomical structures in the human brain," *Neuron*, vol. 33, pp. 341–355, 2002.

[88] J. Sled, A. Zijdenbos, and A. Evans, "A nonparametric method for automatic correction of intensity nonuniformity in mri data," *IEEE Trans Med Imaging*, vol. 17, pp. 87–97, 1998.

[89] B. Fischl, A. Liu, and A. Dale, "Automated manifold surgery: Constructing geomatrically accurate and topologically correct models of the human cerebral cortex," *IEEE Transactions on Medical Imaging*, vol. 20, no. 1, pp. 70–80, 2001.

[90] F. Segonne, J. Pacheco, and B. Fischl, "Geometrically accurate topology-correction of cortical surfaces using nonseparating loops," *IEEE Trans Med Imaging*, vol. 26, pp. 518–529, 2007.

[91] A. Dale and M. Sereno, "Improved localization of cortical activity by combining eeg and meg with mri cortical surface reconstruction: a linear approach," *J Cogn Neurosci*, vol. 5, pp. 162–176, 1993.

[92] B. Fischl and A. Dale, "Measuring the thickness of the human cerebral cortex from magnetic resonance images," in *Proc Natl Acad Sci U S A 97*, pp. 11050–11055, 2000.

[93] M. Reuter, H. Rosas, and B. Fischl, "Highly accurate inverse consistent registration: A robust approach," *Neuroimage*, vol. 53, no. 4, pp. 1181–1196, 2010.

[94] B. Fischl, D. Salat, A. van der Kouwe, N. Makris, F. Segonne, B. Quinn, and A. Dale, "Sequence-independent segmentation of magnetic resonance images," *Neuroimage*, vol. 23, no. Suppl 1, pp. S69–84, 2004.

[95] B. Fischl, M. Sereno, and A. Dale, "Cortical surface-based analysis. ii: Inflation, flattening, and a surface-based coordinate system," *Neuroimage*, vol. 9, pp. 195–207, 1999.

[96] B. Fischl, M. Sereno, R. Tootell, and A. Dale, "High-resolution intersubject averaging and a coordinate system for the cortical surface," *Hum Brain Mapp*, vol. 8, pp. 272–284, 1999.

[97] B. Fischl, A. van der Kouwe, C. Destrieux, E. Halgren, F. Segonne, D. Salat, E. Busa, L. Seidman, J. Goldstein, D. Kennedy, V. Caviness, N. Makris, B. Rosen, and A. Dale, "Automatically parcellating the human cerebral cortex," *Cereb Cortex*, vol. 14, pp. 11–22, 2004.

[98] S. Song, S. Sun, W. Ju, S. Lin, A. Cross, and A. Neufeld, "Diffusion tensor imaging detects and differentiates axon and myelin degeneration in mouse optic nerve after retinal ischemia," *Neuroimage*, vol. 20, pp. 1714–1722, 2003.

[99] A. V. Faria, J. Zhang, K. Oishi, X. Li, H. Jiang, K. Akhter, L. Hermoye, S. K. Lee, A. Hoon, E. Stashinko, M. I. Miller, P. C. van Zijl, and S. Mori, "Atlas-based analysis of neurodevelopment from infancy to adulthood using diffusion tensor imaging and applications for automated abnormality detection," *Neuroimage*, vol. 52, no. 2, pp. 415–28, 2010.

[100] S. M. Smith, M. Jenkinson, H. Johansen-Berg, D. Rueckert, T. E. Nichols, C. E. Mackay, K. E. Watkins, O. Ciccarelli, M. Z. Cader, P. M. Matthews, and T. E. Behrens, "Tract-based spatial statistics: voxelwise analysis of multi-subject diffusion data," *NeuroImage*, vol. 31, no. 4, pp. 1487–505, 2006.

[101] Y. Shi, S. J. Short, R. C. Knickmeyer, J. Wang, C. L. Coe, M. Niethammer, J. H. Gilmore, H. Zhu, and M. A. Styner, "Diffusion tensor imaging-based characterization of brain neurodevelopment in primates," *Cerebral cortex*, vol. 23, no. 1, pp. 36–48, 2013.

[102] B. J. Liu, Z. Liu, Y. Wang, G. Gerig, S. Gouttard, R. Tao, T. Fletcher, M. Styner, and W. W. Boonn, "¡title¿quality control of diffusion weighted images¡/title¿," vol. 7628, pp. 76280J–76280J–9, 2010.

[103] L. K. Jacobsen, M. R. Picciotto, C. J. Heath, S. J. Frost, K. A. Tsou, R. A. Dwan, M. P. Jackowski, R. T. Constable, and W. E. Mencl, "Prenatal and adolescent exposure to tobacco smoke modulates the development of white

matter microstructure," *The Journal of neuroscience : the official journal of the Society for Neuroscience*, vol. 27, no. 49, pp. 13491–8, 2007.

[104] R. H. Paul, S. M. Grieve, R. Niaura, S. P. David, D. H. Laidlaw, R. Cohen, L. Sweet, G. Taylor, R. C. Clark, S. Pogun, and E. Gordon, "Chronic cigarette smoking and the microstructural integrity of white matter in healthy adults: a diffusion tensor imaging study," *Nicotine Tob Res*, vol. 10, no. 1, pp. 137–47, 2008.

[105] Y. Liao, J. Tang, Q. Deng, Y. Deng, T. Luo, X. Wang, H. Chen, T. Liu, X. Chen, A. L. Brody, and W. Hao, "Bilateral fronto-parietal integrity in young chronic cigarette smokers: a diffusion tensor imaging study," *PloS one*, vol. 6, no. 11, p. e26460, 2011.

[106] M. Hudkins, J. O'Neill, M. C. Tobias, G. Bartzokis, and E. D. London, "Cigarette smoking and white matter microstructure," *Psychopharmacology*, vol. 221, no. 2, pp. 285–95, 2012.

[107] W. Huang, J. R. DiFranza, D. N. Kennedy, N. Zhang, D. Ziedonis, S. Ursprung, and J. A. King, "Progressive levels of physical dependence to tobacco coincide with changes in the anterior cingulum bundle microstructure," *PLoS One*, vol. 8, no. 7, p. e67837, 2013.

[108] X. Zhang, E. A. Stein, and L. E. Hong, "Smoking and schizophrenia independently and additively reduce white matter integrity between striatum and frontal cortex," *Biological psychiatry*, vol. 68, no. 7, pp. 674–7, 2010.

[109] F. Lin, G. Wu, L. Zhu, and H. Lei, "Heavy smokers show abnormal microstructural integrity in the anterior corpus callosum: a diffusion tensor imaging study with tract-based spatial statistics," *Drug and alcohol dependence*, vol. 129, no. 1-2, pp. 82–7, 2013.

[110] S. Zhang, J. S. Ide, and C. S. Li, "Resting-state functional connectivity of the medial superior frontal cortex," *Cerebral cortex*, 2011.

[111] R. A. Gons, A. G. van Norden, K. F. de Laat, L. J. van Oudheusden, I. W. van Uden, M. P. Zwiers, D. G. Norris, and F. E. de Leeuw, "Cigarette smoking is associated with reduced microstructural integrity of cerebral white matter," *Brain : a journal of neurology*, vol. 134, no. Pt 7, pp. 2116–24, 2011.

[112] J. Ashburner and K. J. Friston, "Voxel-based morphometry–the methods," *Neuroimage*, vol. 11, no. 6 Pt 1, pp. 805–21, 2000.

[113] J. Gallinat, E. Meisenzahl, L. K. Jacobsen, P. Kalus, J. Bierbrauer, T. Kienast, H. Witthaus, K. Leopold, F. Seifert, F. Schubert, and M. Staedtgen, "Smoking and structural brain deficits: a volumetric mr investigation," *The European journal of neuroscience*, vol. 24, no. 6, pp. 1744–50, 2006.

[114] D. Das, N. Cherbuin, K. J. Anstey, P. S. Sachdev, and S. Easteal, "Lifetime cigarette smoking is associated with striatal volume measures," *Addiction biology*, vol. 17, no. 4, pp. 817–25, 2012.

[115] T. C. Durazzo, A. Mon, S. Gazdzinski, and D. J. Meyerhoff, "Chronic cigarette smoking in alcohol dependence: associations with cortical thickness and n-acetylaspartate levels in the extended brain reward system," *Addiction biology*, vol. 18, no. 2, pp. 379–91, 2013.

[116] T. C. Durazzo, V. A. Cardenas, C. Studholme, M. W. Weiner, and D. J. Meyerhoff, "Non-treatment-seeking heavy drinkers: effects of chronic cigarette smoking on brain structure," *Drug and alcohol dependence*, vol. 87, no. 1, pp. 76–82, 2007.

[117] T. C. Durazzo, D. Tosun, S. Buckley, S. Gazdzinski, A. Mon, S. L. Fryer, and D. J. Meyerhoff, "Cortical thickness, surface area, and volume of the brain reward system in alcohol dependence: relationships to relapse and extended abstinence," *Alcoholism, clinical and experimental research*, vol. 35, no. 6, pp. 1187–200, 2011.

[118] S. Kuhn, F. Schubert, and J. Gallinat, "Reduced thickness of medial orbitofrontal cortex in smokers," *Biological psychiatry*, vol. 68, no. 11, pp. 1061–5, 2010.

[119] T. Zhu, R. Hu, W. Tian, S. Ekholm, G. Schifitto, X. Qiu, and J. Zhong, "Spatial regression analysis of diffusion tensor imaging (spread) for longitudinal progression of neurodegenerative disease in individual subjects," *Magn Reson Imaging*, vol. 31, no. 10, pp. 1657–67, 2013.

[120] R. B. Patil, R. Piyush, and S. Ramakrishnan, "Identification of brain white matter regions for diagnosis of alzheimer using diffusion tensor imaging," *Conf Proc IEEE Eng Med Biol Soc*, vol. 2013, pp. 6535–8, 2013.

[121] G. Du, M. M. Lewis, S. Sen, J. Wang, M. L. Shaffer, M. Styner, Q. X. Yang, and X. Huang, "Imaging nigral pathology and clinical progression in parkinson's disease," *Mov Disord*, vol. 27, no. 13, pp. 1636–43, 2012.

[122] X. Geng, S. Gouttard, A. Sharma, H. Gu, M. Styner, W. Lin, G. Gerig, and J. H. Gilmore, "Quantitative tract-based white matter development from birth to age 2years," *NeuroImage*, vol. 61, no. 3, pp. 542–57, 2012.

[123] C. Lebel, M. Gee, R. Camicioli, M. Wieler, W. Martin, and C. Beaulieu, "Diffusion tensor imaging of white matter tract evolution over the lifespan," *NeuroImage*, vol. 60, no. 1, pp. 340–52, 2012.

[124] Z. Liu, H. Zhu, B. L. Marks, L. M. Katz, C. B. Goodlett, G. Gerig, and M. Styner, "Voxel-wise group analysis of dti," *Proc IEEE Int Symp Biomed Imaging*, pp. 807–810, 2009.

[125] C. B. Goodlett, P. T. Fletcher, J. H. Gilmore, and G. Gerig, "Group analysis of dti fiber tract statistics with application to neurodevelopment," *NeuroImage*, vol. 45, no. 1 Suppl, pp. S133–42, 2009.

[126] H. Zhu, L. Kong, R. Li, M. Styner, G. Gerig, W. Lin, and J. H. Gilmore, "Fadtts: functional analysis of diffusion tensor tract statistics," *NeuroImage*, vol. 56, no. 3, pp. 1412–25, 2011.

[127] S. Pieper, M. Halle, and R. Kikinis, "3d slicer," *IEEE Press*, pp. 632–635, 2004.

[128] M. Farzinfar, I. Oguz, R. G. Smith, A. R. Verde, C. Dietrich, A. Gupta, M. L. Escolar, J. Piven, S. Pujol, C. Vachet, S. Gouttard, G. Gerig, S. Dager, R. C. McKinstry, S. Paterson, A. C. Evans, I. network, and M. A. Styner, "Diffusion imaging quality control via entropy of principal direction distribution," *Neuroimage*, vol. 82, pp. 1–12, 2013.

[129] B. van Ginneken, T. Heimann, and M. Styner, "3d segmentation in the clinic: A grand challenge," *Medical Image Computing and Computer Assisted Intervention*, pp. 37–46, 2007.

[130] P. A. Yushkevich, J. Piven, H. C. Hazlett, R. G. Smith, S. Ho, J. C. Gee, and G. Gerig, "User-guided 3d active contour segmentation of anatomical structures: significantly improved efficiency and reliability," *NeuroImage*, vol. 31, no. 3, pp. 1116–28, 2006.

[131] K. W. H. Johnson, G. Harris, "Brainsfit: mutual information registrations of whole-brain 3d images, using the insight toolkit," *The Insight Journal*, 2007.

[132] J. M. G. G. Joshi S, Davis B, "Unbiased diffeomorphic atlas construction for computational anatomy," *NeuroImage*, vol. 23 Suppl 1, pp. S151–160, 2004.

[133] B. B. Avants, C. L. Epstein, M. Grossman, and J. C. Gee, "Symmetric diffeomorphic image registration with cross-correlation: evaluating automated labeling of elderly and neurodegenerative brain," *Med Image Anal*, vol. 12, no. 1, pp. 26–41, 2008.

[134] A. Klein, J. Andersson, B. A. Ardekani, J. Ashburner, B. Avants, M. C. Chiang, G. E. Christensen, D. L. Collins, J. Gee, P. Hellier, J. H. Song, M. Jenkinson, C. Lepage, D. Rueckert, P. Thompson, T. Vercauteren, R. P. Woods, J. J. Mann, and R. V. Parsey, "Evaluation of 14 nonlinear deformation algorithms applied to human brain mri registration," *Neuroimage*, vol. 46, no. 3, pp. 786–802, 2009.

[135] V. Arsigny, P. Fillard, X. Pennec, and N. Ayache, "Log-euclidean metrics for fast and simple calculus on diffusion tensors," *Magn Reson Med*, vol. 56, no. 2, pp. 411–21, 2006.

[136] I. Corouge, P. T. Fletcher, S. Joshi, J. H. Gilmore, and G. Gerig, "Fiber tract-oriented statistics for quantitative diffusion tensor mri analysis," *Med Image Comput Comput Assist Interv*, vol. 8, no. Pt 1, pp. 131–9, 2005.

[137] J. MacKillop, "Integrating behavioral economics and behavioral genetics: delayed reward discounting as an endophenotype for addictive disorders," *J Exp Anal Behav*, vol. 99, no. 1, pp. 14–31, 2013.

[138] V. W. Chanon, C. R. Sours, and C. A. Boettiger, "Attentional bias toward cigarette cues in active smokers," *Psychopharmacology*, vol. 212, no. 3, pp. 309–20, 2010.

[139] I. Corouge, P. T. Fletcher, S. Joshi, S. Gouttard, and G. Gerig, "Fiber tract-oriented statistics for quantitative diffusion tensor mri analysis," *Medical image analysis*, vol. 10, no. 5, pp. 786–98, 2006.

[140] T. Heatherton, L. Kozlowski, R. Frecker, W. Rickert, and J. Robinson, "Measuring the heaviness of smoking: using self-reported time to the first cigarette of the day and number of cigarettes smoked per day," *Br J Addict*, vol. 84, no. 7, pp. 791–9, 1989.

[141] N. Mello, *Biology of alcoholism*, ch. Bahvioural studies of alcoholism., pp. 210–219. Plenum Press, 1972.

[142] B. J. Everitt and M. E. Wolf, "Psychomotor stimulant addiction: a neural systems perspective," *J Neurosci*, vol. 22, no. 9, pp. 3312–20, 2002.

[143] S. E. Hyman and R. C. Malenka, "Addiction and the brain: the neurobiology of compulsion and its persistence," *Nat Rev Neurosci*, vol. 2, no. 10, pp. 695–703, 2001.

[144] B. Froeliger, R. V. Kozink, J. E. Rose, F. M. Behm, A. N. Salley, and F. J. McClernon, "Hippocampal and striatal gray matter volume are associated with a smoking cessation treatment outcome: results of an exploratory voxel-based morphometric analysis," *Psychopharmacology (Berl)*, vol. 210, no. 4, pp. 577–83, 2010.

[145] F. Picard, S. Sadaghiani, C. Leroy, D. S. Courvoisier, R. Maroy, and M. Bottlaender, "High density of nicotinic receptors in the cingulo-insular network," *Neuroimage*, vol. 79, pp. 42–51, 2013.

[146] X. Zhang, B. J. Salmeron, T. J. Ross, X. Geng, Y. Yang, and E. A. Stein, "Factors underlying prefrontal and insula structural alterations in smokers," *NeuroImage*, vol. 54, no. 1, pp. 42–8, 2011.

[147] M. N. Smolka, M. Buhler, S. Klein, U. Zimmermann, K. Mann, A. Heinz, and D. F. Braus, "Severity of nicotine dependence modulates cue-induced brain

activity in regions involved in motor preparation and imagery," *Psychopharmacology*, vol. 184, no. 3-4, pp. 577–88, 2006.

[148] A. C. Janes, D. A. Pizzagalli, S. Richardt, B. F. B. de, S. Chuzi, G. Pachas, M. A. Culhane, A. J. Holmes, M. Fava, A. E. Evins, and M. J. Kaufman, "Brain reactivity to smoking cues prior to smoking cessation predicts ability to maintain tobacco abstinence," *Biological psychiatry*, vol. 67, no. 8, pp. 722–9, 2010.

[149] G. M. DiFranza, J. R., "Alcoholism and smoking.," *Journal of Studies on Alcohol*, vol. 51, pp. 130–135, 1990.

[150] M. Rosenbloom, E. V. Sullivan, and A. Pfefferbaum, "Using magnetic resonance imaging and diffusion tensor imaging to assess brain damage in alcoholics," *Alcohol research & health : the journal of the National Institute on Alcohol Abuse and Alcoholism*, vol. 27, no. 2, pp. 146–52, 2003.

[151] A. Khanna, M. Guo, M. Mehra, and r. Royal, W., "Inflammation and oxidative stress induced by cigarette smoke in lewis rat brains," *J Neuroimmunol*, vol. 254, no. 1-2, pp. 69–75, 2013.

[152] P. Mazzone, W. Tierney, M. Hossain, V. Puvenna, D. Janigro, and L. Cucullo, "Pathophysiological impact of cigarette smoke exposure on the cerebrovascular system with a focus on the blood-brain barrier: expanding the awareness of smoking toxicity in an underappreciated area," *Int J Environ Res Public Health*, vol. 7, no. 12, pp. 4111–26, 2010.

[153] A. Csordas and D. Bernhard, "The biology behind the atherothrombotic effects of cigarette smoke," *Nat Rev Cardiol*, vol. 10, no. 4, pp. 219–30, 2013.

[154] H. Y. Benjamini, Y., "Controlling the false discovery rate: a practical and powerful approach to multiple testing," *Journal of the Royal Statistical Society*, vol. 57, no. Series B, pp. 289–300, 1995.

[155] D. Badre and A. D. Wagner, "Left ventrolateral prefrontal cortex and the cognitive control of memory," *Neuropsychologia*, vol. 45, no. 13, pp. 2883–901, 2007.

[156] S. Enriquez-Geppert, T. Eichele, K. Specht, H. Kugel, C. Pantev, and R. J. Huster, "Functional parcellation of the inferior frontal and midcingulate cortices in a flanker-stop-change paradigm," *Hum Brain Mapp*, vol. 34, no. 7, pp. 1501–14, 2013.

[157] L. Jacobson, D. C. Javitt, and M. Lavidor, "Activation of inhibition: diminishing impulsive behavior by direct current stimulation over the inferior frontal gyrus," *J Cogn Neurosci*, vol. 23, no. 11, pp. 3380–7, 2011.

[158] T. Egner, "Right ventrolateral prefrontal cortex mediates individual differences in conflict-driven cognitive control," *J Cogn Neurosci*, vol. 23, no. 12, pp. 3903–13, 2011.

[159] D. A. O'Connor, S. Rossiter, M. Yucel, D. I. Lubman, and R. Hester, "Successful inhibitory control over an immediate reward is associated with attentional disengagement in visual processing areas," *Neuroimage*, vol. 62, no. 3, pp. 1841–7, 2012.

[160] M. Luijten, D. A. O'Connor, S. Rossiter, I. H. Franken, and R. Hester, "Effects of reward and punishment on brain activations associated with inhibitory control in cigarette smokers," *Addiction*, vol. 108, no. 11, pp. 1969–78, 2013.

[161] E. T. Berkman, E. B. Falk, and M. D. Lieberman, "In the trenches of real-world self-control: neural correlates of breaking the link between craving and smoking," *Psychol Sci*, vol. 22, no. 4, pp. 498–506, 2011.

[162] M. R. Brown, R. M. Lebel, F. Dolcos, A. H. Wilman, P. H. Silverstone, H. Pazderka, E. Fujiwara, T. C. Wild, A. M. Carroll, O. Hodlevskyy, L. Zedkova, L. Zwaigenbaum, A. H. Thompson, A. J. Greenshaw, and S. M. Dursun, "Effects of emotional context on impulse control," *Neuroimage*, vol. 63, no. 1, pp. 434–46, 2012.

[163] B. Froeliger, L. A. Modlin, R. V. Kozink, L. Wang, E. L. Garland, M. A. Addicott, and F. J. McClernon, "Frontoparietal attentional network activation differs between smokers and nonsmokers during affective cognition," *Psychiatry research*, vol. 211, no. 1, pp. 57–63, 2013.

[164] T. C. Durazzo, P. S. Insel, and M. W. Weiner, "Greater regional brain atrophy rate in healthy elderly subjects with a history of cigarette smoking," *Alzheimers Dement*, vol. 8, no. 6, pp. 513–9, 2012.

[165] R. H. Paul, A. M. Brickman, R. A. Cohen, L. M. Williams, R. Niaura, S. Pogun, C. R. Clark, J. Gunstad, and E. Gordon, "Cognitive status of young and older cigarette smokers: data from the international brain database," *J Clin Neurosci*, vol. 13, no. 4, pp. 457–65, 2006.

[166] M. Weiser, S. Zarka, N. Werbeloff, E. Kravitz, and G. Lubin, "Cognitive test scores in male adolescent cigarette smokers compared to non-smokers: a population-based study," *Addiction*, vol. 105, no. 2, pp. 358–63, 2010.

[167] F. Baker, M. W. Johnson, and W. K. Bickel, "Delay discounting in current and never-before cigarette smokers: similarities and differences across commodity, sign, and magnitude," *J Abnorm Psychol*, vol. 112, no. 3, pp. 382–92, 2003.

[168] W. K. Bickel, A. L. Odum, and G. J. Madden, "Impulsivity and cigarette smoking: delay discounting in current, never, and ex-smokers," *Psychopharmacology (Berl)*, vol. 146, no. 4, pp. 447–54, 1999.

[169] S. H. Mitchell, "Measures of impulsivity in cigarette smokers and non-smokers," *Psychopharmacology (Berl)*, vol. 146, no. 4, pp. 455–64, 1999.

[170] A. L. Odum, G. J. Madden, and W. K. Bickel, "Discounting of delayed health gains and losses by current, never- and ex-smokers of cigarettes," *Nicotine Tob Res*, vol. 4, no. 3, pp. 295–303, 2002.

[171] Y. Ohmura, T. Takahashi, and N. Kitamura, "Discounting delayed and probabilistic monetary gains and losses by smokers of cigarettes," *Psychopharmacology (Berl)*, vol. 182, no. 4, pp. 508–15, 2005.

[172] B. Reynolds, J. B. Richards, K. Horn, and K. Karraker, "Delay discounting and probability discounting as related to cigarette smoking status in adults," *Behav Processes*, vol. 65, no. 1, pp. 35–42, 2004.

[173] L. H. Epstein, J. B. Richards, F. G. Saad, R. A. Paluch, J. N. Roemmich, and C. Lerman, "Comparison between two measures of delay discounting in smokers," *Exp Clin Psychopharmacol*, vol. 11, no. 2, pp. 131–8, 2003.

[174] G. M. Heyman and S. P. Gibb, "Delay discounting in college cigarette chippers," *Behav Pharmacol*, vol. 17, no. 8, pp. 669–79, 2006.

[175] S. H. Kollins, "Delay discounting is associated with substance use in college students," *Addict Behav*, vol. 28, no. 6, pp. 1167–73, 2003.

[176] J. H. Yoon, S. T. Higgins, S. H. Heil, R. J. Sugarbaker, C. S. Thomas, and G. J. Badger, "Delay discounting predicts postpartum relapse to cigarette smoking among pregnant women," *Exp Clin Psychopharmacol*, vol. 15, no. 2, pp. 176–86, 2007.

[177] J. Dallery and B. R. Raiff, "Delay discounting predicts cigarette smoking in a laboratory model of abstinence reinforcement," *Psychopharmacology (Berl)*, vol. 190, no. 4, pp. 485–96, 2007.

[178] M. Li and M. Burmeister, "New insights into the genetics of addiction," *Nature Reviews Genetics*, vol. 10, pp. 225–231, 2009.

[179] M. Buhler and K. Mann, "Alcohol and the human brain: a systematic review of different neuroimaging methods," *Alcoholism, clinical and experimental research*, vol. 35, no. 10, pp. 1771–93, 2011.

[180] S. Yip, C. Lacadie, J. Xu, P. Worhunsky, R. Fulbright, R. Constable, and M. Potenza, "Reduced genual corpus callosal white matter integrity in pathological gambling and its relationship to alcohol abuse or dependence," *The World Journal of Biological Psychiatry*, vol. 14, no. 2, pp. 129–138, 2013.

[181] J. M. Vink, G. Willemsen, and D. I. Boomsma, "Heritability of smoking initiation and nicotine dependence," *Behav Genet*, vol. 35, no. 4, pp. 397–406, 2005.